UNIVERSIDADE DE LISBOA
FACULDADE DE CIÊNCIAS
DEPARTAMENTO DE ENGENHARIA GEOGRÁFICA, GEOFÍSICA E ENERGIA

Statistical downscaling of air temperature in the Douro Valley for agronomic applications

Andreia Filipa Silva Ribeiro

Dissertação

Mestrado em Ciências Geofísicas

Especialização em Meteorologia

2013

UNIVERSIDADE DE LISBOA

FACULDADE DE CIÊNCIAS

DEPARTAMENTO DE ENGENHARIA GEOGRÁFICA, GEOFÍSICA E ENERGIA

Statistical downscaling of air temperature in the Douro Valley for agronomic applications

Andreia Filipa Silva Ribeiro

Dissertação

Mestrado em Ciências Geofísicas

Especialização em Meteorologia

Dissertação orientada pela Doutora Susana M. Barbosa e co-orientada pelo Professor Pedro Miranda

2013

A Andreia Filipa Silva Ribeiro usufruiu de uma bolsa ANICT para o desenvolvimento da Dissertação de Mestrado “Statistical downscaling of air temperature in the Douro Valley for agronomic applications”.

“Começa por fazer o que é necessário, depois o que é possível e de repente estarás a fazer o impossível”

São Francisco de Assis (1181-1226)

Agradecimentos

À minha orientadora Doutora Susana Barbosa pela sua disponibilidade e apoio em vários momentos durante este Mestrado. O meu mais sincero agradecimento por todos os estímulos durante a orientação deste trabalho e por ter elevado os meus conhecimentos académicos e científicos, contribuindo para o meu crescimento pessoal e profissional. Nunca vou conseguir retribuir o constante incentivo e o testemunho pessoal que me serviram de inspiração e que tornaram possível a conclusão desta tese.

Ao Professor e co-orientador Pedro Miranda pela oportunidade em trabalhar neste tema e pela oportunidade de me ter integrado no seu grupo de investigação. Agradeço igualmente todas as discussões e sugestões relevantes para este trabalho, que permitiram uma maior profundidade na interpretação dos resultados.

Ao Doutor Alexandre Ramos expresso a minha gratidão pela partilha dos dados das estações meteorológicas utilizados neste trabalho. Agradeço igualmente a disponibilidade e amabilidade na revisão dos primeiros resultados obtidos deste trabalho. A sua contribuição foi fundamental para este estudo.

À Doutora Rita Cardoso por disponibilizar os dados de reanálise e do modelo WRF e pelo auxílio prestado numa fase inicial do trabalho. As suas sugestões e recomendações foram de elevada importância para a realização desta tese.

Ao André Amaral e à Sofia Ermida, pela presença, pela força, pela amizade, e por me encorajarem sempre durante este Mestrado. As lágrimas e gargalhadas partilhadas não foram menos importantes para a conclusão deste curso.

A toda a minha família, em particular, aos meus pais, cujas palavras de coragem, apoio e amor incondicionais foram determinantes ao longo de todo o meu percurso académico e pessoal. À minha mana, por todo o carinho e doçura, e por ser sempre um motivo de alegria na minha vida.

A Deus, por mais um motivo de gratidão na minha vida. Obrigada por Seres fonte de inspiração e coragem em todos meus passos.

Abstract

Agronomic activities are very dependent on local climatic conditions. The vineyard in particular is very sensitive to temperature, which significantly affects the composition of grapes and hence the final quality of the produced wine. In a climate change context knowledge of future temperature variability is important to minimize impacts and promote adaptation measures often entailing high costs. However, given the local character of agronomic activities, temperature projections are required at very small spatial scales, and downscaling of climate variables is therefore required. In this thesis temperature data from the high resolution (9km) meteorological model WRF and reanalysis data from ERA-interim are analyzed. Statistical downscaling techniques are applied to the ERA-interim data in order to obtain local temperature estimates for the wine producing region of the Douro valley. Several bioclimatic indices based on downscaled temperature are further calculated in order to evaluate the climatic potential of the Douro Wine Region.

Key-words: Statistical downscaling, Temperature, Bioclimatic indices, Douro Wine Region

Resumo

No contexto das alterações climáticas os impactos da variabilidade da temperatura têm sido um dos principais objectos de estudo ao longo do último século. A prática vitícola, em particular, é uma das actividades agronómicas mais influenciadas pela temperatura, e a sua importância económica para Portugal conduziu a vários estudos sobre este tópico. A Região Vinhateira do Douro constitui um excelente exemplo da contribuição dos produtores de vinho para o crescimento económico, e de como a complexa topografia da região contribui para a variabilidade climática, muitas vezes com consequências directas na qualidade final do vinho. Esta tese contribui para o conhecimento das condições climáticas locais da Região Vinhateira do Douro que influenciam a composição das uvas e a consequente qualidade do vinho produzido.

O impacto das alterações climáticas na qualidade do vinho da Região Vinhateira do Douro usando *GCMs* (*General Circulation Models* também conhecidos como *Global Climate Models*) e *RCMs* (*Regional Climate Models*) é discutido por vários autores. Contudo, a baixa resolução das grelhas dos *GCMs*, dos *RCMs* e da reanálise negligenciam aspectos regionais, e técnicas que permitam a obtenção de informação de menor escala surgem como um requisito essencial nas ciências agronómicas. A Região Vinhateira do Douro em particular é um excelente exemplo da necessidade de climatologia de alta resolução, motivada pela geomorfologia complexa da região. O objectivo deste trabalho é a realização de um *downscaling* estatístico da temperatura do ar para locais particulares de modo a focar em áreas localizadas da Região Vinhateira do Douro, com a intenção de poder ser aplicado no estudo de uma vinha em particular.

Existem vários métodos de *downscaling* com o propósito de colmatar o problema de baixa resolução dos *GCMs* e *RCMs*, que são geralmente subdivididos em duas categorias: *downscaling* dinâmico e estatístico. O *downscaling* dinâmico é uma abordagem numérica que consiste na utilização de modelos globais ou reanálise como forçadores de modo a obter simulações de dados mais detalhadas para uma região particular. O *downscaling* estatístico utiliza modelos estatísticos simples, de modo a estabelecer a relação estatística entre variáveis de grande escala e variáveis locais. Os modelos de regressão são bastante utilizados para *downscaling* estatístico destacando-se pelo seu custo computacional reduzido e a sua fácil aplicação.

Neste trabalho são consideradas três estações meteorológicas na Região Vinhateira do Douro, Vila Real, Pinhão e Régua, representando duas das três sub-regiões da Região Demarcada do Douro: Baixo Corgo (Régua e Vila Real) e Cima Corgo (Pinhão). Baixo Corgo é a sub-região que apresenta as temperaturas mais baixas devido à influência dos ventos do Atlântico, sendo protegida pelas serras do Marão e Montemuro, enquanto Cima Corgo apresenta temperaturas mais elevadas. Em contraste, a sub-região mais a este, Douro Superior, é a sub-região mais quente e mais seca e que tem as plantações de vinhas mais recentes, marcada por episódios de seca recorrentes. As estações meteorológicas em análise são também representativas das características topográficas que contribuem para o clima único da região, com altitudes de 481, 65 e 130 metros respectivamente. A mais recente

reanálise do *ECMWF* (*European Centre for Medium Range Forecasts*), ERA-Interim, e um *RCM* estado-de-arte resultante de um *downscaling* dinâmico, WRF (9km) são utilizados para a realização do *downscaling* estatístico da temperatura do ar para a localização das estações. A suave topografia da reanálise ERA-Interim e do modelo WRF são ajustadas através de um gradiente de temperatura constante de 6ºC/km.

O *downscaling* estatístico realizado neste trabalho é baseado em métodos de regressão. Como pré-processamento na análise dos dados de temperatura é aplicada uma decomposição das séries temporais utilizando o método *STL* (*Seasonal-Trend decomposition procedure based on Loess*), um algoritmo iterativo e robusto baseado em regressão local. O ajuste sazonal das séries temporais é um passo fulcral para a análise de regressão e, neste trabalho, é obtido pela remoção da componente sazonal obtida pelo método *STL*.

Neste trabalho, a técnica de regressão baseada em mínimos quadrados ordinários é primeiro considerada, e posteriormente o método de regressão robusta é aplicado de modo a reduzir o impacto de eventuais *outliers* nos resultados. A relação estatística entre a reanálise/WRF e as observações é estabelecida a partir das séries temporais ajustadas sazonalmente para o período de calibração de 1989-2003. O *downscaling* estatístico da reanálise ERA-Interim e a combinação de *downscaling* dinâmico e estatístico do modelo WRF é realizado no período de validação de 2004-2006. O correspondente ciclo sazonal da reanálise ERA-Interim e do modelo WRF são adicionados posteriormente às séries temporais *downscaled*, dado que o ciclo sazonal médio é semelhante ao das observações. O ciclo sazonal das observações não é considerado neste trabalho dado que não seria possível a sua utilização no caso da aplicação desta técnica de *downscaling* para linhas temporais no futuro. De modo a avaliar o *downscaling* estatístico, quatro medidas de precisão estatística são utilizadas: o viés, a raiz do erro médio quadrático, o erro absoluto médio e o erro percentual absoluto.

Como etapa final, as séries locais de temperatura obtidas por *downscaling* estatístico são utilizadas para avaliar o potencial climático para crescimento da uva, nas estações em estudo da Região Vinhateira do Douro. A caracterização do clima nesta região é realizada a partir de índices bioclimáticos baseados na temperatura durante o período de crescimento das videiras (Abril a Outubro). A temperatura média do período de crescimento (*GST, Average growing season temperature*) é calculada a partir da soma da média da temperatura média, durante os sete meses do período de crescimento. O índice *GDD* (*Growing degree-days*) corresponde à temperatura média acima de uma temperatura base de 10ºC, uma vez que não existe crescimento da uva abaixo desta temperatura, e permite descrever o tempo envolvido nos processos biológicos da videira. Semelhante a este último é o índice helio-térmico de Huglin (*HI, Heliothermal Index of Huglin*) que dá mais peso à temperatura máxima e considera um coeficiente de ajustamento devido à variação em latitude. A duração do período de crescimento é dada pelo *LGS* (*Length growing season*) que considera o número de dias em quem a temperatura média está acima dos 10ºC. O CI (*Cool Nigth Index*) é complementar ao HI e tem conta a média da temperatura mínima durante o período de maturação (Setembro). De acordo com os valores de cada índice é possível definir classes climáticas características do potencial climático de cada região.

Um dos principais resultados deste trabalho reside na excelente representação da variabilidade da temperatura máxima, mínima e média pelas séries temporais *downscaled* estatisticamente. De um modo geral, a regressão baseada em mínimos quadrados ordinários e a regressão robusta apresentam resultados semelhantes, indicando que o impacto de eventuais *outliers* não é significativo na variabilidade média. Verifica-se que o *downscaling* estatístico reduz significativamente as diferenças entre a ERA-Interim/WRF e as observações, revelando a importância do *downscaling* estatístico em aumentar a *performance* da reanálise ERA-Interim e do modelo WRF, e o valor adicional em combinar *downscaling* dinâmico e estatístico. Os índices bioclimáticos calculados a partir das séries *downscaled* estatisticamente destacam-se como sendo uma excelente aproximação dos índices calculados a partir das observações e constituem uma melhoria significativa do que se obteria a partir apenas da reanálise ERA-Interim e do modelo WRF. No que diz respeito à aplicação na vinha, o *downscaling* estatístico revela ser uma mais-valia ao capturar características locais, tal como a influência da altura das estações.

Palavras-chave: Downscaling estatístico, Temperatura, Índices bioclimáticos, Região Vinhateira do Douro

Índice

1. Introduction

During the last century the climate system has been suffering changes caused by human interference leading to increased vulnerability of various natural systems. Agronomic sciences have been facing major challenges in the last few years, trying to optimize systems and techniques to help endure and overcome climatic change impacts. Viticulture is one of the agronomic activities most directly influenced by climatic conditions and with high economic relevance for many countries, in particular Portugal. Recently, there has been an effort to bring together the scientific community and the wine-making sector to understand how climate affects wine production and quality and thus minimize the impacts and promote adaptation measures.

The Douro region is a good example of the importance of vineyards cultures to Portugal's economic growth. Composed by a rugged terrain with a particular topography, this wine region was crafted giving rise a stunning stairway covered by vineyards that produce excellent wine grapes. Among other high quality wines, the Douro region produces the world famous Porto Wine that has the highest wine classification in Portugal, exerting a strong economic and cultural contribution. A combination of numerous factors contributes to this distinctive wine region, and climate characteristics are a key factor to understand the dynamics behind this high quality wine production. Understanding how temperature affects yield and the composition of grapes is important to assess the impacts in the final quality of the produced wine. In this context, the study of relationships between temperature and wine production is a bridge to quantify the effects of global warming and promote adaptive measures.

Portugal, in particular the Douro region, is a fine example of the need of high resolution climatology, motivated by both geomorphologic complexity and large climate gradients. Downscaling techniques allow to obtain regional information, overcoming the problem of misrepresentation of small-scale features of the most widely used models for climate studies. In the next sub-chapter a literature review summarizing introductory concepts is followed by a brief overview of statistical downscaling techniques and its scientific motivation. Emphasis is given on the influence of climate variability in the vineyards of the Douro region, and climate scenarios associated to higher wine production.

1.1 Agrometeorology and vineyard

The importance of agriculture in human history arises when man began to domesticate animals and grow food, and soon realized that agriculture is dependent on climate. Particularly the characteristics of the Mediterranean climate make it unique in all climates of the world with both advantages and disadvantages for agriculture. Qualitatively the climate of the Portuguese territory is temperate with hot and dry summers, and rainfall concentrated in winter (see Koppen's classification in *"Atlas Climático Ibérico (1971-2000)"*). Some major drawbacks for agriculture are the lack of rain during the

summer which limits the moisture available for plant growth, and excessive rains in winter that compromise the soils with poor drainage. However, these characteristics can be beneficial for some species, revealing to be favorable for a couple of agricultural practices. Vineyards are generally located in regions with climate as described above, in particular the most common species *Vitis vinifera* which requires long, warm-to-hot, dry summers and cool winters (Winkler et al. 1974). In fact, humid conditions are susceptible to certain fungus diseases causing vining plants to be poorly suited to humid summers, and long and dry summers are required for a desirable maturation of grapes (Mariano Feio, 1991). During the winter it is a plant with an extremely high resistance when faced with cold conditions, dying only with negative temperatures between -13º and -15ºC, which never happens in Portugal (Mariano Feio, 1991). Moreover, the consequences of climate change depend on the characteristics of each region and the capacity of grape varieties and producers to adapt (Jones et al. 2005).

In viticulture, climate is assessed differentiating three levels of climate: macroclimate, mesoclimate and microclimate (Smart and Robinson, 1991). While macroclimate refers to the climate of a region, extending over tens of kilometers depending on e.g. topography and distance from ocean, mesoclimate refers to a particular site, generally associated to a particular vineyard. Mesoclimate effects concern to e.g. sunlight, conditioning if vineyards are planted in hill-sides facing south or north in order to promote sunlight absorption. Microclimate is the climate within a surrounding plant canopy (above ground part of a particular vine), whose effects can occur over few centimeters. Using again the sunlight example, in the top of the canopy the sunlight may affect far more than in the center. Microclimate is appropriate when an individual vine is considered, while the climate of a vineyard is concerned with macroclimate or mesoclimate. In addition to the spatial scale, climate operates in temporal scales varying from broad to singular weather events, such as extreme weather events, manifested in temperature, precipitation and humidity parameters.

A set of climate conditions influence the grapevine depending on the region of viticulture, the most influential factor in growth of wine grapes being the temperature (Mullin et al. 1992), and generally temperatures of grapevine parts are at or near air temperature (Smart and Robinson, 1991). One effect of air temperature in the plant is water lost through transpiration: the higher the air temperature the most water is loss through transpiration, which enables to regulate the temperature of the leaf. The temperature has also a very important role in photosynthesis, varying with the stage of development of the grapes. Other factors, such as precipitation, radiation, humidity, fog, may also have effects, but much more limited (Winkler et al. 1974). In fact, although *Vitis vinifera* grows best in regions that have few or no summer rains, winter must be rainy in order to store water in the soil to carry vines through the summer, although irrigation can mitigate these deficiencies (Weaver, 1976).

Due to the important role of temperature in almost all biological aspects of the vine, knowledge of the developmental stages of the grapes is significant to understand how climate influences the different growth stages (Figure 1). Each year, the grapevine growth starts with the budburst corresponding to the growing point when the leaves are separated at the tip. After the budburst, the flowering begins, followed by the stage of fruit set where a grape berry begins to develop. The stage when grape berries start a color change and maturation is called *véraison* followed by the harvest that corresponds to the grape maturity. The grapes are then removed from the vine and are ready to begin the wine making process. The temperature largely influences the growing season length, which is crucial in the optimization of the maturation of grapes, determining the levels of sugar and the final wine (Jones et al. 2005). For many of the world benchmark regions, a study based on both climate and plant growth shows that high quality wine production is limited to 13 to 21ºC average temperatures during the growing season (Jones, 2006). Average temperatures higher than 21ºC are possible, but are mostly limited to fortified wines, table grapes and raisons (Jones and Alves 2012).

Figure 1 – Vegetative cycle of Vitis vinifera. Photos source: Sogrape Vinhos, S.A. (http:/ http://www.sograpevinhos.eu/)

The time between the different developmental stages of *Vitis vinifera* greatly depends on climate and geographic location (Jones and Davis 2000). In order to define climate regions more favorable to the development of grapes there are several bioclimatic indices based directly or indirectly on temperature during the growing season. Based on the values of each index it is possible to fit groups or classes varying from very cool to very hot regions characterizing the climatic potential of a geographic location. One of the earliest indices was intended to determine the time required for grapes to reach maturity, expressed by the total amount of heat received, yielding the concept of temperature-time values called degree days or heat units (Amerine and Winkler, 1944). Heat summation corresponds to the sum of the mean monthly temperature above 10ºC, since there is no growth below that temperature. Winkler et al. (1974) adopted this concept to the growing season (April 1 to October 31) at various locations in California and as a result it was classified into five regions according to heat summations values. Also called the Winkler index (WI), Jones et al. (2010) derived this variable for the western United States, classifying it as Growing Degree-Days (GDD), and a further Growing Season average Temperature index (GST) calculated by taking the average of the seven months of the growing season. With similar information, Malheiro et al. (2010) calculated the Length Growing

Season (LGS) as the number of days with mean temperatures above 10ºC, considering 182 days or higher an appropriate LGS for vine growing (Jackson, 2001).

Table 1 - Bioclimatic indices resumed in this work, their equations and references. Variables: GDD (Growing degree-days), GST (Average growing season temperature), LGS (Length growing season), HI (Heliothermal Index of Huglin), CI (Cool night index), DI (Dryness index), HyI (Hydrothermic Index of Branas) and CompI (Composite Index).

Index	Equation	References (e.g.)
GDD (ºC)	$\sum_{Apr}^{Oct} \max[([T_{\max} + T_{\min}]/2) - 10]$	Winkler (1974) Jones et al. (2010) Santos et al. (2012)
GST (ºC)	$\frac{1}{N}\sum_{Apr}^{Oct}([T_{\max} + T_{\min}]/2)$ Where *N* is the number of observations	Jones et al. (2010)
LGS (days)	Number of days with $T_{mean} > 10^{o}C$	Jackson (2001) Malheiro et. al. (2010)
HI	$\sum_{Apr}^{Oct} \max([T_{mean} - 10] + [T_{\max} - 10]/2).d$ Where *d* is an adjustment for latitude	Tonietto and Carbonneau (2004) Malheiro et. al. (2010) Blanco-Ward et al. (2007) Santos et al. (2012)
CI	September average $T_{\min}$	Tonietto (1999) Malheiro et. al. (2010) Blanco-Ward et al. (2007) Santos et al. (2012)
DI	$\sum_{Apr}^{Sep}(W_0 + P + T_v - E_s)$ Where W_0 is the initial soil-water, *P* the precipitation, T_v the potential transpiration and E_s the evaporation from the soil	Riou et al. (1994) Tonietto and Carbonneau (2004) Malheiro et. al. (2010) Blanco-Ward et al. (2007) Santos et al. (2012)
HyI	$\sum_{Apr}^{Aug}(T \times P)$	Branas et al. 1946 Tonietto and Carbonneau (2004) Malheiro et. al. (2010) Blanco-Ward et al. (2007) Santos et al. (2012)
CompI	Ratio of years combining 4 criteria: HyI ≥ 1400, DI ≥-100, HyI≤5100 and $T_{\min}$ always ≥-17ºC	Malheiro et. al. (2010) Santos et al. (2012)

Similar to the heat summation concept, the classical Heliothermal Index of Huglin (HI) (Huglin, 1978) is widely used, giving more weight to maximum temperatures above mean temperatures and applying a coefficient which expresses the day-length adjustment due to latitude varying, which takes into account the average daylight period for the latitude studied (e.g., Tonietto and Carbonneau 2004, Jones et al. 2010, Malheiro et al. 2010). Complementary to HI is the Cool Night Index (CI) which provides a relative measure of maturation potential taking into account the minimum temperatures (mean of minima) during maturation period (September in the Northern Hemisphere and March for the Southern Hemisphere (Tonietto 1999)). This index allows to assess grape and wine qualitative potential, such as color and aroma, supplementing the Dryness Index (DI) which gives information about soil-water availability based on an adaptation of the potential water balance of Riou (Riou et al.

1994). HI, CI and DI combined define the Multicriteria Climatic Classification System (*Géoviticulture MCC System*) developed by Tonietto and Carbonneau (2004) for 97 grape-growing regions in 29 countries, among them Portugal. This system is a research tool for grape-growing and wine-making zoning, distinguishing 36 different climate types, recognized by Blanco-Ward et al. (2007) as a good method for viticultural zonation in the northwest of Spain, defining 6 climate types for that region.

Assessing the potential risk of grapevine exposure to diseases is performed by the Hydrothermic Index of Branas (HyI) (Branas et al., 1946) combining the precipitation and temperature during the growing season by the sum of the product between the variables (e.g. Blanco-Ward et al. 2007, Malheiro et al. 2010). The risk is considered high if HyI exceeds 5100ºC.mm and low for values below 2500ºC.mm.

The Composite Index (CompI), which provides the fraction of winegrowing optimal years in a specific time period, was developed by Malheiro et al. (2010), combining 4 criteria: HyI ≥ 1400, DI ≥-100, HyI≤5100 and T_{min} always ≥-17ºC. A value of 0 corresponds to the total absence of suitable years, while a value of 1 means that all years are suitable for grapevine growing. More recently Santos et al. (2012) adapted this index by removing the Hydrothermic Index of Branas (HyI) criteria, since according to these authors it contributes to unrealistically low values of CompI for several established viticultural regions. The additional value of Santos et al. (2012) study was the update of information for viticultural zoning by mapping bioclimatic indices, and also the analyses of the inter-annual variability of the indices and possible long-trends, potentially related to large-scale atmospheric forcing.

1.2 Douro Valley case study

A combination of numerous factors such as topography, soil and Mediterranean climate characteristics contribute to the distinctive wine region of the Douro Valley. The Douro region produces the world famous Port Wine, among other high quality wines, achieving the highest wine classification as a denomination of controlled origin (DOC) in Portugal and has been classified by UNESCO (United Nations Educational, Scientific and Cultural Organization) as a World Heritage Site. It is a very rugged mountainous region situated in the province of Trás-os-Montes e Alto Douro in the northeastern Portugal, confined by the western mountains of Marão and Montemuro (Figure 2), which block the flow of moist air from the Atlantic Ocean (Fanet, 2004). The Douro River and its affluents (Figure 2), such as Tua and Corgo, extend into deep valleys and most crops are embedded in the river basins whose soils are mainly composed by schist that is beneficial to the longevity of the vines (Mayson, 2012). Many factors contribute to the unique Douro wines which are strong contributors to Portugal's economy, thus understanding its production and how climate affects vineyards is of the highest importance, for the region and for the whole country.

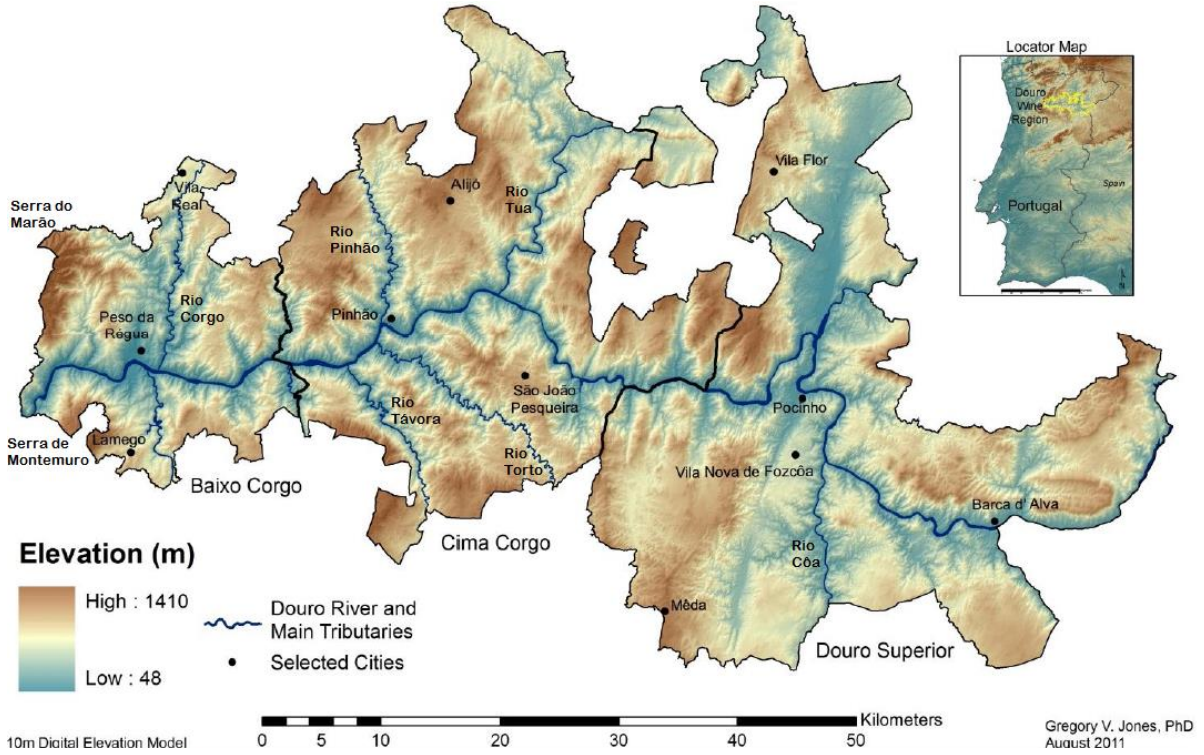

Figure 2 – The Douro Wine Region topography, Douro River and main tributaries, and the location of the region within Portugal (top right). Identification of the three sub-regions: Below Corgo, Above Corgo and Upper Douro. The western high elevations correspond to the mountains of Marão and Montemuro. Data source: IVDP (2011)

In order to improve the cultivation of vineyards and to safeguard the quality of wine, an administrative delimitation was marked in the Douro region, the Demarcated Region of Douro (DRD). Generally the DRD is characterized by hot and dry summers, followed by cool winters, thus governed by warm and dry conditions with heat and water stress in most years (Jones and Alves, 2012). According to the growing season average temperatures (GST) index for 1950-2000 the overall DRD is 65% a warm climate type, 24% an intermediate climate and nearly 10% hot climate type (ADVID (Associação para o Desenvolvimento da Viticultura Duriense), 2012). However, the complex topography of the Douro Valley promotes climate variability since the region extends over steep valleys at different solar exposures and different altitudes. Hence the distribution area of vineyards is not uniform and the DRD is usually subdivided into three sub-regions (Figure 1), from the west to the east, each one with its own mesoclimate: Below Corgo on the left margin of the River Corgo (west of DRD), Above Corgo on the right margin of the River Corgo (center of the DRD) and Upper Douro on the right margin of River Tua (east of DRD). Below Corgo is the coolest and rainy sub-region due to the influence of the Atlantic winds, while Above Corgo is a little warmer and drier (Mayson, 2012). In contrast, Upper Douro is the hottest and driest of the sub-regions and the most recently planted, marked by recurrent drought episodes (Mayson, 2012). This heterogeneous climate conditions are in agreement with the historic climate normal (1931-1960) describing generally wetter and cooler areas to the west in contrast with drier and warmer areas to the east (ADVID, 2012). The sub-region Below Corgo has

more area as a warm climate type than the other two sub-regions, Above Corgo has more area as an intermediate climate type than the other two sub-regions and Douro Superior has twice the area in hot climate type than the other two regions on growing season average temperatures (GST) profile (ADVID, 2012). In addition Douro Superior has warmer maximum and minimum temperatures, on average, compared to the other sub-regions (ADVID, 2012).

To fully understand how climate parameters vary during the stages of growth of the grapes it is important to examine the evolution of the main stages of the vegetative cycle. In the DRD budburst typically occurs during March followed by flowering in May and *véraison* (coloring of the grapes) in July (Malheiro, 2005). In mid-August begins the evaluation of the maturation of the grapes to determine the start of the harvest that generally occurs in late September. In contrast with northwestern-Spain, where budburst occurs between April and June, delaying all the other stages compared to DRD (Lorenzo et al. 2012). Spring and early summer are the months of the most intensive growth period and the climate conditions of those seasons largely influence crop production and quality, being crucial for DRD wine production. Usually the time periods used for climate assessment in wine regions are the growing season (April-October) and dormant season (November-March). The historic climate normal (1931-1960) shows that maximum temperatures during growing season ranges from 22º4ºC to 30.3ºC (Table 2; ADVID, 2012).

Table 2 - Historic climate normal (1931-1960) statistics in the DRD for the growing season (April-October), dormant season (November-March) and annual values from 57 stations of temperature. Adapted from ADVID (2012).

Variable	Period	Mean	Median	Std. Dev.	Max.	Min.	Range
Average Temperature (ºC)	Annual	14.3	14.3	1.3	16.8	11.4	5.4
	Growing Season	18.7	18.7	1.5	21.8	15.3	6.5
	Dormant Season	8.1	8.2	1.1	10.0	5.1	4.9
Maximum Temperature (ºC)	Annual	20.7	20.5	1.7	24.1	16.6	7.5
	Growing Season	26.3	26.1	2.0	30.3	22.4	7.9
	Dormant Season	12.8	12.6	1.5	15.4	8.4	7.0
Minimum Temperature (ºC)	Annual	7.9	7.9	1.2	10.5	5.0	5.4
	Growing Season	11.2	11.0	1.3	14.2	7.8	6.3
	Dormant Season	3.4	3.4	1.1	6.0	1.1	4.9

Several authors provide information about the most favorable climatic conditions for wine production in the DRD during the different stages of the growth of grapes. According to Santos et al. (2012a) higher wine production in DRD is associated to wet and cool springs during budburst, and warmer conditions during flowering, noting that precipitation in March and high temperatures in May are favorable to yield. Similarly, other results show that high rainfall in March (budburst) and high temperatures and low precipitation in May (flowering) and June (*véraison*) favor grapevine yield (Santos et al., 2011).

The vegetative cycle is also a good indicator of favorable conditions for wine production. Vineyards exposed to an Atlantic Mediterranean climate exhibit a typical feature in their vegetative cycle characterized by a maximum of the photosynthetic activity at the end of spring and a minimum during winter (Gouveia et al., 2011). During the period of intense growth (budburst), in March, an increase in the photosynthetic activity is evident, starting to decrease in July. Gouveia et al. (2011) results indicate that lower photosynthetic activity in the previous autumn and the current spring, along with higher greenness during the summer, corresponds to a lower wine production.

Looking into the past decades, both maximum and minimum temperatures show increasing trends during the growing season, with similar changes in the annual mean (ADVID, 2012). This study of the longest available records, covering 1967-2010 for the DRD, shows that the years with the warmest minimum temperatures during the growing season were 2003 and 2006, and the years with the warmest maximum temperatures were 1995, 2006 and 2010. Winter exhibits a significant warming in minimum temperatures during 1967-2010, while no significant changes were observed in maximum temperatures. Other studies identified similar trends for Portugal, such as the increase in the daily mean temperature of 0.52ºC per decade since 1976 found by Ramos et al. (2011) based on 23 Portuguese stations. The inter-disciplinary studies about climatic changes for Portugal of Miranda et al. (2006) have shown an increase in minimum temperatures and a smaller rise in maximum temperatures as well. However, correlations between annual, growing season and dormant season weather regimes and temperature in DRD are not significant. While weather regimes exhibit weak trends, the significant trends in annual, growing season and dormant season temperatures, point towards a general warming that is not significantly driven by regional circulation changes (ADVID, 2012). In contrast, Santos et al. (2011) showed a clear connection between large-scale atmospheric flow (composites of mean sea level pressure) and yield (NCEP/NCAR reanalysis parameters for precipitation and 2 m air temperature of March, May and June). Concerning the North Atlantic Oscillation (NAO), the correlation with winegrape production is little or none (Jones, 1997) probably due to the fact that NAO is largely a wintertime mechanism and its effects diminish over the growing season.

In particular, the last winery year of 2012 experienced changes in the evolution of the main vine growth stages and most of the territory was in state of severe drought. The report performed by ADVID noted a delay in the vegetative cycle with the beginning of flowering and véraison occurring two weeks later than average. During winter, minimum air temperature reached very low values, and from February to December it was the driest period of the last 40 years. In addiction, many studies on future climate conditions in the DRD found the occurrence of more extreme heat events and a decrease in cold events (Santos et al. 2011, Gouveia et al. 2011, Jones and Alves 2012).

The late 20th century has been characterized by a warming in wine producing regions that has been mostly beneficial for high-quality wine production, while in some cases the cause for better quality is the improvement of viticulture and enological practices (Jones et al., 2005). To assess the viticultural suitability of DRD, bioclimatic indices provide useful information, in particular the Huglin Index (1950-2000) which describes 50% of the territory as warm temperate climate for viticulture, 35% as temperate climate, 10% as warm climate, and 4% as cool climate for crops (ADVID, 2012). A viticultural zoning for Europe during 1950-2009 show that most areas of the Iberian Peninsula are suitable for wine production, although a warming is expected to occur according to the Winkler (WI) and the Huglin (HI) indices (Santos et al., 2012). Future projections of winegrape suitability across Europe show a Dryness Index (DI) pattern for southern Europe projected to become very dry, namely in southern Iberia (Malheiro et al., 2010). The results are found to be similar to the ADVID (2012) assessment using a single climate model (HADCM3) that predicts a warming increase based on the Average Growing Season Temperature (GST) index, increase of Growing Degree Days (GDD) and an increase of the warm temperate class, and the forthcoming of a warm class for the Huglin Index (HI). Despite the fact that an increase of warm and dry conditions during the growing season is associated with the risk of plant pathogens exposure, the Hydrothermal Index (HyI) pattern reveals that all areas with a Mediterranean climate in southern Europe (e.g. Portugal, Spain and Italy) present low risk of contamination of diseases in vines, both in present and in future scenarios (Santos et al. 2012, Malheiro et al. 2010). In contrast, the Composite Index (CompI) predicts negatives effects in southern Europe regions, namely the Douro Valley. European Huglin Index (HI) patterns describe a northward extension of the wine-producing potential areas, since long day-lengths compensate the lower temperatures, leading to a northward extension of the viticultural zones (Malheiro et al., 2010). In addition a significant increase of the Cool Night Index (CI) with potential negative impacts in the Mediterranean Basin is predicted (Santos et al. 2012, Malheiro et al. 2010).

1.3 Climate downscaling

Climate models are typically the tools for modeling climate dynamics by simulating the interactions of the atmosphere, ocean and surface, based on the integration of physical, chemical, and sometimes biological equations. The coupled atmosphere-ocean models, General Circulation Models (GCMs, also known as a Global Climate Models) are widely used to understand the dynamics of the climate system, and generate future and past climate data. These computationally intensive numerical models are quite complex, and typically divide the planet in a 4-dimensional grid, by latitude, longitude, time and upward through the atmosphere. The spatial and temporal grid resolution indicates how detailed is the representation of information, depending on how large the grid cells are (in kilometers or degrees of latitude and longitude), how many vertical layers there are, and the size of the used time steps (how often calculations of the various properties occur).

The weather simulated by these models greatly depends on the assumed atmospheric concentration of greenhouse gases and different scenarios simulate different concentrations of gases. In IPCC (Intergovernmental Panel Climate Change) AR4 there were 40 different scenarios which are organized into six families, A1FI, A1B, A1T, A2, B1 and B2, each containing scenarios that are similar to each other. These scenarios came from the Special Report on Emissions Scenarios (SRES), in order to make projections of possible climate change making assumptions about the future e.g. technological development, economic growth, population increase, and thus estimating greenhouse gas concentrations.

Global climatological datasets are also built based on global atmospheric reanalysis such as the reanalysis from the European Centre for Medium Range Forecasts (ECMWF) or the reanalysis from the National Centers for Environmental Prediction (NCEP/NCAR). While GCMs do not necessarily use actual observations to generate initial conditions, reanalysis are generated from observations and assimilated data, providing a complete record of global atmospheric circulation. ERA-Interim is the latest global atmospheric reanalysis produced by ECMWF to replace the ERA-40 reanalysis and extend to the present date.

Models can be generated with higher or lower resolutions. GCMs and reanalysis operate with typical grid sizes of a few hundreds of kilometers, and thus are able to reproduce large-scale climate features. However, the low resolution of GCMs and reanalysis grid cells cannot resolve features on smaller scales, and regional aspects are overlooked. But information on smaller scales is required for the study of climate impacts since local climate change is largely influenced by local orography and other local parameters, which are not represented by a GCM. A way of solving this problem is to derive small scale information from a model or process with larger scale, which is known as downscaling technique.

There are several possible downscaling methods designed to fill this resolution problem, which are generally divided in two categories: dynamical and statistical downscaling. Dynamical downscaling is a numerical approach that consists in *nesting* a global model or reanalysis data to provide more detailed simulations for a particular location (Figure 3). Regional Climate Models (RCMs) are models with higher resolution than GCMs, which can be forced by GCMs or by reanalysis data, using those initial conditions to drive high resolution information. RCMs forced by ERA-40 reanalysis such as PRUDENCE and ENSEMBLES projects are valuable tools of atmospheric data for Europe, with resolutions ranging 25 and 50km. Recently Soares et al. (2012) proposed a regional climate dataset for the Portuguese mainland based on the Weather Research and Forecast Modeling System (WRF) model which was used to downscale ERA-Interim reanalysis trough two nested grids, one with 27 km and another with 9km of resolution.

The impact of climate change on wine quality using GCMs and RCMs is discussed by several authors. Santos et al. (2011) performed future grapevine yield projections for the Douro region using two GCM ensemble simulations, ECHAM5/MPI-OM1 with a spatial resolution of 1.875º for recent-past climate, and two integrations following the A1B scenario for future climate. COSMO-CLM was nested in ECHAM5 in order to obtain a finer-scale grid with 18km approximately, in a total of 3x5 grid-points in the Douro Valley. Santos et al. (2012) assessed climate change projections with 15 different GCM/RCM chains by dynamical downscaling: two ECHAM5/COSMO-CL simulations and 13 based on simulations of the ENSEMBLES project following the A1B scenario. Data from these simulations were extracted for the Douro Valley containing 3x4 grid-points of the ENSEMBLES project with 25km of resolution, and 4x7 grid points of the COSMO-CL simulations with 18km of resolution. Of even greater resolution is the global database WorldClim which is a result of several GCM's output (http://www.worldclim.org) and incorporates weather station records providing monthly maximum and minimum temperatures and precipitation with ~1km of resolution. ADVID (2012) compared WorldClim data with records from Vila Real, Pinhão and Régua for 1967-2010 and found a high correlation between the station values and model indicating WorldClim adequacy. For future climate projections, downscaled models for the same grid of the WorldClim are used, interpolating the anomalies between the GCM and the baseline years of the WorldClim for three greenhouse emission scenarios, B2, A1B and A2 of the HADCM3 model.

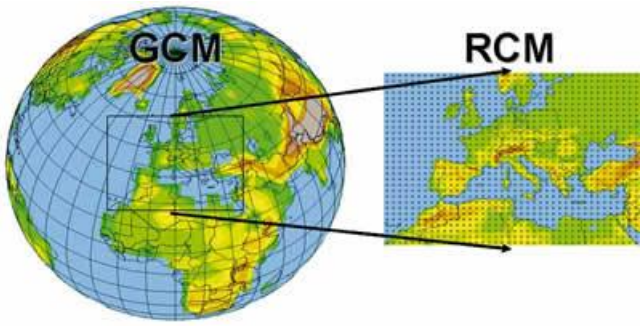

Figure 3 – Schematic depiction of the Regional Climate Model nesting approach. Data source: World Meteorological Organization (WMO) (http://www.wmo.int)

Instead of spatial interpolation or *nesting* two models, statistical downscaling makes use of simple statistical models in order to establish the relationship between large-scale climate variables and local climate variables. A statistical downscaling model describes the functional relationship between a small scale variable *y* (predictand) and a large scale variable *x* (predictor):

$$y = f(x) \tag{1}$$

A pre-requisite for statistical downscaling is the good representation of the predictor *x* by the climatic models and eq. (1) must be understood as a stochastic equation, which implies that different

predictands *y* are consistent with the same predictor *x* (von Storch, 1999). This statistical relationship is based on the fact that regional climate is governed by the large scale climate state *x* and local features *y*. Heyen et al. (1995) refer to downscaling as a term that describes a procedure in which information about a process with smaller scale is derived from a process with larger scale. The authors state four fundamental steps to perform downscaling: (1) identify a large scale parameter that governs the local parameter, (2) find the statistical relationship between the parameters, (3) validate the relationship with independent data and (4) given a successful validation the local parameter can be estimated from GCM results.

To determine the statistical relationship, a large number of downscaling techniques have been developed and generally good simulations from GCMs are chosen as predictors. Regression models are widely used for downscaling (e.g. Kilsby et al. 1997, Wilby et al. 1998, Schoof et al. 2001), since the focus of this statistical technique is to establish a relationship between a dependent variable and one or more independent variables. Among downscaling approaches, regression models stand out because they require much less computing power, and are easier to perform.

Other alternatives have arisen in response to the limitations of classic regression models. Tareghian et al. (2013) overstep some problems inherent in the standard regression models implementation by applying quantile regression (QR) instead. Their main motivation was the poor effectiveness of traditional linear regression models concerning different quantiles of the conditional distribution, rather than the mean. When the interest is in extreme events, standard regression models may fail to provide the desired information, but QR may overcome this limitation and produce more satisfactory results. In comparison with a standard regression model the QR performed by Tareghian et al. (2013) showed better performance and the functional relationship between predictor and predictand formulated by QR is clearer than by neural networks (Baur et al., 2004). In addiction Cannon (2011) developed a quantile regression neural network for downscaling.

Despite the popularity of multiple linear regression, other optional approaches, such as Artificial Neural Networks (ANN) (e.g. Schoof et al., 2001) have been applied and compared with regression based methods (e.g. Wilby et al. 1998, Schoof et al. 2001). Although ANNs are analogous to multiple regression in terms of describing a quantitative relationship between a predictand and a predictor, neural networks make no assumption about the form of the function or the degree of nonlinearity (Wilby et al., 1998) and in general the performance of neural networks is better than for multiple regression models (Schoof et al., 2001). Alternative models are based on Single Value Decomposition (SVD) (e.g. Widman et al., 2003) and Canonical Correlation Analysis (CCA) (e.g. Heyen et al. 1995, von Storch 1999) which involve different technical details like filtering predictors and predictands or the use of Principal Component Analysis (PCA) (e.g. Palatella et al. 2010).

The aim of conventional downscaling methods is to derive information about regional processes from large scale processes which generally implies that while involved variables are not the same, the predictor governs the predictand. In fact, the main objective is precisely to describe the link between those different features. However, sometimes it is also convenient to estimate local features assuming that predictor and predictand fields are the same climate variable, for instance, precipitation. Widman et al. (2003) compared standard downscaling methods using a 1000 hPa geopotential and simulated precipitation as a predictor field: while the geopotential predictor was able to predict about 30% of the observed monthly precipitation variance, models using simulated precipitation as a predictor explained over 60% of the observed monthly precipitation variability. Maak et al. (1997) investigated if it is possible to link a climatological parameter with a non-meteorological parameter such as phenological state of a plant. The authors used canonical correlation analysis (CCA) to derive a downscaling model capable to reproduce flowering date anomalies of *Galanthus nivalis* L. based on GCM air temperature data. More recently Abatzoglou et al. (2012) developed statistical downscaling techniques for wildfire applications by tracking fire danger indices. The variety of possible applications of the downscaling methodology highlights its importance for climate studies and suggests that there must be an ongoing effort in the improvement of these techniques and their application to Agrometeorology.

1.4 Goals and research objectives

The purpose of this work is to obtain local temperature estimates for the wine producing region of the Douro valley since temperature is a key factor to understand the link between climate conditions and vineyards. In this thesis, temperature data from the high resolution 9km meteorological model WRF, reanalysis data from ERA-interim and local observations recorded at the meteorological stations of Vila Real, Pinhão and Régua are analyzed. First, ERA-Interim reanalysis is used to perform a statistical downscaling of temperature to the stations points. Second, an evaluation of dynamical downscaling is performed by comparing the 9km WRF model temperature simulations to observational data. Third, dynamical and statistical downscaling are combined by statistically downscaling the 9km WRF simulations to stations points. Furthermore, to classify the climatic potential of the Douro Wine Region to the vine growing, several bio-climatic indices based on downscaled temperature values are analyzed.

In the next chapter the meteorological variables and the corresponding pre-processing are described. The following chapter is entirely devoted to the methodology for statistical downscaling and validation applied in this work. The fourth chapter presents the major results of the analysis and in the last chapter a summary of the results is presented followed by final considerations.

2. Data and pre-processing

The Demarcated Region of the Douro (DRD) extends through the valley of the Douro River from about 100km upstream from Porto, to the border with Spain. A selected area within the DRD is typically considered to delimit the area of vineyards of the Douro region named the Douro Valley between 41.0-41.4ºN latitude and 7.0-7.8W longitude (Figure 4, blue dashed box) (Santos et al. 2011). For the current regional study an area between 40.5-42.0ºN latitude and 6.4-8.1ºW longitude is considered covering a significant network of available grid points of reanalysis, WRF model and meteorological stations (Figure 4).

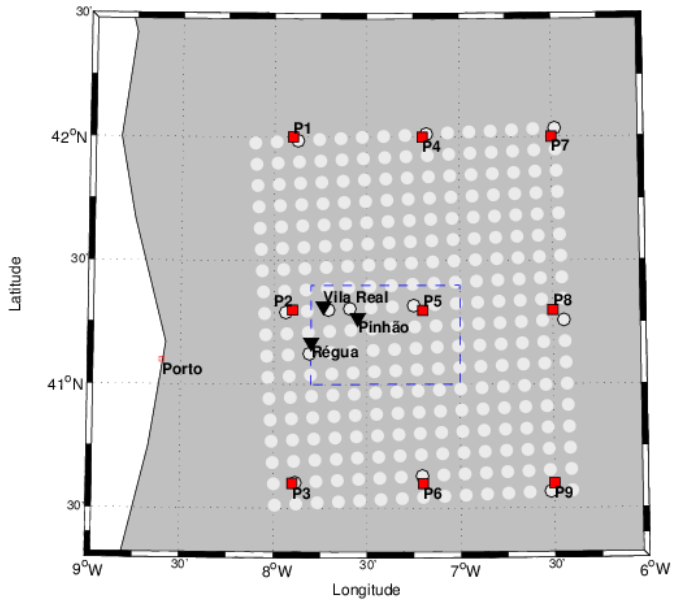

Figure 4 – Map of the Douro Valley sector (blue dashed box), including the 9 grid points of ERA-Interim reanalysis (red), the 270 grid points of the WRF model simulation (white, black border denotes the grid-points closer to ERA-Interim grid-points and stations) and the location of the meteorological stations of Vila Real, Pinhão and Régua (black triangles).

2.1 Observational data

Three meteorological stations situated in the Douro Valley are considered: Vila Real, Pinhão and Régua (Table 3, Figure 4 black triangles). This study uses surface observations of daily Tmax and Tmin, recorded at 2m, already used by Ramos et al. (2011), and from these time series mean temperatures (Tmean) are calculated as Tmax+Tmin/2. Daily time series of Tmax, Tmin and Tmean from the meteorological stations of Vila Real, Pinhão and Régua, respectively, are displayed in Figure 5 to Figure 7 for the period 1989-2006. The observations are from the Instituto Português do Mar e da Atmosfera (IPMA) and are available for the period 1941-2006. Daily Tmax above 45 º C and below 0 º C and daily Tmin above 30 º C are set as missing, to avoid erroneous outliers. The time period 1989-2006 common to the WRF model and reanalysis data is considered. According to the applied criteria,

Pinhão and Régua present 0.02 and 0.03% (Table 3) of missing values while Vila Real remains nearly complete.

Table 3 - Characteristics of the meteorological stations considered in the Douro Valley.

Station	Lat. (ºN)	Lon. (ºW)	Altitude. (m)	Missing days (Tmax)	Missing days (Tmin)
Vila Real	41.32	7.73	481	1	0
Pinhão	41.27	7.55	65	128	130
Régua	41.17	7.80	130	190	189

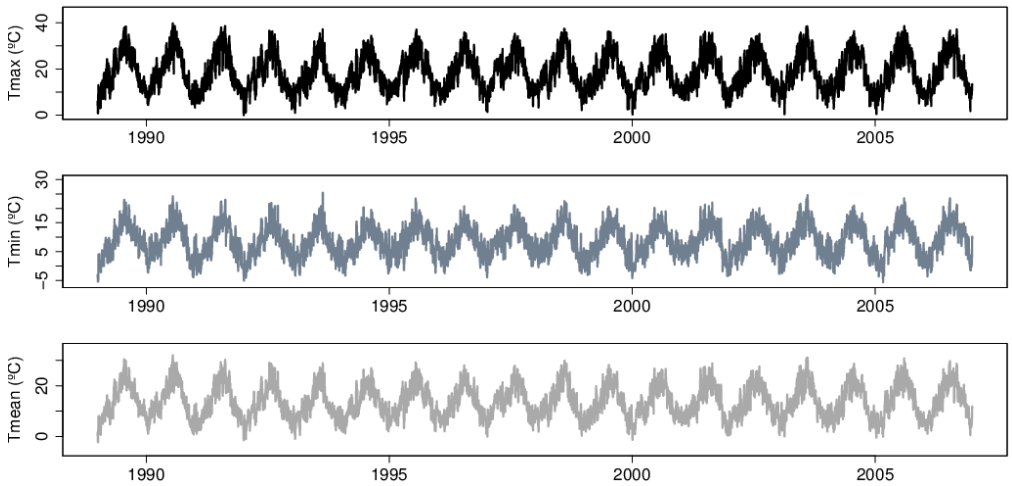

Figure 5 – Daily maximum (top), minimum (center) and mean (bottom) temperature of Vila Real meteorological station for the period 1989-2006.

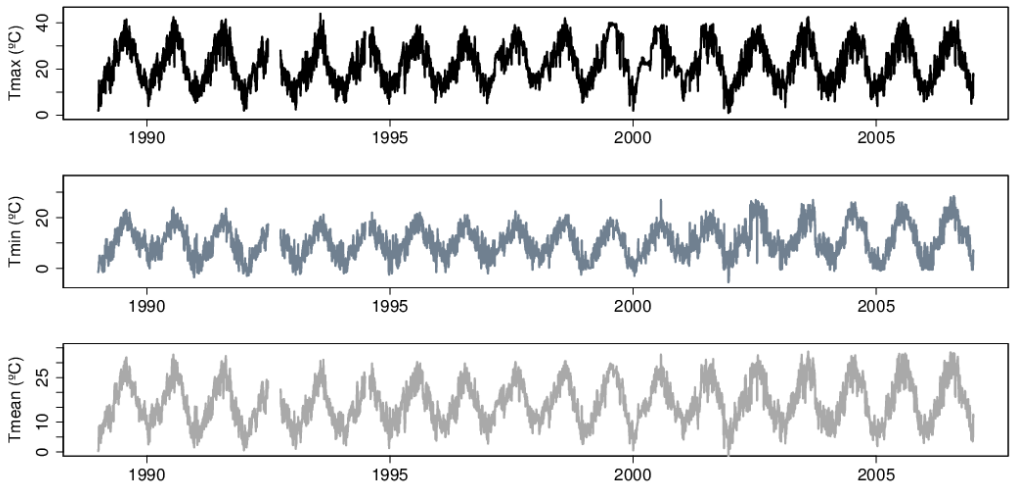

Figure 6 – Daily maximum (top), minimum (center) and mean (bottom) temperature of Pinhão meteorological station for the period 1989-2006.

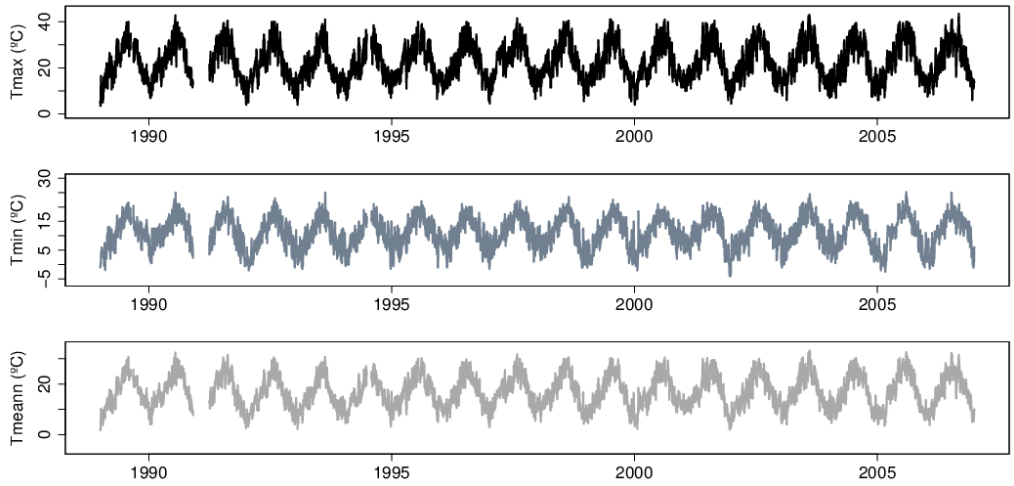

Figure 7 – Daily maximum (top), minimum (center) and mean (bottom) temperature Régua meteorological station for the period 1989-2006.

2.2 WRF and ERA-Interim reanalysis data

This work uses a high resolution simulation of the WRF model, at 9km of horizontal resolution for the period of 1989-2008 corresponding to 18x15 grid points (Figure 4 white circles). Soares et al. (2012) proposed a regional climate dataset for the Portuguese mainland based on the WRF model, with a horizontal grid of 9km resolution, with the aim to use WRF as an RCM. In their study, the version 3.1.1 of the WRF model was used to downscale ERA-Interim reanalysis through two nested grids, one with 27 km and another with 9km of resolution. The outermost grid of 27 km resolution was forced in its interior by grid nudging, performed every 6 h at all levels above the planetary boundary layer, in order to mitigate problems in the propagation of large-scale features through boundaries of the model. Initial and boundary conditions for this outer domain were derived from the ERA-Interim reanalysis. The innermost 9 km resolution grid was performed by one-way nesting defined as a finer grid resolution driven by the coarse grid output as initial and boundary conditions. In a simplistic form, the coarser grid was forced by the atmospheric reanalysis, and the finer grid was forced by the output of the coarser grid. Both grids are centered in the Iberian Peninsula and the 27 km resolution grid domain covers a relatively large ocean area to reduce spurious boundary effects in the 9 km resolution domain. The present work uses the results of the WRF high resolution simulation of minimum and maximum temperatures that were previously evaluated against observations (Soares et al., 2012). Both 27 km and 9 km resolutions showed an improvement relatively to ERA-Interim on the representation of these parameters, but the finer grid was found to be generally better.

The ERA-Interim reanalysis data used by Soares et al. (2012) were interpolated to a regular grid of 0.7º of spatial resolution for the period of 1989-2008, and the same reanalysis data is used in the present study including 3x3 grid points in the study region (Figure 4). The smooth topography of the WRF model and reanalysis (Figure 8) requires a correction of temperature associated with altitude

differences, here adjusted trough a constant lapse rate of 6ºC/km applied to both maximum and minimum temperatures (Soares et al., 2012). This correction is applied for both grid points of WRF and ERA-Interim reanalysis data.

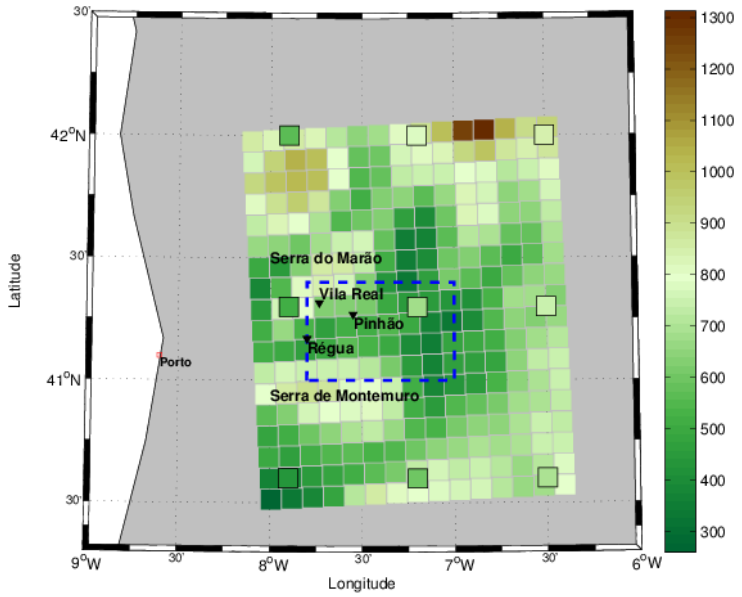

Figure 8 – Map of the Douro Valley (blue dashed box) and ERA-Interim reanalysis and WRF model topographies showing the western mountains of Marão and Montemuro.

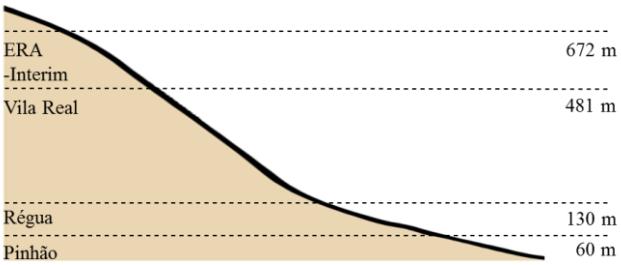

Figure 9 – Schematic illustration of the altitude of the meteorological stations and of the ERA-Interim grid-point centered in the Douro Valley.

Figure 8 highlights the western mountains of Marão and Montemuro, which limit and shield the Douro Valley, the sixth and eighth higher elevations of Portugal, respectively. Since it is located in a less mountainous area than the closest grid-point, the ERA-Interim grid-point centered in the Douro Valley is considered henceforth for the analysis. The ERA-Interim closest grid-point is situated neighboring to Serra do Marão (Figure 8) becoming more difficult to represent local temperature due to the complex topography. The complex terrain of the Douro Valley makes the three meteorological stations network very distinct in altitudes with emphasis to Pinhão which is at very low altitude (Figure 9). The altitude of the ERA-Interim grid-point centered in the Douro Valley (672 m) is above all stations being closer to the altitude of Vila Real.

Figure 10 shows daily Tmax, Tmin and Tmean orography-corrected time series of reanalysis at the grid-point centered in the Douro Valley (Figure 4) for the available period 1989-2008. The same data for the WRF grid-point nearest to station of Vila Real is graphed in Figure 11 and both figures show similar seasonal cycles.

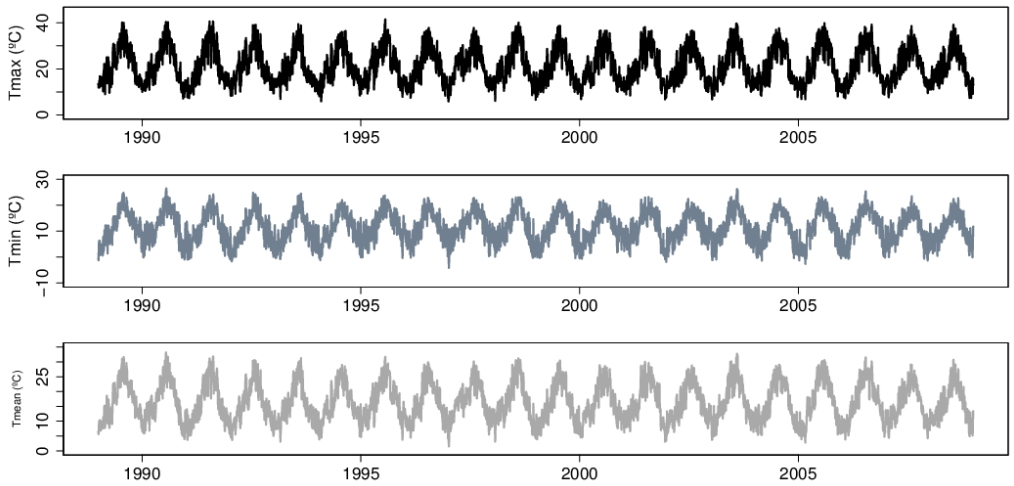

Figure 10 – Daily time series maximum (top), minimum (center) and mean (bottom) temperature of the ERA-Interim grid point within the Douro Valley (P5) for the period 1989-2008.

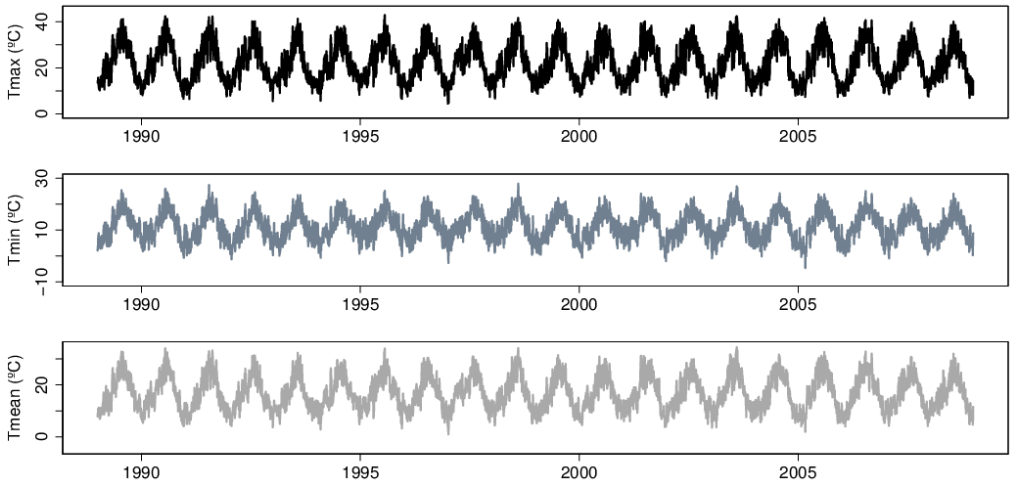

Figure 11 – Daily time series maximum (top), minimum (center) and mean (bottom) temperature of the WRF model grid point closer to Vila Real for the period 1989-2008.

Considering the available time period of observational data (1989-2006), WRF model and reanalysis data (1989-2008), the common period of 1989-2003 is considered for model calibration. The data for the period 2004-2006 are not used in the modeling stage being only used afterwards for validation purposes. Henceforth the 1989-2003 calibration period is considered.

2.3 Seasonal decomposition

As a pre-processing step in the analysis of temperature data, a time series decomposition is performed based on the STL method, the Seasonal-Trend decomposition procedure based on Loess and implemented in the R-package *stl*. The STL algorithm is based on locally-weighted regression, or loess (Cleveland et al., 1990), a robust method for curve estimation enabling STL to perform rather well even in the case of extreme observations and/or outliers. STL makes use of two smoothing parameters, one for the trend component and another for seasonality which controls how the seasonal component can change in time. Figure 12 illustrates the result of STL decomposition for Tmax at Vila Real using a seasonal smoothing parameter of 365 days. The time series (top) is decomposed from top to bottom into seasonal and trend components, and a remainder component corresponding to the residual variation of the data that is not modeled as seasonal or trend components. The STL decomposition implemented in the R-package *stl* requires time series with no missing values therefore gaps in observational records are replaced by interpolated values according to the algorithm of Stineman (1980) implemented in the R-package *stinepack*. After the decomposition, the interpolated values are again set as missing, and thus the resulting component time series have the same missing values as the original record.

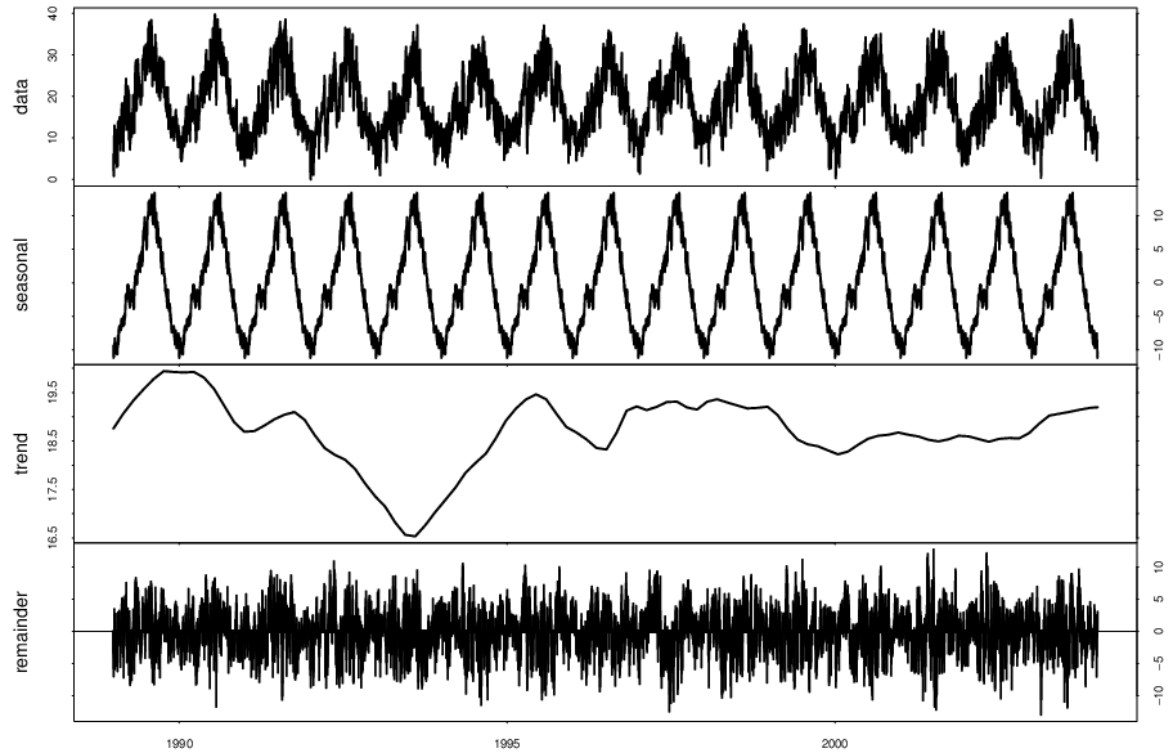

Figure 12 – STL decomposition of the Vila Real maximum temperatures time series using a seasonal smoothing parameter of 365 days for the calibration period 1989-2003. From top to bottom: station records, seasonal component, trend component and remainder. The units on the vertical scales are in ºC.

2.3.1 Seasonal cycle

The mean seasonal cycle of temperature time series is obtained by averaging each calendar day over the whole 1989-2003 period and is shown for the three meteorological stations, the reanalysis grid-point centered in the Douro Valley and the WRF model closest points in Figure 13. The mean seasonal cycle shows similar behavior for the three meteorological stations with Pinhão exhibiting slightly higher temperatures during summer.

The non-averaged seasonal cycle of Tmax, Tmin and Tmean resulting from the STL decomposition is shown for Vila Real in **Erro! A origem da referência não foi encontrada.**. The amplitude of the seasonal cycle is slightly larger for Tmax and Tmean than Tmin, and all seasonal cycles are apparently in phase. Annual amplitudes are computed as the difference between the maximum and the minimum of seasonal component for each calendar year and are approximately constant over the period 1989-2003.

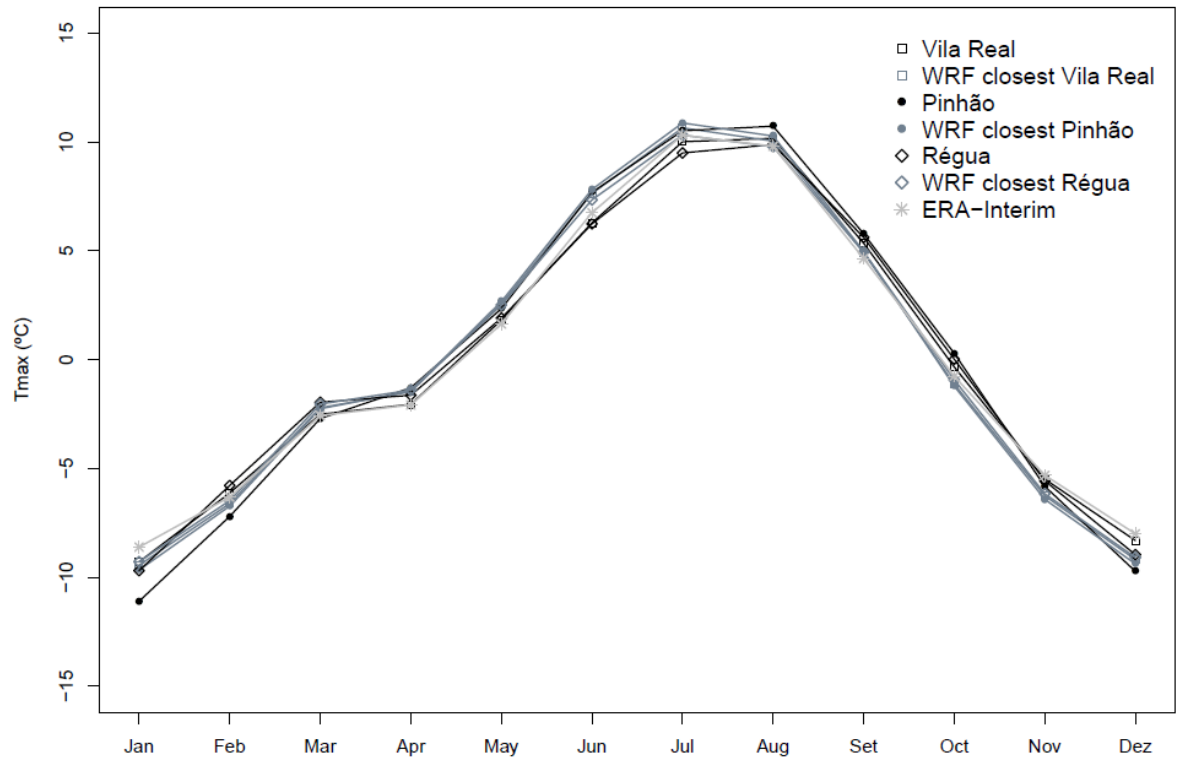

Figure 13 – Tmax mean seasonal cycle of the meteorological stations records (black), reanalysis grid-point centered in the Douro Valley (gray) and WRF closest point (slate gray) of Tmax (top) Tmin (center) and Tmean (bottom) for the calibration period 1989-2003.

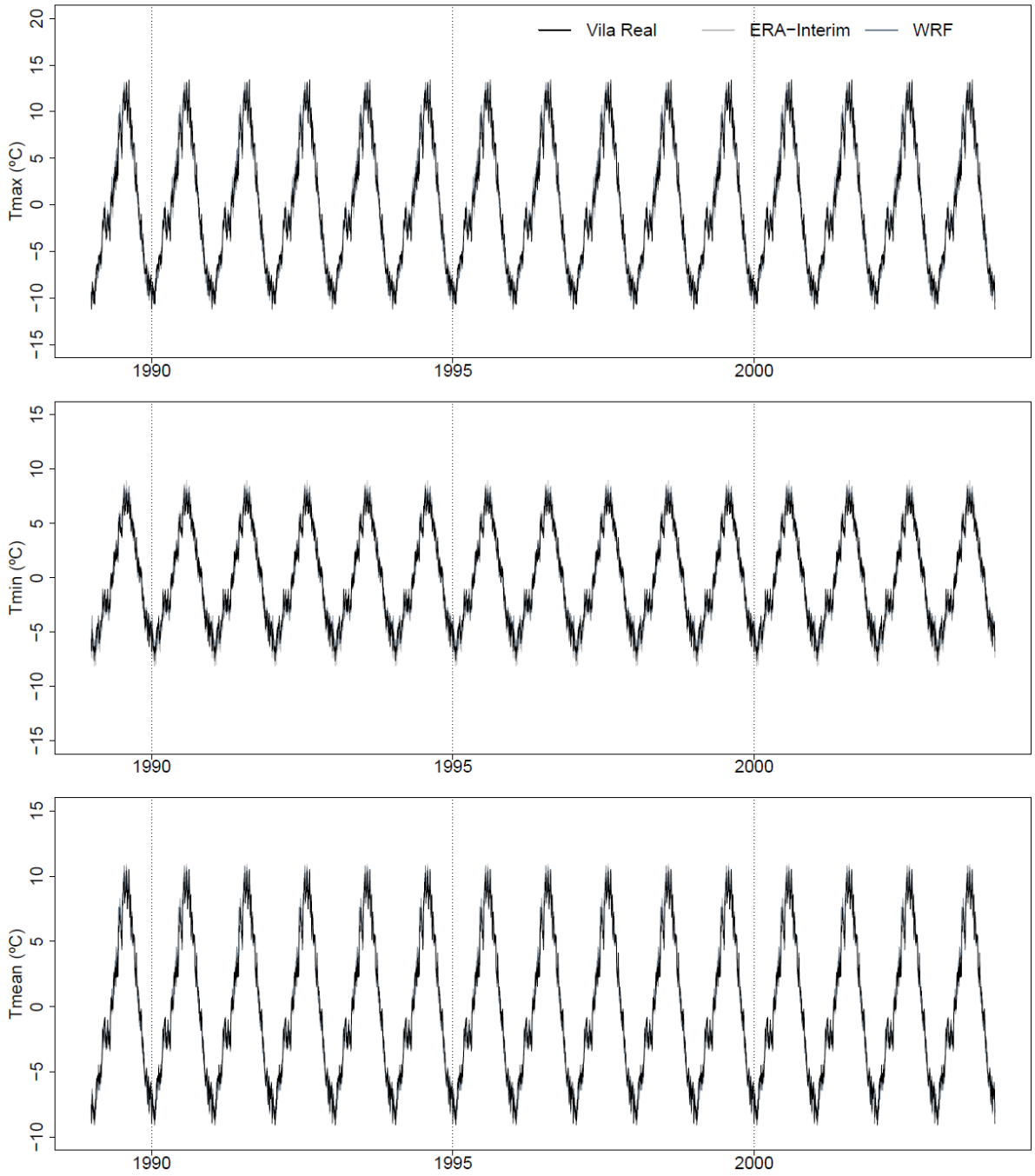

Figure 14 - Seasonal component of the Vila Real station records (black), reanalysis grid-point centered in the Douro Valley (gray) and WRF closest point (slate gray) of Tmax (top) Tmin (center) and Tmean (bottom) for the calibration period 1989-2003.

2.3.1 Seasonal adjustment

Seasonally adjusted temperature time series are obtained by removing the seasonal component derived by STL (previous section) and are shown for the Vila Real station in Figure 15. Seasonal adjustment is a crucial step before any regression analysis when the interest of the study is not on the seasonal cycle. Considering that the seasonal cycle is approximately constant trough the calibration period (Figure 13) only seasonally adjusted time series are considered in the analysis hereafter (Figure 15).

The bias between the seasonally-adjusted time series of the WRF model grid-cell and the observations are illustrated for the daily Tmin in Figure 16 for the calibration period 1989-2003. Generally the higher biases correspond to steeper topography areas (Figure 8, section 2.1) and the grid-points around the stations have smaller biases. Correlations and bias of seasonally-adjusted station data and the reanalysis grid-point centered in the Douro Valley and WRF closest point are shown in Table 4. Pinhão exhibits weaker correlations than the other stations possibly due to local effects not reproduced by the models. Both WRF and ERA-Interim seasonally adjusted time series tend to display higher bias at Vila Real, the station with highest altitude. At Pinhão and Régua WRF displays the smaller biases.

Table 4- Bias and correlation of seasonally-adjusted station data, ERA-Interim grid-point centered in the Douro Valley and WRF nearest points (confidence intervals in parenthesis).

Station/Point	ERA-Interim			WRF		
	Variable (ºC)	Correlation	Bias (ºC)	Variable (ºC)	Correlation	Bias (ºC)
Vila Real	Tmax	0,79 (0,78-0,80)	2,71	Tmax	0,77 (0,76-0,78)	3,61
	Tmin	0,81 (0,80-0,82)	2,80	Tmin	0,83 (0,82-0,84)	2,80
	Tmean	0,86 (0,70-0,73)	2,76	Tmean	0,84 (0,83-0,85)	3,20
Pinhão	Tmax	0,63 (0,61-0,64)	-1,23	Tmax	0,62 (0,60-0,63)	-0,20
	Tmin	0,64 (0,62-0,65)	1,07	Tmin	0,58 (0,57-0,60)	0,86
	Tmean	0,72 (0,71-0,73)	-0,08	Tmean	0,68 (0,67-0,69)	0,33
Régua	Tmax	0,77 (0,76-0,78)	-1,02	Tmax	0,76 (0,75-0,78)	0,14
	Tmin	0,80 (0,79-0,80)	0,31	Tmin	0,72 (0,71-0,73)	-0,15
	Tmean	0,84 (0,83-0,84)	-0,36	Tmean	0,80 (0,79-0,81)	-0,01

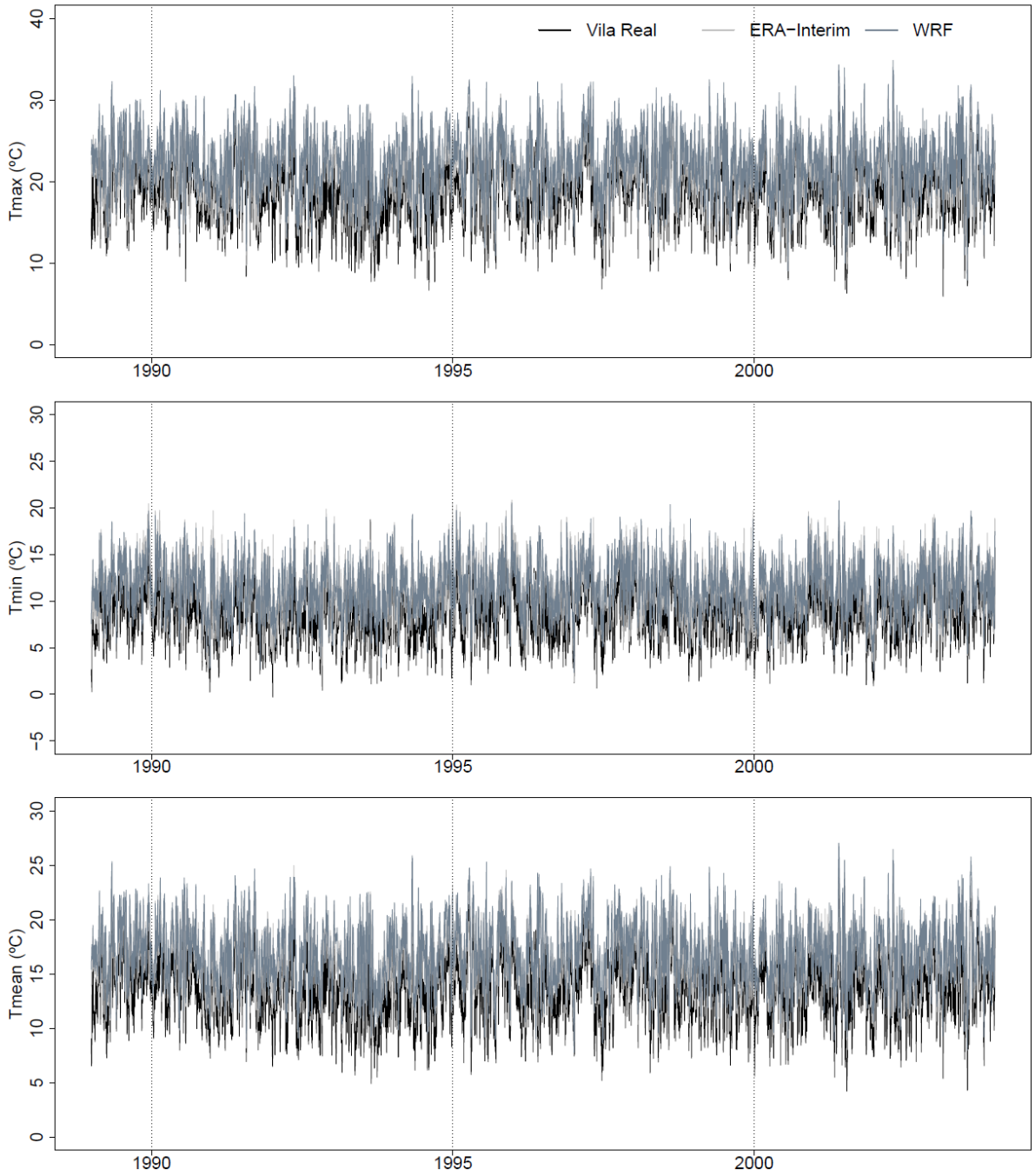

Figure 15 – Seasonally adjusted time series of the Vila Real station records (black), reanalysis grid-point centered in the Douro Valley (gray and WRF closest point (slate gray) of Tmax (top) Tmin (center) and Tmean (bottom) for the calibration period 1989-2003.

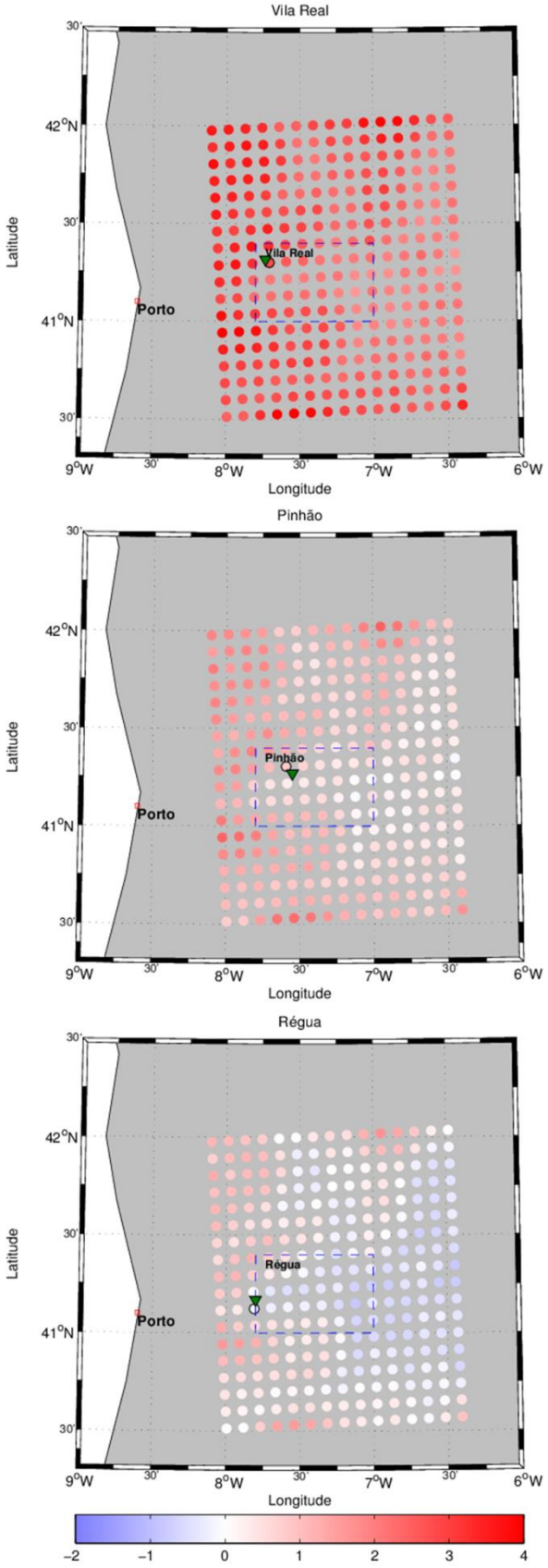

Figure 16 - Bias between the seasonally-adjusted daily Tmin time series of the WRF grid-cell (circles) and the observations for the calibration period (1989-2003). Map of the Douro Valley (blue dashed box) and meteorological stations location (triangles).

3. Methods

An overview of the main steps of the applied downscaling methodology (Figure 17) is presented in this section. The statistical downscaling procedure starts from the seasonally-adjusted time series of the three stations records, of the ERA-Interim grid-point centered in the Douro Valley and of the closest grid-points of the WRF model. The seasonal cycle is assumed to be approximately the same at the station and the considered grid-points (see section 2.3.1) and is added after the downscaling to the simulated time series.

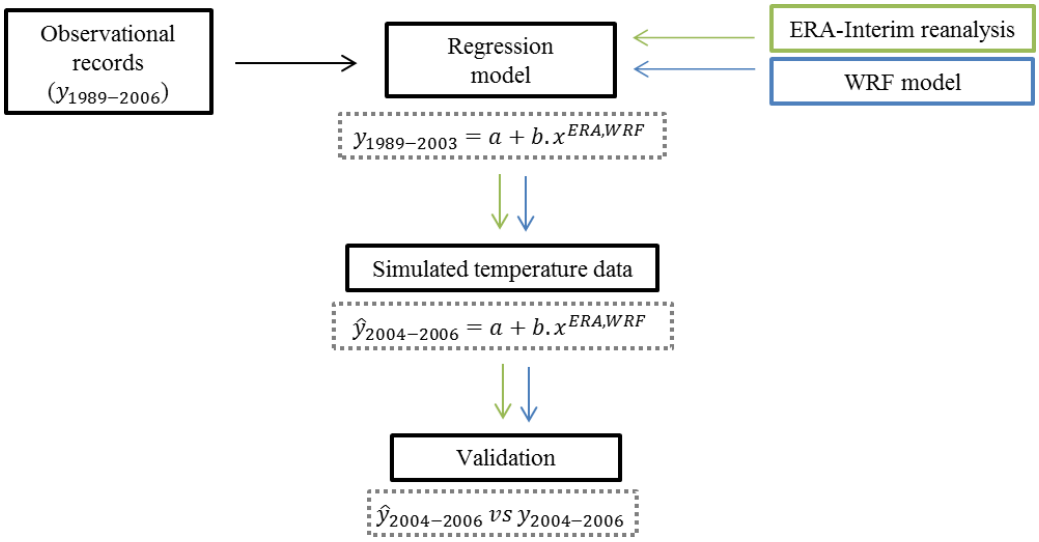

Figure 17 – Schematic overview of the applied downscaling methodology.

The relationship between the reanalysis/WRF model data and observational data is established during the calibration period (1989-2003) for Tmax, Tmin and Tmean. The statistical relationship is subsequently used on the reanalysis/WRF model data during the validation period (2004-2006) to obtain local temperature estimates for subsequent agronomical applications. The local simulated temperature data is then evaluated to the observations.

Statistical downscaling of temperature to the stations points is based on regression methods. The ordinary linear regression is first considered (section 3.1). Robust regression (section 3.2) is then applied in order to reduce the impact of eventual outliers in regression results. To evaluate the statistical downscaling, four statistical accuracy measures are used: the bias, the roots mean squared error (RMSE), the mean absolute error (MAE) and the mean absolute percentage error (MAPE) (Table 5).

Table 5- Bias, root-mean squared error (RMSE), mean absolute error (MAE) and mean absolute percentage error (MAPE) equations with $\hat{y}$ representing the downscaled temperatures, y the observations and *N* is the number of records.

Error	Equation
BIAS	$\frac{1}{N}\sum(\hat{y}-y)$
RMSE	$\sqrt{\frac{1}{N}\sum(\hat{y}-y)^2}$
MAE	$\frac{1}{N}\sum\lvert\hat{y}-y\rvert$
MAPE	$\frac{1}{N}\sum\left\lvert\frac{\hat{y}-y}{y}\right\rvert\times 100\%$

As a final step, the downscaled temperature data are used for assessing the climatic potential of the Douro Wine Region to vine growing. The climate assessment is performed based on the following bioclimatic indices (see Table 1): GDD (Growing degree-days), GST (Average growing season temperature), LGS (Length growing season), HI (Heliothermal Index of Huglin) and CI (Cool night index).

3.1 Ordinary linear regression

Ordinary linear regression methods are very common in many branches of geophysical data analysis (e.g. Helsel and Hisch, 2002). Recalling the generic functional relationship (Eq. (1), section 1.3), in the present study, let *y* represent the observational station records, *x* represent the reanalysis or regional model data, and the error *ε* be the difference between the observed value of *y* and the linear model estimates. The functional relationship of Eq. (1) can be described by a simple linear regression model as:

$$y_i = \alpha + \beta x_i + \varepsilon_i \qquad i = 1,2,\dots,n \qquad (2)$$

where α is the intercept and β is the slope of the regression line, usually called regression coefficients. The errors are assumed to be uncorrelated, to have mean zero and variance $\sigma_\varepsilon{}^2$, and to follow a normal distribution such that $\varepsilon \sim N(0, \sigma_\varepsilon{}^2)$.

The method of ordinary least squares (OLS) is a common statistical tool to estimate the regression coefficients by minimizing the sum of the squared differences between the observations and the regression line:

$$min\sum_{i=1}^{n}(y_i - x_i\beta)^2 = min\sum_{i=1}^{n}(\varepsilon_i)^2 \qquad (3)$$

In matrix notation eq. (2) can be written as:

$$\boldsymbol{y} = \boldsymbol{X\beta} + \boldsymbol{\varepsilon} \tag{4}$$

where $\boldsymbol{y}$ is an $n \times 1$ vector of observations, $\boldsymbol{X}$ an $n \times p$ matrix of regression variables, $\boldsymbol{\beta}$ an $p \times 1$ vector of regression coefficients, and $\boldsymbol{\varepsilon}$ an $n \times 1$ vector of random errors. The ordinary least squares (OLS) estimator of $\boldsymbol{\beta}$ is then given by:

$$\widehat{\boldsymbol{\beta}} = (\boldsymbol{X}^T\boldsymbol{X})^{-1}\boldsymbol{X}^T\boldsymbol{y}. \tag{5}$$

3.2 Robust regression

Ordinary least squares (OLS) assume that the errors are normally distributed, and thus it is not robust to eventual outliers present in the data. In such circumstances, robust regression is a good alternative since it gives less weight to outliers, reducing their influence on the estimated model (e.g. Hampel, 1986).

A robust regression M-estimator minimizes the sum of the objective function ρ instead of minimizing the sum of the squared residuals:

$$min \sum_{i=1}^{n} \rho(y_i - x_i\beta) = min \sum_{i=1}^{n} \rho(\varepsilon_i) \tag{6}$$

where the objective function ρ gives the contribution of each residual (for OLS regression $\rho(\varepsilon_i) = {\varepsilon_i}^2$). The estimating equations can be written as:

$$\sum_{i=1}^{n} \omega_i(y_i - x_i\beta)x_i = 0 \tag{7}$$

where ω_i is a weight function.

The M-estimation is performed by the Huber's method (Huber, 1981) using the *rlm()* command in the *MASS* R-Package. Since residuals cannot be found until the model is fitted, an iterative procedure is necessary. As a result, iteratively reweighted least squares are used:

1. Ordinary least squares (OLS) is fitted in order to find estimates of the regression coefficients.
2. The residuals are extracted and used to calculate initial estimates for the weights.
3. A weight function is solved for the initial OLS residuals.
4. Weight least squares (WLS) estimates of the regression coefficients are obtained as:

$$\widehat{\boldsymbol{\beta}} = (\boldsymbol{X^T W X})^{-1} \boldsymbol{X^T W y} \quad (8)$$

where $\boldsymbol{W}$ is an $n \times p$ matrix of weights.

5. New weights are calculated and used in the next iteration for a new estimate of the regression coefficients.
6. Steps 4 and 5 are repeated until the estimated coefficients converge.

4. Results

The following section presents the statistical downscaling of the ERA-Interim reanalysis and of the WRF model data to the Douro Valley weather stations of Vila Real, Pinhão and Régua. The regression-based statistical models are established during the calibration period (1989-2003) to infer the statistical relationship that will be applied to the local estimation of temperature during the validation period (2004-2006). Local temperature data is obtained and compared with the local observations recorded at the meteorological stations. Differences on the performance of the applied regression methods (see section 3) are discussed, and the difference between the statistical downscaling performed by ERA-Interim and by WRF model is addressed. The seasonal dynamics of the downscaled temperature data is discussed as well. Statistical downscaling is also evaluated in order to assess if there is any systematic difference in performance of the methods between the weather stations, since topographic signatures may be a key factor in temperature data modeling.

4.1 Statistical downscaling of ERA-Interim reanalysis

The assessment of the statistical relationship between the seasonally adjusted time series of the meteorological stations and the ERA-Interim reanalysis is first presented based on least squares and robust regression for the calibration period (1989-2003). The results are illustrated for the daily Tmax (Figure 18). The three different regression lines obtained from each regression technique show how the ordinary least squares method can be influenced by outlier observations, standing out an apparent fit improvement in robust regression lines.

The model coefficients (Table 6) show that robust regression slopes are always higher than ordinary least squares slopes. The coefficient of determination R^2 (Table 6) indicates that the ordinary least squares models explain more than 50% of the local temperature variation except at Pinhão (Tmax and Tmin). The strongest linear relationship is exhibited by the Tmean and the best fit is achieved at Vila Real reaching 75% of the temperature variability explained by the model.

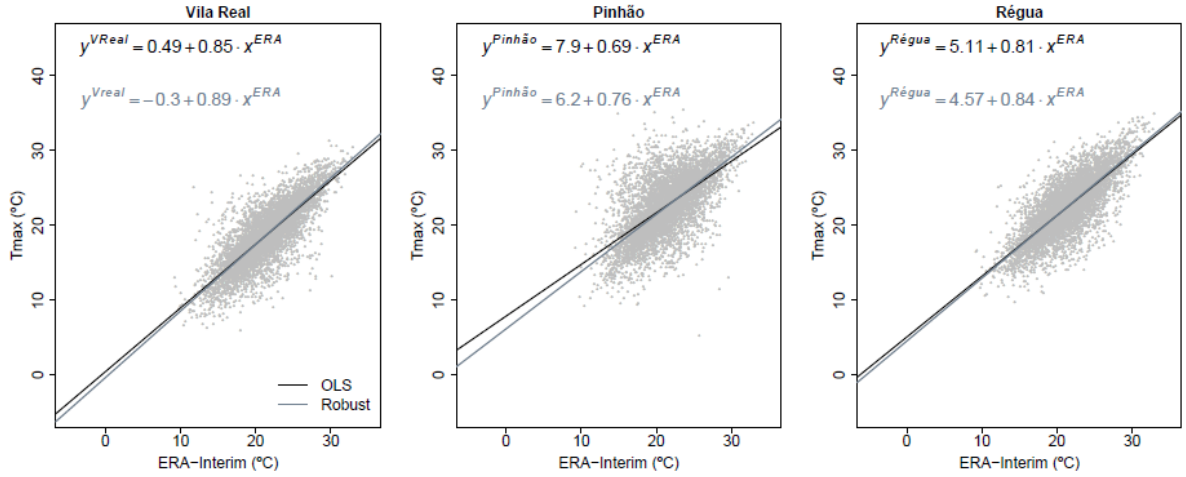

Figure 18 – Scatter diagrams of daily Tmax station records against ERA-Interim for the calibration period 1989-2003. Regression lines are obtained by ordinary least squares (black) and robust regression (gray).

Table 6 - Least squares (OLS) and robust regression model coefficients.

Station	Variable	Slope (ºC)		R^2 (%)
		OLS	Robust	
Vila Real	Tmax	0,85	0,89	63
	Tmin	0,83	0,85	66
	Tmean	0,96	0,99	75
Pinhão	Tmax	0,69	0,76	39
	Tmin	0,70	0,74	40
	Tmean	0,76	0,79	52
Régua	Tmax	0,81	0,84	60
	Tmin	0,78	0,79	64
	Tmean	0,83	0,84	70

Diagnostic plots are performed for all regression models and are illustrated for the daily Tmax at Vila Real in Figure 19. The residuals present some deviations from the normal distribution but have a mean close to zero and the scale location plots show that variance slightly decreases. The Cook's distance plot, a measure of how much influence a single observation has in the model, shows that the robust model significantly reduces the influence of outliers in the estimated regression line.

The statistical relationship set by the regression coefficients (Table 6) is then used on the seasonally-adjusted daily reanalysis data for the validation period (2004-2006) to obtain local temperature estimates. Figure 20 shows the bias between observations and ERA-Interim in comparison with the bias between observations and the statistically downscaled time series by ordinary least squares and robust regression. The bias between ERA-Interim and observations is significantly reduced using both regression-based downscaling methods, mostly below 1ºC and above -1ºC, except at Pinhão (Tmin). In general robust and ordinary least squares give similar results.

The overall performance of the statistical downscaling by ordinary least squares and robust regression applied to the seasonally-adjusted time series is also summarized in Table 7. The RMSE, MAE and

MAPE values indicate a good performance by the downscaled time series at Vila Real and Régua. Indeed, the MAPE of the statistically-downscaled Tmin at Vila Real, the station with the highest coefficient of determination, is reduced to half the value given by ERA-Interim. Hereafter results are presented only for ordinary least squares since the difference between the two regression-based downscaling methods is negligible.

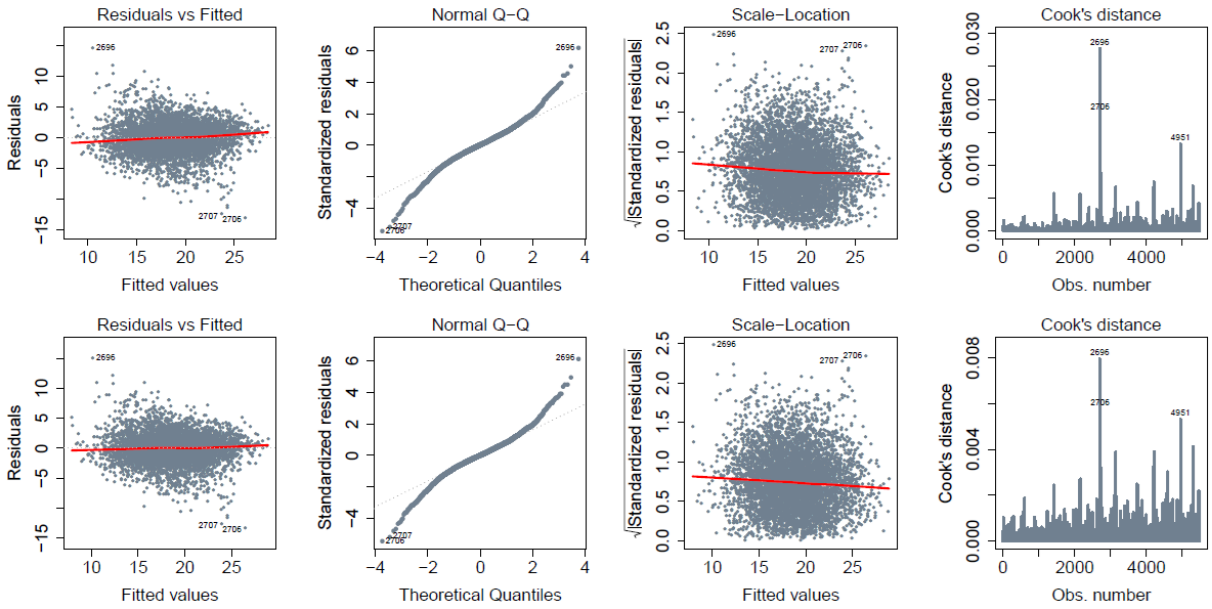

Figure 19 – Residual plots of daily Tmax at Vila Real for ordinary least squares (top) and robust regression (bottom).

After the statistical downscaling of the seasonally-adjusted time series, the seasonal cycle (see section 2.3) of the ERA-Interim time series for the validation period 2004-2006 is added to the respective simulated time series. The bias of the ERA-Interim and the downscaled time series for Tmax is illustrated in Figure 21. The statistical downscaling considerably improves the ERA-Interim performance in representing the temperature data. In fact the ERA-Interim bias at Vila Real is reduced by approximately two degrees. At Régua and Pinhão the bias of the two time series are very similar but the downscaled temperature data display biases closer to zero.

Table 8 summarizes the errors found for daily statistical downscaling time series based on ordinary least squares after adding the seasonal cycle. Similarly to seasonally-adjusted time series (Table 7) the MAPE at Vila Real is reduced to about half the value reproduced by ERA-Interim. The RMSE and MAE of the downscaled time series only exceed 3ºC at Pinhão (Tmin) and Régua (Tmax). Generally a good improvement is found in the downscaled time series based on ERA-Interim concluding that the linear approximations applied to the original series of ERA-Interim are suited to the observations. However, at Pinhão (Tmin) the ERA-Interim displays lower errors than the downscaled time series. The lack of improvement of the statistical downscaling at Pinhão may be a result of the weak linear relationship estimated by the regression model (Table 6).

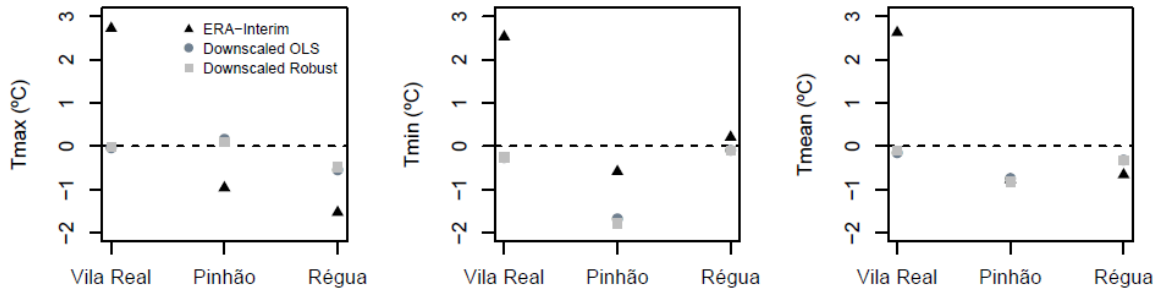

Figure 20 - Bias of the seasonally-adjusted time series of ERA-Interim and the downscaled time series based on ordinary least squares (OLS) and robust regression.

Table 7- Root mean squared error (RMSE), mean absolute error (MAE) and mean absolute percentage error (MAPE) of the seasonally-adjusted time series of ERA-Interim and the downscaled time series by ordinary least squares (OLS) and robust regression.

Vila Real

	Variable (ºC)	ERA-Interim	Downscaled (OLS)	Downscaled (Robust)
RMSE (ºC)	Tmax	3,66	2,38	2,39
	Tmin	2,96	1,51	1,51
	Tmean	3,00	1,45	1,44
MAE (ºC)	Tmax	3,04	1,87	1,88
	Tmin	2,62	1,19	1,19
	Tmean	2,67	1,15	1,15
MAPE (%)	Tmax	17,55	10,37	10,42
	Tmin	34,05	14,22	14,19
	Tmean	21,00	8,64	8,60

Pinhão

	Variable (ºC)	ERA-Interim	Downscaled (OLS)	Downscaled (Robust)
RMSE (ºC)	Tmax	2,62	2,35	2,34
	Tmin	2,05	2,47	2,56
	Tmean	1,74	1,73	1,77
MAE (ºC)	Tmax	2,09	1,88	1,87
	Tmin	1,64	2,03	2,12
	Tmean	1,39	1,40	1,43
MAPE (%)	Tmax	9,20	8,66	8,56
	Tmin	14,09	16,30	17,05
	Tmean	7,97	7,95	8,07

Régua

	Variable (ºC)	ERA-Interim	Downscaled (OLS)	Downscaled (Robust)
RMSE (ºC)	Tmax	3,13	2,68	2,68
	Tmin	1,67	1,54	1,55
	Tmean	1,71	1,56	1,57
MAE (ºC)	Tmax	2,52	2,14	2,14
	Tmin	1,31	1,21	1,21
	Tmean	1,36	1,24	1,24
MAPE (ºC)	Tmax	10,72	9,36	9,37
	Tmin	12,34	11,28	11,29
	Tmean	7,89	7,26	7,27

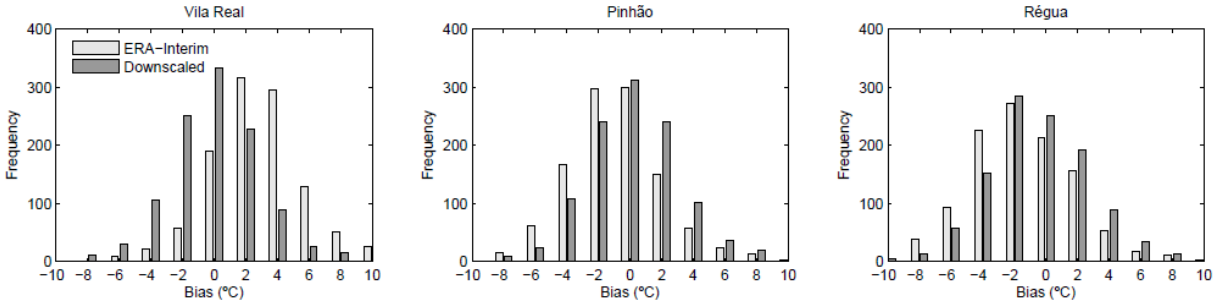

Figure 21 – Bias histograms of the Tmax downscaled time series based on ordinary least squares (gray) and of the ERA-Interim (white).

Table 8- Root mean squared error (RMSE), mean absolute error (MAE) and mean absolute percentage error (MAPE) of the ERA-Interim and the downscaled time series based on ordinary least squares.

Vila Real

	Variable (ºC)	ERA-Interim	Downscaled
RMSE (ºC)	Tmax	4,00	2,87
	Tmin	3,26	2,04
	Tmean	3,18	1,80
MAE (ºC)	Tmax	3,25	2,18
	Tmin	2,77	1,62
	Tmean	2,74	1,41
MAPE (ºC)	Tmax	28,30	18,34
	Tmin	91,22	54,36
	Tmean	38,31	18,17

Pinhão

	Variable (ºC)	ERA-Interim	Downscaled
RMSE (ºC)	Tmax	3,20	2,98
	Tmin	2,91	3,22
	Tmean	2,37	2,36
MAE (ºC)	Tmax	2,49	2,32
	Tmin	2,35	2,61
	Tmean	1,88	1,89
MAPE (ºC)	Tmax	13,85	13,76
	Tmin	79,00	65,74
	Tmean	14,04	14,06

Régua

	Variable (ºC)	ERA-Interim	Downscaled
RMSE (ºC)	Tmax	3,62	3,24
	Tmin	2,02	1,92
	Tmean	2,08	1,95
MAE (ºC)	Tmax	2,92	2,59
	Tmin	1,56	1,49
	Tmean	1,66	1,56
MAPE (ºC)	Tmax	14,92	13,70
	Tmin	31,01	29,74
	Tmean	11,70	11,09

4.2 Statistical downscaling of WRF model data

The following section considers temperature daily data of a high resolution simulation of the WRF model at 9km of horizontal resolution which derives from a dynamical downscaling based on ERA-Interim reanalysis performed by Soares et al. (2012) (see section 2.1). In Figure 22 the previous statistical downscaling of ERA-Interim (section 4.1.1) is compared to the dynamical downscaling of the WRF model at the grid-points closest to the meteorological stations for the validation period 2004-2006. The correlation between the observations and the ERA-Interim downscaled values is higher at Régua and Pinhão, while at Vila Real the dynamically downscaled WRF series are more correlated with observations.

Here the WRF dynamical downscaling is combined with statistical downscaling by performing the statistical downscaling of the WRF model data to weather stations points. Similarly to the downscaling performed in section 4.1.1, the assessment of the statistical relationship between the seasonally adjusted time series of the three stations and the WRF model is first presented on least squares and robust regression for the calibration period (1989-2003). The obtained model coefficients are shown in Table 9. Similarly to Table 6 robust regression slopes are always higher than ordinary least squares slopes, but all slopes are lower than those displayed by the regression models based on ERA-Interim.

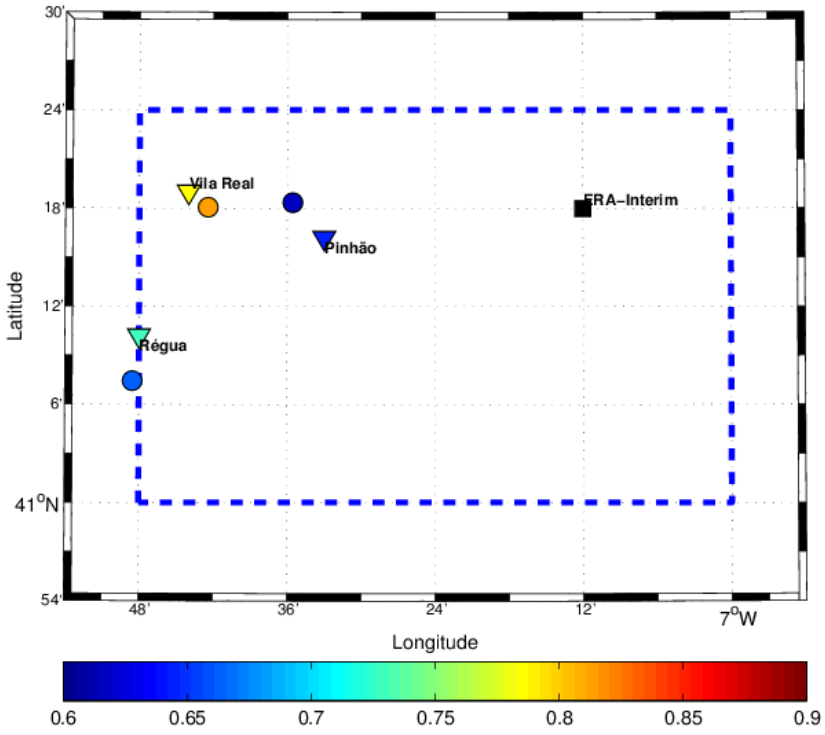

Figure 22 – Map of the Douro Valley (blue dashed box) and correlations of the seasonally-adjusted daily Tmin time series of the WRF model (circles) and the statistically downscaled ERA-Interim time series (triangles) for the validation period (2004-2006).

Table 9 - Least squares (OLS) and robust regression model coefficients.

Station	Variable	Slope (ºC)		R^2 (%)
		OLS	Robust	
Vila Real	Tmax	0.80	0.84	59
	Tmin	0.88	0.90	69
	Tmean	0.88	0.91	70
Pinhão	Tmax	0.66	0.74	38
	Tmin	0.66	0.68	34
	Tmean	0.68	0.71	46
Régua	Tmax	0.78	0.81	59
	Tmin	0.70	0.71	52
	Tmean	0.74	0.75	63

A comparison between Table 9 and Table 6 indicates that ordinary least squares models based on WRF model data exhibit weaker linear relationships than ERA-Interim, except at Vila Real (Tmin). Vila Real presents the best fit reaching 70% of the temperature variability explained by the regression model based on WRF model data. Similarly to the ordinary least squares models of ERA-Interim the strongest linear relationship is displayed by Tmean.

Diagnostic plots have been performed for all models and the residuals behave similarly as described in the previous section.

Local temperature estimates are obtained based on the regression coefficients (Table 9) applied to the seasonally-adjusted daily WRF data for the validation period (2004-2006). At Vila Real, statistical downscaling significantly reduces WRF bias using both regression methods (Figure 23), to values as low as for the statistical downscaling based on ERA-Interim. Similarly to Figure 20, most bias of downscaled time series are below 1ºC and above -1ºC, except at Pinhão (Tmin). Ordinary least squares and robust regression still give similar results.

The seasonal cycle (section 2.3) obtained for the validation period of the daily data of the WRF model is afterwards added to the respective simulated time series. The results are only presented for the ordinary least squares regression since no outstanding improvement was found using robust regression. Figure 24 illustrates the bias of the WRF model and of the statistical downscaled time series of Tmax. Similar to Figure 21, the large bias displayed by WRF model at Vila Real is quite apparent and considerably improved by the statistical downscaling. At Pinhão the bias is also reduced by the statistical downscaling, while at Régua the WRF dynamical downscaling displays lower bias.

The RMSE, MAE and MAPE values also indicate a good performance by the downscaled time-series based on WRF (Table 10). Despite the fact that WRF model at 9km of resolution is already a RCM, the regression models are crucial in further reducing errors in the WRF data, emphasizing the added value of combining dynamical and statistical downscaling. In fact, at Vila Real the MAPE is reduced to over half the value reproduced by the WRF model, and the RMSE and MAE values of the Tmin are lower than the statistical downscaling of ERA-Interim. However, at Pinhão (Tmin and Tmean) the

WRF dynamical downscaling displays lower RMSE and MAE values than the downscaled time series, similarly to what was found in the statisitcal downscaling of ERA-Interim. A possible explanation for the no visible improvement of both statistical downscaling of ERA-Interim and WRF at Pinhão, might be related to the low percentage of temperature variability explained by the regression models (below 50% in most cases).

A comparison between the ERA-Interim and WRF downscaled time series at the seasonal scale is illustrated in Figure 25. In terms of seasonal scale the statistically-downscaled temperature data performance is remarkable and much more consistent with observations than the original ERA-Interim and WRF data. Generally both ERA-Interim and WRF data indicate warmer conditions at Vila Real, with WRF warmer than ERA-Interim, while at Pinhão and Régua the ERA-Interim data underestimates the observations. The median quantile is greatly improved by the statistically-downscaled data with a minor improvement during the winter season. Vila Real is the weather station most enhanced by the statistical downscaling of both ERA-Interim and WRF model data. However, the improvement of the seasonal dynamics towards a quite good temperature representation by the downscaled time series during the growing season, at all meteorological station locations, shows the added value of the statistical downscaling in agronomic applications.

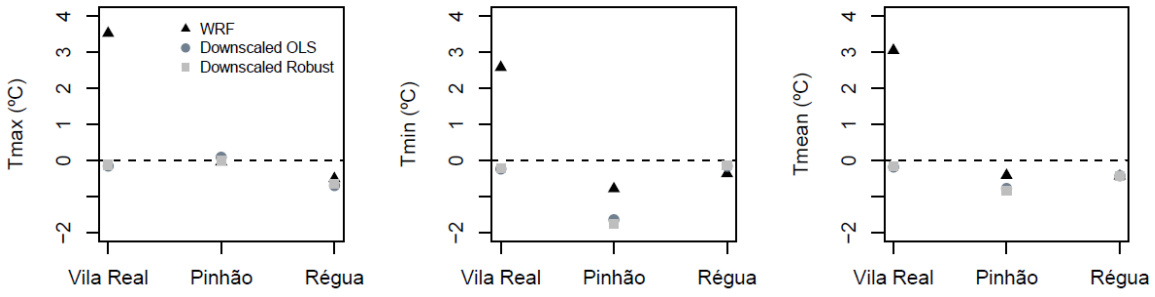

Figure 23 - Bias of the seasonally-adjusted time series from the WRF model data and the downscaled time series.

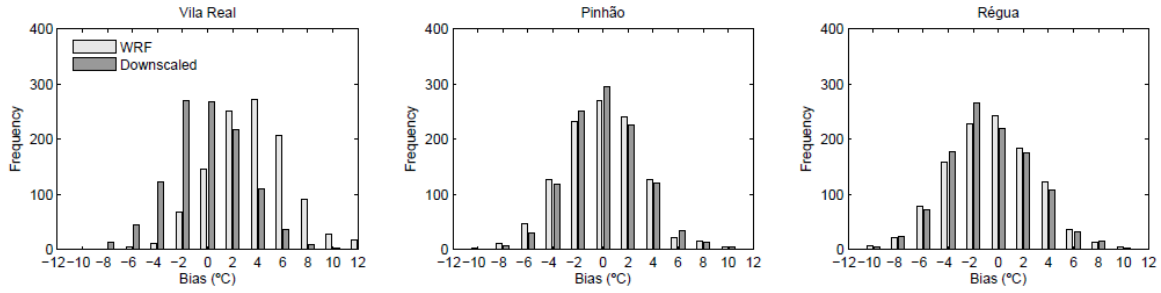

Figure 24 – Bias histograms of the Tmax statistical downscaled time series (gray) and of the WRF model (white).

Table 10- Bias, root mean squared error (RMSE), mean absolute error (MAE) and mean absolute percentage error (MAPE) of the WRF model and the downscaled time series.

Vila Real

	Variable (ºC)	WRF	Downscaled
RMSE (ºC)	Tmax	4,73	3,06
	Tmin	3,11	1,74
	Tmean	3,64	1,97
MAE (ºC)	Tmax	3,92	2,41
	Tmin	2,72	1,32
	Tmean	3,17	1,54
MAPE (%)	Tmax	31,91	19,58
	Tmin	112,19	45,63
	Tmean	43,53	21,78

Pinhão

	Variable (ºC)	WRF	Downscaled
RMSE (ºC)	Tmax	3,07	2,93
	Tmin	3,22	3,43
	Tmean	2,36	2,38
MAE (ºC)	Tmax	2,43	2,32
	Tmin	2,57	2,76
	Tmean	1,85	1,89
MAPE (%)	Tmax	13,74	13,12
	Tmin	96,69	85,24
	Tmean	14,72	14,10

Régua

	Variable (ºC)	WRF	Downscaled
RMSE (ºC)	Tmax	3,54	3,41
	Tmin	2,37	2,17
	Tmean	2,26	2,11
MAE (ºC)	Tmax	2,84	2,77
	Tmin	1,86	1,71
	Tmean	1,80	1,69
MAPE (%)	Tmax	14,92	14,47
	Tmin	32,21	34,71
	Tmean	13,08	12,20

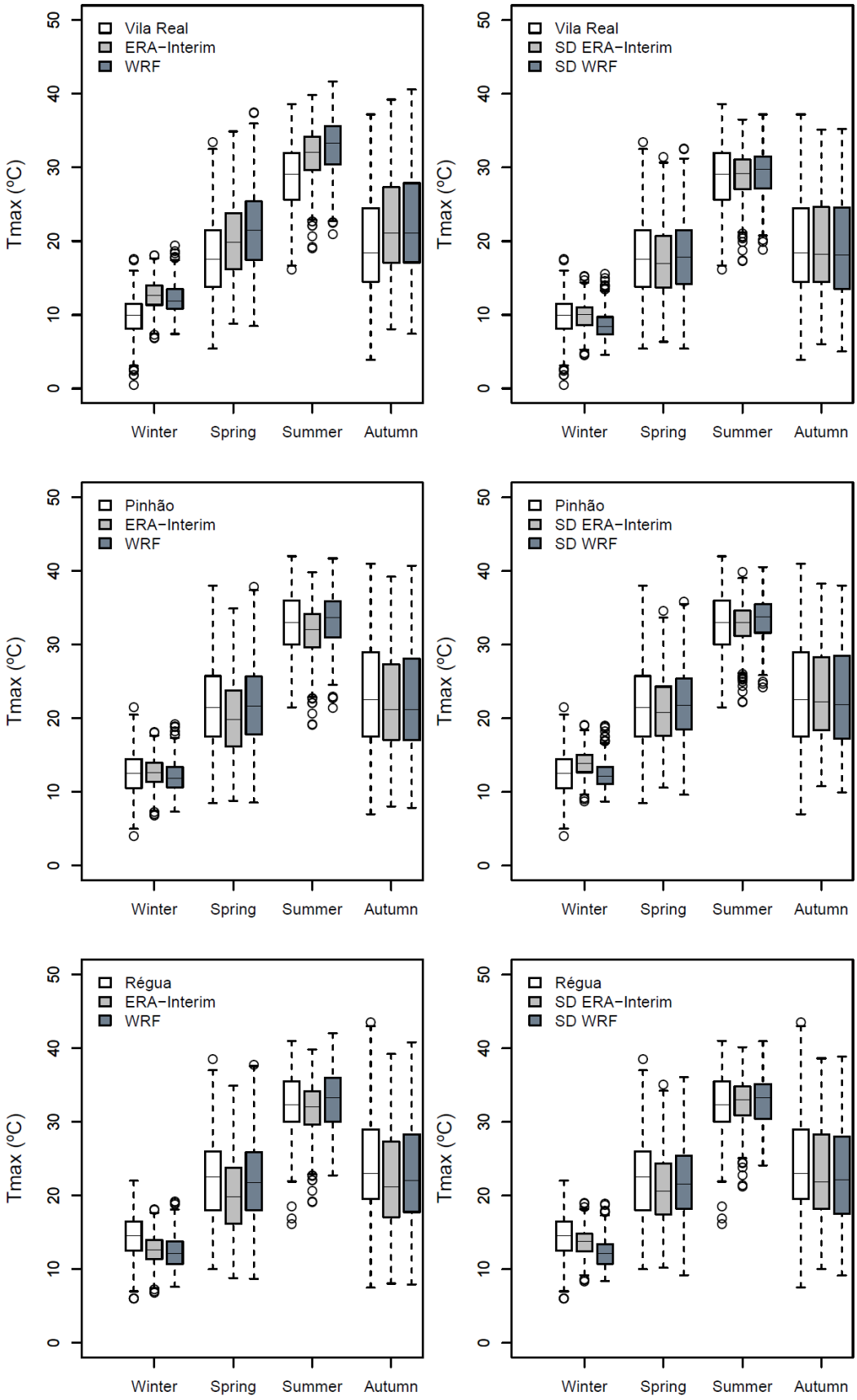

Figure 25 – Boxplot of seasonal daily Tmax from ERA-Interim/WRF and statistically-downscaled time (SD) series based on ordinary least squares for the validation period (2004-2006).

4.3 Application of statistically-downscaled data to viticulture

Given the local character of agronomic activities, climate downscaling is required to provide local temperature data in order to focus on a very local region, e.g. the area surrounding a particular vineyard. In the following section the mesoclimate in the Douro Wine Region viticultural areas of Vila Real, Pinhão and Régua is characterized by bioclimatic indices based on the previously downscaled local temperature during the growing season (April-October) and compared with observations. Winegrape cultivation suitability is assessed for the validation period (2004-2006) and differences between the statistical downscaling of ERA-Interim and the combined dynamical and statistical downscaling of WRF are discussed. The indices calculated in this section are summarized in Table 12 along with the viticultural climate class groups.

Table 11 - Class limits for the GST (Average growing season temperature), GDD (Growing degree-days), HI (Heliothermal Index of Huglin), CI (Cool night index) and LGS (Length growing season). GST and GDD classes are based on limits given by Jones et al. (2010), which use GDD classes defined by Winkler et al (1974), and HI and CI classes are based on Tonietto and Carbonneau (2002).

Index	Class of viticultural climate	Class interval
Average Growing Season Temperature GST (ºC)	Too cool	<13ºC
	Cool	13-15ºC
	Intermediate	15-17ºC
	Warm	17-19ºC
	Hot	19-21ºC
	Very hot	21-24ºC
	Too hot	>24ºC
Growing Degree Days GDD (ºC units)	Too cool	<850
	Region I	850-1389
	Region II	1389-1667
	Region III	1667-1944
	Region IV	1944-2222
	Region V	2222-2700
	Too hot	>2700
Heliothermal Index of Huglin HI	Very cool	≤ 1500
	Cool	1500-1800
	Temperate	1800-2100
	Temperate warm	2100-2400
	Warm	2400-3000
	Very warm	>3000
Cool Night Index CI	Very cool nights	≤12
	Cool nights	12-14
	Temperate nights	14-18
	Warm nights	>18
Length Growing Season LGS (days)	Appropriate for vine growing	≥ 182

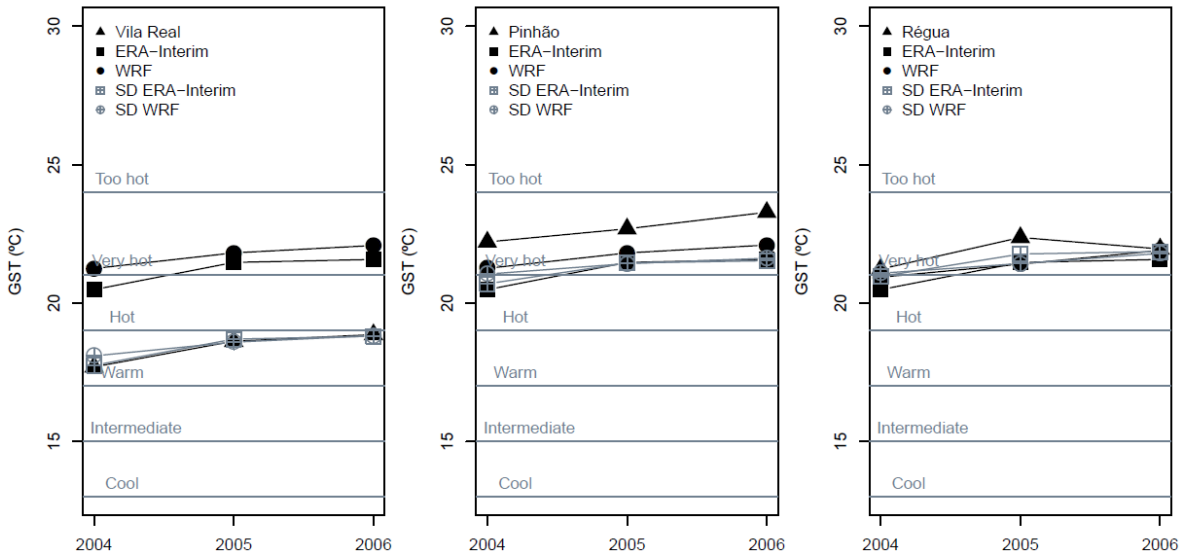

Figure 26 – Average growing season temperature (GST) (ºC) for the validation period (2004-2006).

The average growing season temperature (GST) calculated by the sum of the Tmean average during the growing season is illustrated in Figure 26. An increase of GST values over the three years of the validation period is observed with a maximum in 2005 at Vila Real and Régua. Vila Real is typically a warm climate type during this period, while Pinhão and Régua describe a very hot climate type, wherein Pinhão is warmer than Régua. In fact, Régua and Vila Real are the westerner weather stations, located in the sub-region of Below Corgo, which is characterized by being the coolest region. Pinhão is located further east in the sub-region of Above Corgo and presents warmer conditions. Despite Régua being further west than Vila Real cooler conditions are expected at the upper elevation station.

The performance of both statistically-downscaled time series from ERA-Interim and WRF in representing the GST at Vila Real is remarkable. While the statistically-downscaled temperature data describe accurately the viticultural climatic classes at Vila Real, the same is not true for the original ERA-Interim and WRF model data. Based on ERA-Interim and WRF model data, the region of Vila Real would correspond to a Very hot climate class, while observations and both statistically-downscaled time series describe a Warm climate class. At Régua, both ERA-Interim and WRF model data are slightly improved by the statistical downscaling. At Pinhão, the WRF model is slightly closer to observations, while at Régua the statistical downscaling of ERA-Interim is the best approximation.

Table 12 and Table 13 show the temperature maximum and minimum values during the growing season and the number of days with temperatures higher than 35ºC for the validation period 2004-2006. The year of 2005 displays the highest Tmax at Vila Real and Pinhão and the minimum Tmin at all weather stations. The annual maximum decreases in 2006 while the minimum increases, but even so the temperature is always higher than in 2004. Generally, the statistically downscaled time series are capable to reproduce these features. The largest number of days with temperature higher than 35ºC

also occurs during the year of 2005 reaching 59 hot days at Régua and 50 hot days at Pinhão. Despite being the least successful regression model, both statistically-downscaled temperature data, at Pinhão, perform remarkably in representing the hot days with temperatures higher than 35ºC (Table 12). In particular, the number of hot days described by ERA-Interim, at Pinhão, is greatly improved by the statistical downscaling. The statistically downscaled time series by WRF clearly stands out at Vila Real, while at Pinhão and Régua the WRF dynamical downscaling is a good approximation.

Table 12 - Annual maximum and minimum values for the growing season (April-October) from observations, ERA-Interim and statistically downscaled time series from ERA-Interim for the validation period (2004-2006). The number of days with temperatures higher than 35ºC is also given.

		Vila Real			**Pinhão**			**Régua**		
		Obs.	ERA-Interim	SD	Obs.	ERA-Interim	SD	Obs.	ERA-Interim	SD
Max. (ºC)	**2004**	36,40	37,67	34,30	40,00	37,67	37,56	39,50	37,67	37,91
	2005	38,60	39,84	36,52	42,00	39,84	39,83	40,10	39,84	40,14
	2006	37,20	39,22	35,15	41,00	39,22	38,26	43,50	39,22	38,62
Min. (ºC)	**2004**	0,90	4,06	1,64	6,00	4,06	3,66	5,50	4,06	4,25
	2005	0,70	3,06	0,71	3,50	3,06	2,78	5,00	3,06	3,34
	2006	1,90	4,92	2,18	7,50	4,92	3,93	7,00	4,92	4,69
T ≥ 35ºC (nº days)	**2004**	2	8	0	25	8	13	24	8	11
	2005	14	25	2	50	25	32	59	25	35
	2006	8	17	2	48	17	23	28	17	24

Table 13 - Annual maximum and minimum values for the growing season (April-October) from observations, WRF model data and statistically downscaled time series from WRF for the validation period (2004-2006). The number of days with temperatures higher than 35ºC is also given.

		Vila Real			**Pinhão**			**Régua**		
		Obs.	WRF	SD	Obs.	WRF	SD	Obs.	WRF	SD
Max. (ºC)	**2004**	36,40	41,09	35,72	40,00	41,49	38,95	39,50	41,32	39,03
	2005	38,60	41,65	37,20	42,00	41,71	40,53	40,10	42,01	40,95
	2006	37,20	40,73	35,71	41,00	40,72	38,97	43,50	41,29	39,36
Min. (ºC)	**2004**	0,90	3,80	1,06	6,00	3,58	2,91	5,50	2,27	2,99
	2005	0,70	3,18	0,65	3,50	3,03	2,89	5,00	2,00	3,00
	2006	1,90	4,59	1,76	7,50	4,40	3,45	7,00	4,20	4,18
T ≥ 35ºC (nº days)	**2004**	2	24	2	25	29	24	24	22	19
	2005	14	47	6	50	46	36	59	43	32
	2006	8	37	7	48	40	31	28	39	30

To describe the timing of biological processes, Growing degree-days (GDD) are frequently used, corresponding to the Tmean above a base temperature (Tbase) of 10ºC, since there is no wine grapes growth below this temperature. A degree base of 10ºC is assumed and the values of Tmean below Tbase are set to Tbase. A discussion about how Tbase is incorporated into the GDD equation can be found in McMaster and Wilhelm (1997). The GDD during the growing season is illustrated in Figure 27 and displays a pattern similar to GST (Figure 26). According to the classes limit based on the

standard Winkler Index (Winkler, 1974) Vila Real is typically a Winkler Region III, Pinhão is mainly a Winkler Too hot region and Régua is a Winkler Region V during the validation period. An increase of GDD is observed in all stations with a maximum at 2005 which is not observed at Pinhão. The GDD at Vila Real is clearly best represented by the statistically-downscaled time series. Similarly to Figure 26, WRF model is closer to observations at Pinhão, and at Régua the statistical downscaling of ERA-Interim is the best approximation.

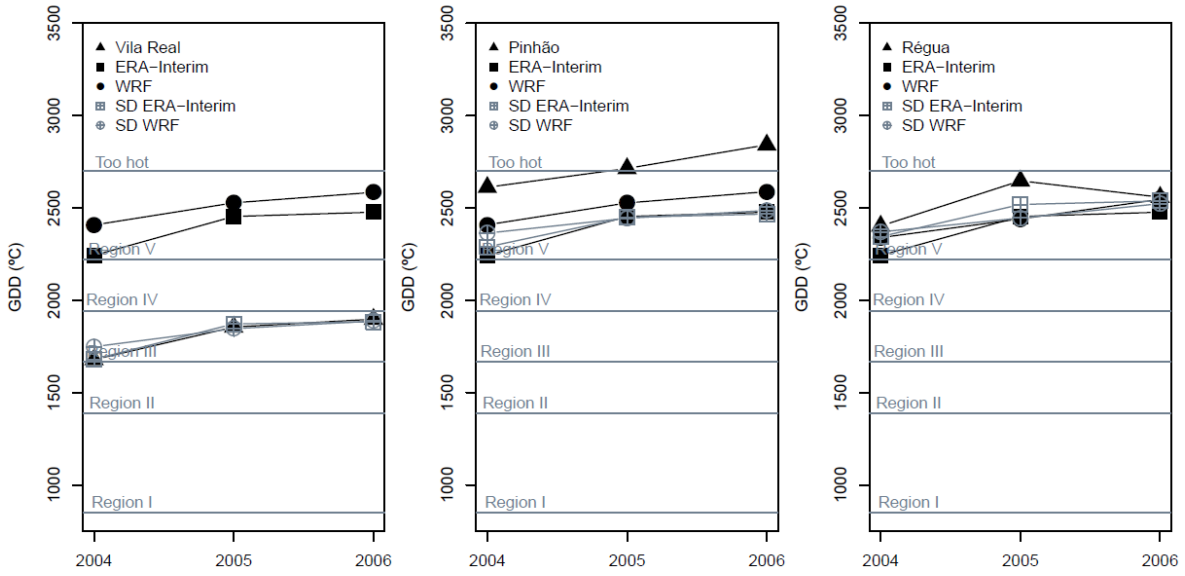

Figure 27 - Growing degree days (ºC units) for the validation period.

Figure 28 illustrates the annual cumulative GDD for the validation period which can be used to estimate the level of grapes growth. In the end of October the GDD is higher and grapes reach maturity and are ready for harvest. Cumulative GDD is highest at Pinhão, followed by Régua and Vila Real. Analogously to the GST pattern (Figure 26) the warmer area has highest GDD, and the higher station displays the lowest GDD, despite its most westerly location. The cumulative GDD of 2006 is the highest at Vila Real and Pinhão, while at Régua 2005 displays the highest cumulative GDD (the year and the station with more frequency of hot days).

Generally, at Vila Real, the cumulative GDD calculated based on the statistically-downscaled time series is much more similar to observations than ERA-Interim and WRF. Figure 29 shows the elevation of each meteorological station and the respective GDD during the growing season for each year of the validation period (2004-2006). Every year, the higher the station, the lower the GDD. At Vila Real and Régua the GDD is well reproduced by the statistically-downscaled temperature, highlighting a vast improvement by the downscaling of ERA-Interim and WRF model data at Vila Real. At Pinhão, both statistically-downscaled temperature data misrepresent the GDD values, similar to Figure 27.

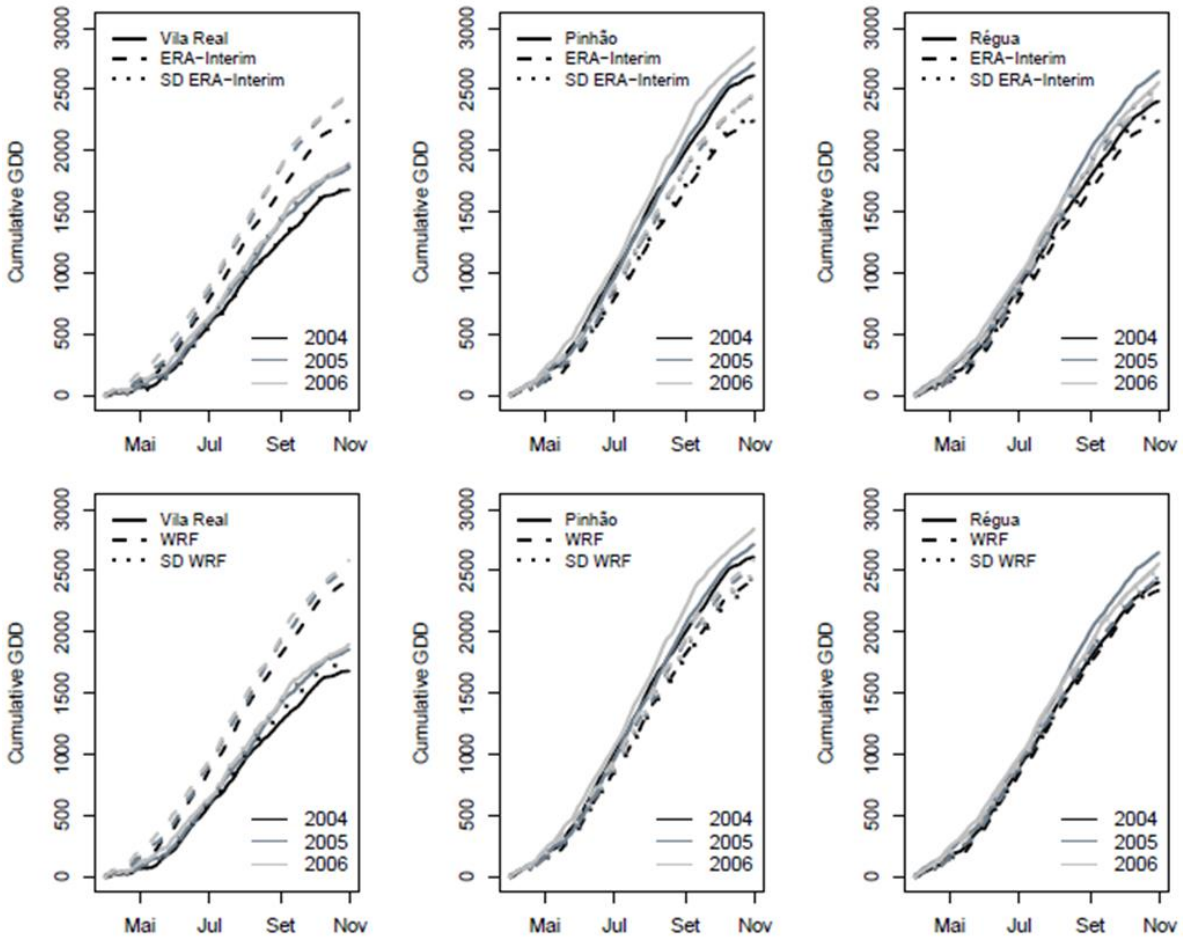

Figure 28 – Annual cumulative growing degree-days (GDD) for the validation period 2004-2006.

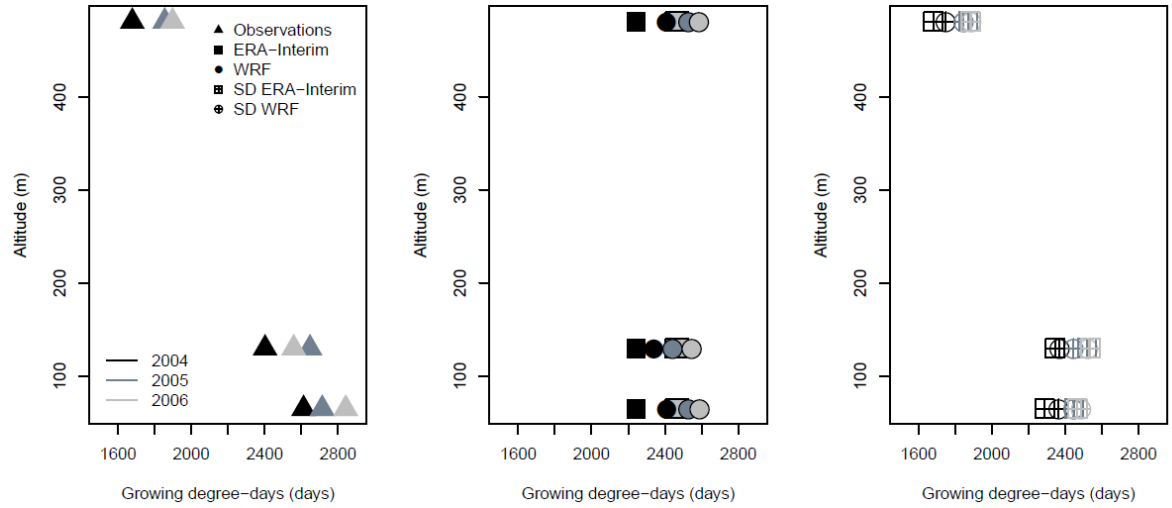

Figure 29 - Annual Growing degree-days (GDD) as a function of altitude of the weather stations by the statistically downscaled time series (right) and observations (left).

The classical Heliothermal Index of Huglin (HI) is obtained by the sum of the mean between Tmean and Tmax above Tbase, multiplied by the day length coefficient *d* of 1.02 (Tonietto and Carbonneau,

2004) due to latitude varying. HI is similar to the GDD concept, but giving more weight to maximum temperatures, and taking into account the average daylight period of the latitude of the Douro Valley. According to the class limits of Tonietto and Carbonneau (2004), Vila Real largely displays a Warm viticultural climate class, while Pinhão and Régua present a Very warm climate class, with HI of Pinhão being the highest. Similar to the previous indices, HI presents an increasing trend with a maximum in 2005 at Vila Real and Régua. Similar to the GST and GDD patterns, HI is better represented by the statistically downscaled time series, at Vila Real, than ERA-Interim and WRF model data. However, the statistically-downscaled time series of WRF is closer to observations at Pinhão and Régua. At Pinhão and Régua, the WRF dynamical downscaling is a good approximation.

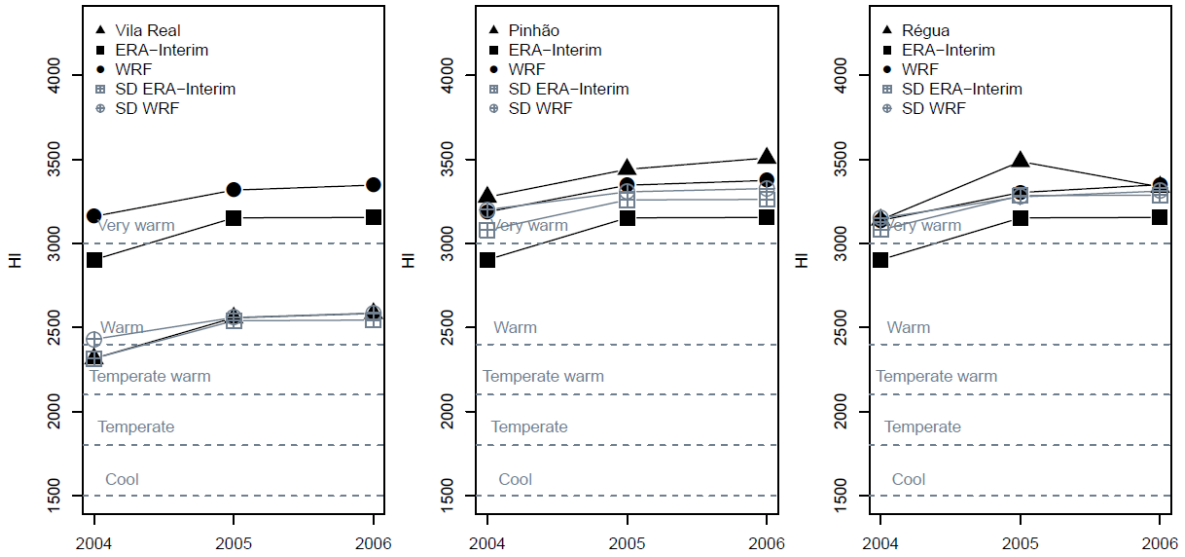

Figure 30 - Huglin Index (HI) for the validation period (2004-2006)

The Cool night index (CI) is obtained by the mean of Tmin during the maturation period which corresponds to the month of September. CI is a viticultural climate index to assess secondary metabolites such as aroma and color in grapes and wines. CI is warmer in 2006 at Vila Real and Régua and warmer in 2004 at Pinhão. Typically Vila Real presents Cool nights viticultural climate class while Pinhão and Régua display Temperate nights class. Both statistically-downscaled time series performance are remarkable at Vila Real, while at Régua the statistically-downscaled time series of WRF are the closest to observations. At Pinhão the CI is poorly represented by all models.

The number of days with Tmean above Tbase is given by the Length growing season (LGS), considering 182 days or higher an appropriate LGS for vine growing (Jackson, 2001). According to LGS, 2004 and 2005 were the most suitable years for viticulture, corresponding to the period characterized by one of the worst droughts ever recorded in Portugal. Both statistically-downscaled time series are capable to capture these features.

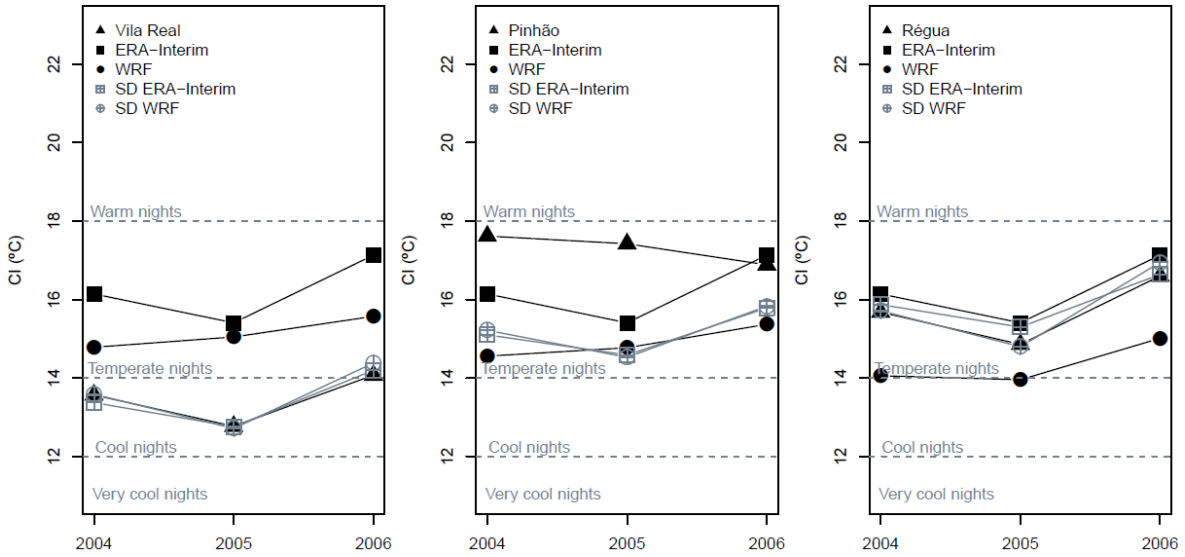

Figure 31 - Night cold index (CI) (ºC) for the validation period (2004-2006).

Table 14- Annual values of LGS (Length growing season) for the growing season (April-October) from observations, ERA-Interim and statistically downscaled time series from ERA-Interim for the validation period (2004-2006).

		Vila Real			Pinhão			Régua		
		Obs.	ERA-Interim	SD	Obs.	ERA-Interim	SD	Obs.	ERA-Interim	SD
LGS	**2004**	194	214	196	214	214	214	213	214	214
	2005	205	214	205	214	214	214	214	214	214
	2006	212	214	213	214	214	214	214	214	214

Table 15- Annual values of LGS (Length growing season) for the growing season (April-October) from observations, WRF model data and statistically downscaled time series from WRF for the validation period (2004-2006).

		Vila Real			Pinhão			Régua		
		Obs.	WRF	SD	Obs.	WRF	SD	Obs.	WRF	SD
LGS	**2004**	194	212	199	214	212	214	213	213	214
	2005	205	214	206	214	214	214	214	214	214
	2006	212	214	213	214	214	214	214	214	214

5. Discussion

In a climate change context, the impacts of temperature variability in agriculture have become a major concern over the last century. Viticulture is one of the agronomic activities most directly influenced by temperature, which largely influences the grapevines composition and consequently the quality of the produced wine. The aim of this work was to perform a statistical downscaling of air temperature to local sites in order to focus on very local areas of the Douro Wine Region, which could be used to study a particular vineyard. Three meteorological stations situated in the Douro Valley were considered, Vila Real, Pinhão and Régua, accounting for two of the three Demarcated Region of

Douro sub-regions: Below Corgo (Régua and Vila Real) and Above Corgo (Pinhão). Below Corgo is the coolest sub-region due to the influence of the Atlantic winds, while Above Corgo is a little warmer. The analyzed weather stations are also representative of the topographic features which contribute to the unique climate variability of the Douro Wine Region, with altitudes of 481, 65 and 130 m respectively (Figure 9, see section 2.2). The most recent reanalysis from ECMWF, ERA-Interim, and a state-of-the-art RCM resulting from a dynamical downscaling, WRF (9km), were used to perform a statistical downscaling of air temperature to the station points.

The performed statistical downscaling was based on regression methods which are widely used, standing out for their modest computing requirements and easy implementation. Ordinary least squares and robust regression models were established for seasonally-adjusted time series during the calibration period 1989-2003, and statistical downscaling of reanalysis and the combined dynamical and statistical downscaling of WRF model data were performed for the validation period 2004-2006. In general, ordinary least squares and robust regression gave similar results, indicating that the impact of eventual outliers, assessed by the robust regression, was not significant in the mean variability. The corresponding seasonal cycle of ERA-Interim and WRF time series is then added to the simulated time series since the mean seasonal cycle shows a behavior similar to that of the observations (Figure 13, section 2.3.1). Despite being available for this validation period, the seasonal cycle of observational records is not considered, since it would not be possible to take it into account in the case of statistical downscaling procedures for scenarios in the future. The statistical errors between the seasonally-adjusted time series and observations were slightly lower than for the time series with seasonal cycle. However the difference between ERA-Interim/WRF and the respective downscaled time series remains nearly the same after the addition of the seasonal cycle.

Prior to the application of the statistical downscaling, both ERA-Interim and WRF model data display lower bias at the lower altitude stations, Pinhão and Régua, and a higher bias at Vila Real. This feature may suggest that, before the application of the statistical downscaling technique, reanalysis and dynamical downscaling model may be a good approximation at valley sites, but that an improvement at higher elevation sites is required. In any case, WRF model data displays lower biases than ERA-Interim at Pinhão and Régua, indicating significant advantages in using WRF dynamical downscaling as a regional climate model, rather than reanalysis.

The variability of Tmax, Tmin and Tmean is very well represented by the statistically-downscaled time series of ERA-Interim and WRF. Generally a good improvement is found in the statistically-downscaled time series of both ERA-Interim and WRF, showing the added value of statistical downscaling in further reducing the statistical errors of both the reanalysis and RCM data. The sole exception is Pinhão, where WRF model data displays lower errors than the statistically-downscaled time series, probably due to the weaker linear relationships established by both ERA-Interim and WRF

regression models. In addition, the performance of downscaled temperature data at the seasonal scale is noteworthy, highlighting the importance of statistical downscaling in viticulture practices. In a region with such rugged topography, statistical downscaling proves to be essential since it significantly improves the ability of representing temperature variability.

The growth stages of the wine grapes are largely influenced by local climate conditions, in particular by temperature, since it significantly affects the main biological aspects of the vine, namely the composition and maturation of grapes. Bioclimatic indices based on temperature are indicative of the climate scenarios associated to winegrape cultivation suitability, including those calculated in this work: average growing season temperature (GST), growing degree-days (GDD), heliothermal index of Huglin (HI), cool night index (CI) and length growing season (LGS). Except for CI and LGS, the bioclimatic indices are increasing over the three years of the validation period (2004-2006) displaying a maximum in 2005 at Vila Real and Régua (western weather stations located at Below Corgo) while at Pinhão (eastern weather station located at Above Corgo), the increase was linear in time. At Pinhão the bioclimatic indices are not lower than at Vila Real and Régua in 2005, but the increase lasted until 2006 in Above Corgo while at Below Corgo the bioclimatic indices have recovered in 2006. This feature may suggest an influence of the intense drought of 2004/2005 at Vila Real and Régua, one of the worst droughts ever recorded (Garcia-Herrera et al., 2007). In fact most of the Portuguese territory is characterized by a temperate climate with hot and dry summers favorable to the occurrence of droughts, where several events stand out, mainly since 1910 (Vicente Serrano, 2006). Although it is generally accepted that wine grapes benefit from long, warm-to-hot and dry summers, excessive drought is not desirable. However, despite the highest Tmax, the year of 2005 did not record a drop in wine production (wine production during this period is discussed by e.g. Santos et al. 2011 and Gouveia et al. 2011).

Although the GST, GDD, HI and LGS are all indicative of grape growing stages, they are not directly comparable (e.g., a warm GST is not equivalent to a warm GDD or a warm HI and vice versa (ADVID, 2012)). The CI is a measure of maturation potential, depending only on Tmin during the maturation period (September). While CI displays a minimum in 2005 at Vila Real and Régua, it is decreasing in Pinhão, and similarly to the other indices, the nights are cooler at Vila Real and warmer at Régua and Pinhão. Warmer conditions are verified at Above Corgo (Pinhão) than at Below Corgo (Vila Real and Régua) and cooler conditions are verified at the upper elevation weather station (Vila Real) than at the valley stations (Pinhão and Régua).

The use of WRF and ERA-Interim data to calculate the bioclimatic indices may lead to misrepresentations of the viticultural suitability of the region of Vila Real. In fact, both statistically-downscaled temperature data of WRF and ERA-Interim stand out as an improved approximation to observations at Vila Real, providing a significant improvement of both reanalysis and RCM data at

higher elevation sites. At Régua, both statistically-downscaled temperature data estimate rather well the viticultural climate classes of the three meteorological stations, with the statistical downscaling of ERA-Interim being closer to observations at 2005. In respect to viticultural applications, the statistical downscaling is indeed an advantage in capturing local details such as the impact in the results of the elevation of the sites. However, at Pinhão the WRF dynamical downscaling is a good approximation, as expected from the low percentage of temperature variability explained by the regression models and the lower errors displayed by the WRF model data.

The use of this statistical downscaling technique in future climate data can be a useful research tool for agronomical applications due to the local character of the corresponding processes. Understanding how climate will affect yield in the future is important to minimize the impacts of climate changes and promote adaptation measures. Despite the very good performance of the statistical downscaling of ERA-Interim, reanalysis data is only available for the past. In turn, the statistical downscaling of WRF show results as good as the statistical downscaling of ERA-Interim for computation of bioclimatic indices, and WRF dynamical downscaling display a better ability to represent the number of hot-days and the bioclimatic indices at Pinhão. Evaluation of the future climate of the Douro Wine Region based on statistical downscaling of future WRF model data may be a promising approach to assess the impacts of climate change henceforward.

6. Concluding remarks and future work

In the past decades, several agroclimatic studies have focused on the influence of climate variability in agricultural crops. Arguably, climate exerts strong influence worldwide in the suitability of a region to crops growth, in particular wine grapes, and high resolution climate data is of high importance to understand how temperature affects viticultural practices in a changing climate. In this dissertation, statistical downscaling based on regression models was applied to ERA-Interim and WRF model data in order to obtain local temperature estimates for the regions of Vila Real, Pinhão and Régua, located at one of the most distinctive wine producing regions, the Douro Valley. Bioclimatic indices were subsequently obtained from the downscaled data with the goal of providing an illustration of possible agronomic applications of statistical downscaling of air temperature and to examine climate conditions of the Douro Wine Region.

By establishing statistical relationships based on a simple regression model, the ERA-Interim reanalysis and the WRF (9km) dynamical downscaling data were easily combined with observational data for the period 1989-2003. The performed statistical downscaling was validated for the period 2004-2006 and a good agreement with observations was found. The errors of both ERA-Interim and WRF were significantly reduced using the regression-based downscaling methodology, and the added value of combining dynamical downscaling (WRF) and statistical downscaling was demonstrated.

The climate assessment obtained with the bioclimatic indices based on the downscaled temperature data provided additional evidence of the great potential of statistical downscaling for viticultural applications. The results obtained show that the use of reanalysis and WRF model data without application of statistical downscaling can lead to inaccuracies in the characterization of the Douro Wine Region viticultural suitability. These findings add substantial information on the use of reanalysis and RCM data to viticultural applications and hold great promise for future application of statistical downscaling to a broader network of local stations. A larger number of observational records to guarantee spatial representativeness of the Douro Wine Region would be very advantageous to assess the regional viticultural suitability. Evaluation of the future climate by WRF statistical downscaling for a broad network of weather stations in the Douro Wine Region would be an asset in terms of assessment of agronomic impacts in a changing climate.

An issue that was not addressed in this study is related to the constant lapse rate for the topographic correction here assumed. In a region with such a complex topography like the Douro Valley, at higher stations the temperature variability may be more pronounced in altitude and a constant lapse rate may not be adequate. This limitation can be one of the reasons for the reanalysis and RCM lack of performance. However the statistical downscaling enhances significantly the ERA-Interim and WRF ability of representing observations at the highest altitude stations and therefore is particularly valuable in a region with such rugged topography and could a good alternative to more complex topographic correction methods.

More broadly, further investigation on the information given by bioclimatic indices would have a number of important implications since bioclimatic indices may not explain all the variability of sugar content and acidity of a vineyard. An attempt to improve the explained wine grapes qualitative variability can be the development of new bioclimatic indices (e.g. Malheiro et al., 2010) based on the downscaled time series.

Taken together, the results from this thesis suggest that both statistical downscaling of ERA-Interim and statistical downscaling of WRF are adequate for the Douro Wine Region. However, the WRF dynamical downscaling and the combined WRF dynamical and statistical downscaling are much better in representing the frequency of hot days than ERA-Interim, in the Douro Wine Region, suggesting a significant improvement of WRF in the higher quantiles. Soares et al. (2012) obtained similar results for the precipitation, showing that ERA-Interim completely lacks events with strong precipitation and the high precipitation quantiles, in comparison to WRF model data. In addition, the bioclimatic indices considered here are based only on temperature data, and a combination of temperature and precipitation data would be the ideal for a complete evaluation of the Douro Wine Region climate. The development of downscaling approaches based on other regression methods, such us the quantile

regression technique (e.g. Tareghian et al., 2013) is a highly relevant topic for further research, to apply to both temperature and precipitation data.

7. References

Amerine A.. A. J. Winkler. 1944. Composition and quality of musts and wines of California grapes. *Hilgardia*. **15**. 493-675.

Atlas Climático Ibérico. Instituto de Meteorologia de Portugal. Agencia Estatal de Meteorología de Espana. 2011

ADVID (Associação para o Desenvolvimento da Viticultura Duriense). 2012. A Climate Assessment for the Douro Wine Region; and examination of the Past. Present and Future Climate Conditions for Wine Production. ADVID (www.advid.pt)

Abatzoglou J. T.. T. J. Brown. 2012. A comparison of statistical downscaling methods suited for wildfire applications. *Int. J. Climatol.*. **32**. 772-780.

Blanco-Ward D.. J. M. G. Queijeiro. G.V. Jones. 2007. Spatial climate variability and viticulture in the Mino River Valley of Spain. Vitis. **46**. 63-70.

Branas J.. G. Bernon. L. Levadoux. 1946. Eléments de viticulture générale. Imp. Dehan. Montpelier

Cleveland R. B.. W. S. Cleveland. J.E. McRae. and I. Terpenning .1990. STL: A Seasonal-Trend Decomposition Procedure Based on Loess. *Journal of Official Statistics*. **6**. 3–73.

Fanet J.. 2004. Great wine terroirs. University of California Press. Berkeley.

Feio. M.. 1991. Clima e Agricultura: exigências climáticas das principais culturas e potencialidades agrícolas do nosso clima. Ministério da Agricultura. Pescas e Alimentação. Lisboa

Garcia-Herrera, R., Paredes, D., Trigo, R. M., Trigo, I. F, Hérnandez, E., Barriopedro, D., Mendes, M. A., 2007: The Outstanding 2004/05 Drought in the Iberian Peninsula: Associated Atmospheric Circulation. *American Meteorological Society*, **8**, 483-489

Gouveia C. M. L. R. Liberato. C. C. DaCamara. R. M. Trigo. A. M. Ramos. 2011. Modelling past and future wine production in the Portuguese Douro Valley. *Clim. Res.*. **48**. 349–362.

Heyen H.. E. Zorita. H. V. Storch. 1995. Statistical downscaling of monthly mean North Atlantic air-pressure to sea level anomalies in the Baltic Sea. *Tellus*. **48A**. 312-323

Huglin P.. 1978. Nouveau mode d'évaluation des possibilities héliothermiques d'un milieu viticole. *CR Acad. Agr.*. **64**. 1117-1126

Helsel, D.R. and R. M. Hirsch, 2002. Statistical Methods in Water Resources Techniques of Water Resources Investigations. U.S. Geological Survey.

Huber, P. J., 1981. Robust Statistics. Wiley

Hampel, F. R., Ronchetti E. M., Rouseeauw, P. J., Stahel, W. A., 1986. Robust Statistics: The Approach based on Influence Functions. Wiley.

Jackson D.. 2001. Climate: Monographs in cool climate viticulture-2. Daphne Brasell Associates. Wellington

Jones G.V.. F. Alves. 2012. Impact of climate change on wine production: a global overview and regional assessment in the Douro Valley of Portugal. *Int. J. Global Warming*. **4**. 383-406.

Jones G. V.. A. A. Duff. A. Hall. J. W. Myers. 2010. Spatial Analysis of Climate in Winegrape Growing Regions in the Western United States. *Am. J. Enol. Vitic.*. **61**. 313-326

Jones G. V.. 2006. Climate and Terroir: Impacts of Climate Variability and Change on Wine. *Fine Wine and Terroir - The Geoscience Perspective*. Macqueen R. W. and L. D. Meinert (eds.). *Geoscience Canada Reprint Series Number 9*. Geological Association of Canada. St. John's. Newfoundland.

Jones G.V.. M. A. White. O. R. Cooper. K. Storchmann. 2005. Climate change and global wine quality. *Climate Change*. **73**. 319–343

Jones G.V.. R. Davis. 2000a. Climate Influences on Grapevine Phenology. Grape Composition. and Wine Production and Quality for Bordeaux. France. *Am. J. Enol. Vitic.*. **51**. 249-261.

Jones G.V.. R. Davis. 2000b. Using a synoptic climatological approach to understand climate-viticulture relationships. *Int. J. Climatol.*. **20**. 813–837

Jones G.V.. 1997. A Synoptic Climatological Assessment of Viticultural Phenology. Dissertation. University of Virginia. Department of Environmental Sciences

Koenker, R. and Hallock, K. 2001. Quantile Regression. *J. Econ. Perspect.* **15**, 143-156.

Kilsby C. G.. P. S. P. Cowpertwait. P. E. O'Connel. P. D. Jones. 1998. Predicting rainfall statistics in England and Wales using atmospheric circulation variables. *Int. J. Climatol.*. **48**. 523-539.

Lorenzo M. N.. J. J. Taboada. J. F. Lorenzo. A. M. Ramos. 2012. Influence of climate on grape production and wine quality in the Rías Baixas. north-western Spain. *Reg. Environ. Change*. DOI: 10.1007/s10113-012-0387-1

Mayson R.. 2012. Port and the Douro. Infinite Ideas Limited. Oxford

Maak K.. H. von Storch. 1997. Statistical downscaling of monthly mean air temperature to the beginning of flowering of *Galanthus nivalis* L. in Northern Germany. *Int. J. Biometeorol.*. **41**. 5-1.

Malheiro. A. N. C.. 2005. Microclimate. yield and water-use of vineyards in the Douro Region. Portugal. Dissertation. Cranfield University. UK.

Malheiro A. C.. J. A. Santos. H. Fraga. J. G. Pinto. 2010. Climate change scenarios applied to viticultural zoning in Europe. *Clim. Res*.. **43**. 163–177.

McMaster, G. S., Wilhelm W. W. 1997. Growing degree-days: one equation, two interpretations. *Agricultural and Forest Meteorology*, **87**, 291-300.

Mullins M. G.. A. Bouquet. L. E. Williams. 1992. Biology of the Grapevine. Cambridge University Press. Great Britain

Palatella L.. M. M. Miglietta. P. Paradisi. P. Lionello. 2010. Climate change assessment for Mediterranean agricultural areas by statistical downscaling. *Nat. Hazards Earth Syst. Sci.*. **10**. 1647-1661.

Ramos A. M.. R. M. Trigo. F. E. Santo. 2011. Evolution of extreme temperatures over Portugal: recent Changes and future scenarios. *Climate Research*. **48**. 177-192.

Riou C. B.. N.. V R.. Sotes. V. Gomez-Miguel. A. Carbonneau. M. Panagiotou. A. Calo. A. Costacurta. Castro R.. A. Pinto. C. Lopes. L. Carneiro. P. Climaco. 1994. Le déterminisme climatique de la maturation du raisin: application au zonage de la teneur em sucre dans la communauté européenne. Office des Publications Officielles des Communautés Européennes. Luxembourg

Santos J. A.. S. D. Gratsch. M. K. Karremann. G. V. Jones. J. G. Pinto. 2012a. Ensemble projections for wine production in the Douro Valley of Portugal. *Climatic Change*. DOI 10.1007/s10584-012-0538-x

Santos J. A.. A. C. Malheiro. J. G. Pinto. G. V. Jones. J. G. Pinto. 2012b. Macroclimate and viticultural zoning in Europe: observed trends and atmospheric forcing. *Clim. Res.*. **51**. 89-103

Santos J. A.. A. C. Malheiro. M. K. Karremann. J. G. Pinto. 2011. Statistical modelling of grapevine yield in the Port Wine region under present and future climate conditions. *Int. J. Biometeorol.*. **55**. 199-131.

Santos J. A.. S. Leite. 2009. Long-term variability of the temperature time series recorded at Lisbon. J. *Appl. Stat.*. **36**. 323-137.

Santos F. D.. P. M. A. Miranda. 2006. Alterações climáticas em Portugal: cenários. impactos e medidas de adaptação. (Projecto SIAM II). Gradiva. Lisboa

Santos J. A.. J. Corte-Real. S. Leite. 2005. Weather regimes and their connection to the winter rainfall in Portugal. *Int. J. Climatol.*. **25**. 33–50

Soares P. M. M.. R. M. Cardoso. P. M. A. Miranda. J. Medeiros. M. Belo-Pereira. F. Espirito-Santo. 2012. WRF high resolution dynamical downscaling of ERA-Interim for Portugal. *Clim. Dyn.*. DOI 10.1007/s00382-012-1315-2

Schoof J. T.. S. C. Pryor. 2001. Downscaling temperature and precipitation: a comparison of regression-based methods and artificial neural networks. *Int. J. Climatol.*. **21**. 773-790.

Stineman. R. W.. 1980. A Consistently Well Behaved Method of Interpolation. Creative Computing . **6**. Number 7. p. 54-57.

Smart R.. M. Robinson. 1991. Sunlight into wine. A handbook for winegrape canopy management.Winetitles. Adelaide

Tareghian R.. P. F. Rasmussen. 2013. Statistical Downscaling of Precipitation using Quantile Regression. *Journal of Hydrology*. http://dx.doi.org/10.1016/j.jhydrol.2013.02.029

Tonietto J.. 1999. Les macroclimats viticoles mondiaux et l'influence du mésoclimat sur la typicité de la Syrah et du Muscat de Hambourg dans le sud de la France: méthodologie de caráctérisation. PhD dissertation. Ecole Nationale Supérieure Agronomique. Montpellier

Tonietto J. A. Carbonneau. 2004. A multicriteria climatic classification system for grape-growing regions worldwide . *Agric Meteorol.***124**. 81−97

Vicente-Serrano, S.M., 2006: Spatial and temporal analysis of droughts in the Iberian Peninsula (1910–2000). *Hydrological Sciences Journal*, **51**, 83-97

von Storch H.. 1999. On the use of "Inflation" in Statistical Downscaling. *J. Climate*. **12**. 3505–3506

Widman M.. C. S. Bretherton. E. P. Salathé. 2003. Statistical Precipitation Downscaling over the Northwestern United States Using Numerically Simulated Precipitation as a Predictor. *J. Climate*. **16**. 799–816

Wilby R. L.. T. M. L. Wigley. D. Conway. P. D. Jones. B. C. Hewitson. J. Main. D. S. Wilks. 1998. Statistical Downscaling of general circulation model output: A comparison of methods. *Water Resources Research*. **34**. 2995-3008.

Winkler A. J.. J A. Cook. W. M. Kliwer. L. A. Lider. 1974. General viticulture. University of California Press. Berkeley

Weaver R. J.. 1976. Grape Growing. John Wiley & Sons. New York

Appendix

Notation and acronyms

Vectors are denoted as italic, bold and lower case letters.

Matrixes are denoted as italic, bold and capital letters.

The transpose of a matrix is indicated by (^{T}).

Model estimates are represented by a hat (^).

The derivative of a function is denoted by a (‘).

Figures not shown in the dissertation

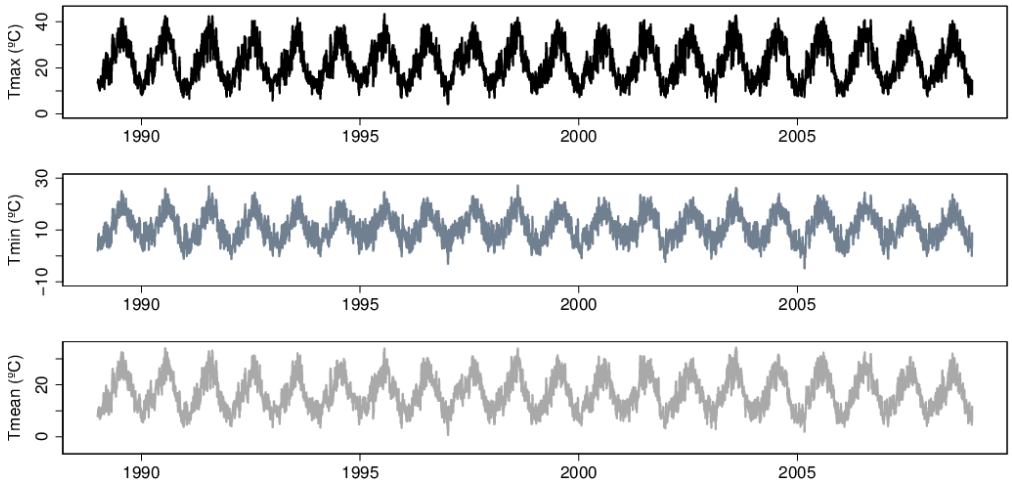

Figure 32 - Daily time series maximum (top), minimum (center) and mean (bottom) temperature of the WRF model grid point closer to Pinhão for the period 1989-2008.

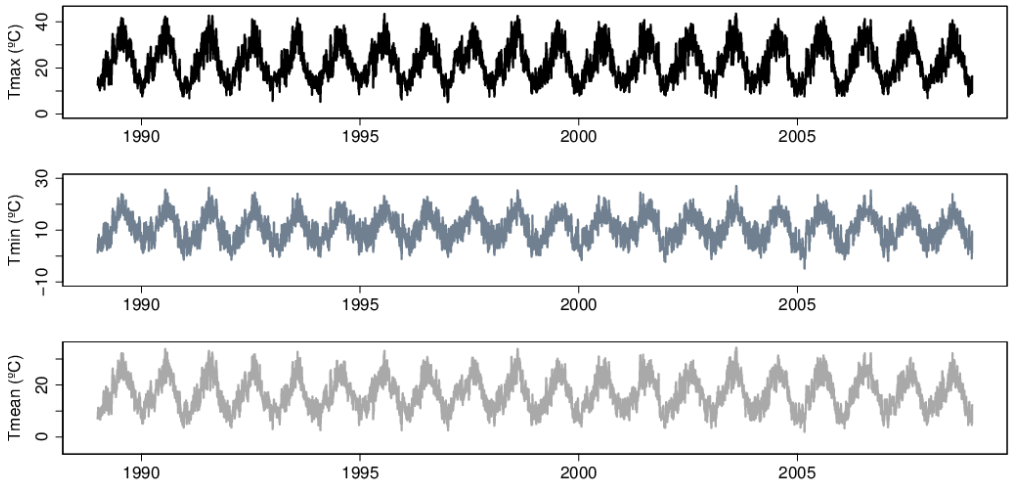

Figure 33 - Daily time series maximum (top), minimum (center) and mean (bottom) temperature of the WRF model grid point closer to Régua for the period 1989-2008.

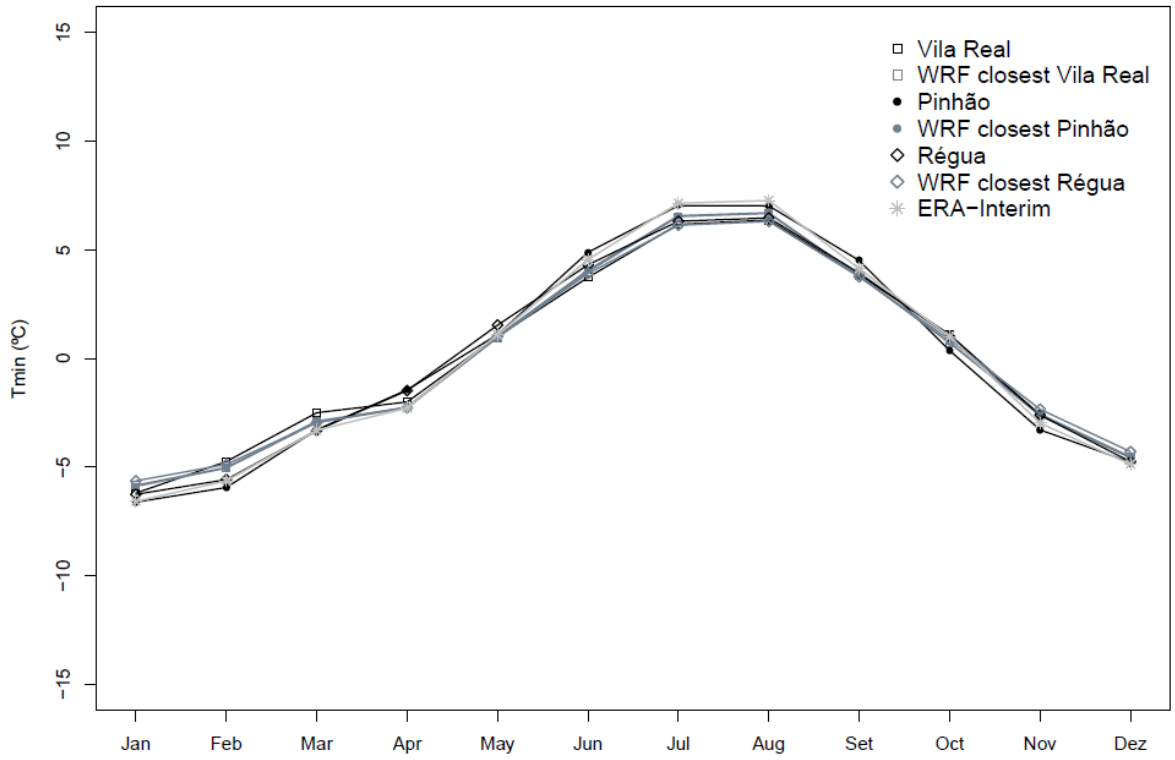

Figure 34 - Tmin mean seasonal cycle of the meteorological stations records (black), reanalysis grid-point centered in the Douro Valley (gray) and WRF closest point (slate gray) of Tmax (top) Tmin (center) and Tmean (bottom) for the calibration period.

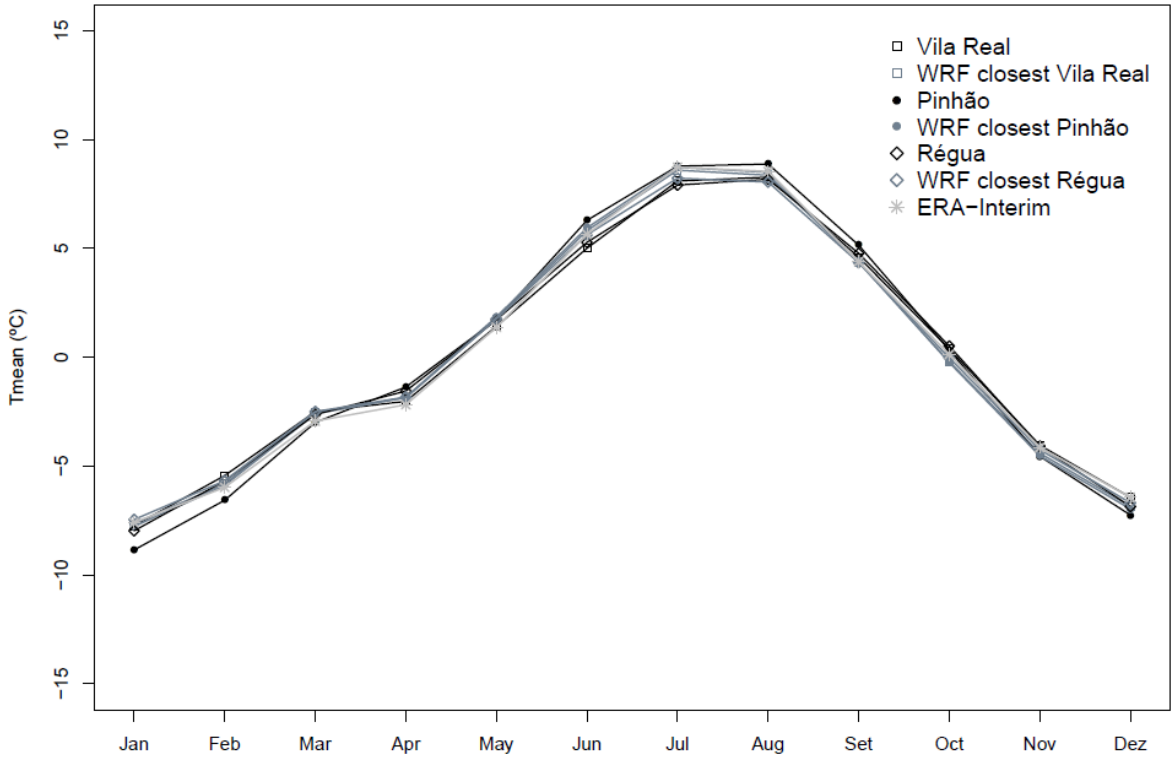

Figure 35 - Tmean mean seasonal cycle of the meteorological stations records (black), reanalysis grid-point centered in the Douro Valley (gray) and WRF closest point (slate gray) of Tmax (top) Tmin (center) and Tmean (bottom) for the calibration period.

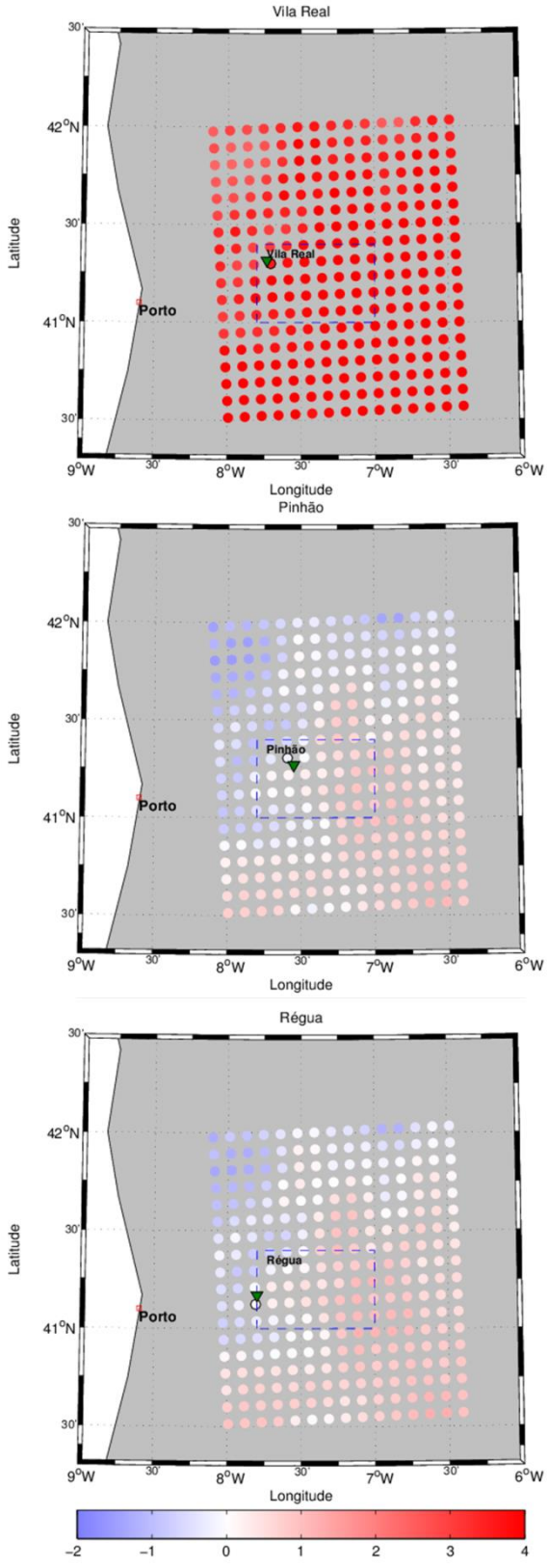

Figure 36- Bias between the seasonally-adjusted daily Tmax time series of the WRF grid-cell (circles) and the observations for the calibration period (1989-2003). Map of the Douro Valley (blue dashed box) and meteorological stations location (triangles).

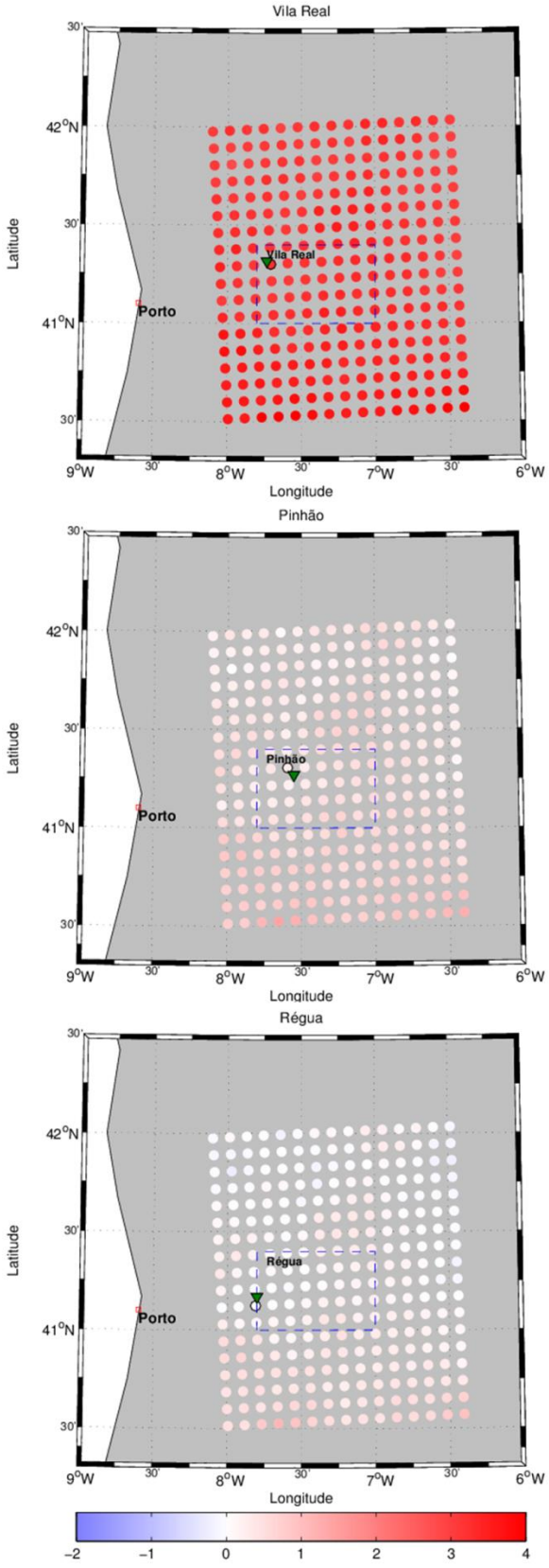

Figure 37- Bias between the seasonally-adjusted daily Tmean time series of the WRF grid-cell (circles) and the observations for the calibration period (1989-2003). Map of the Douro Valley (blue dashed box) and meteorological stations location (triangles).

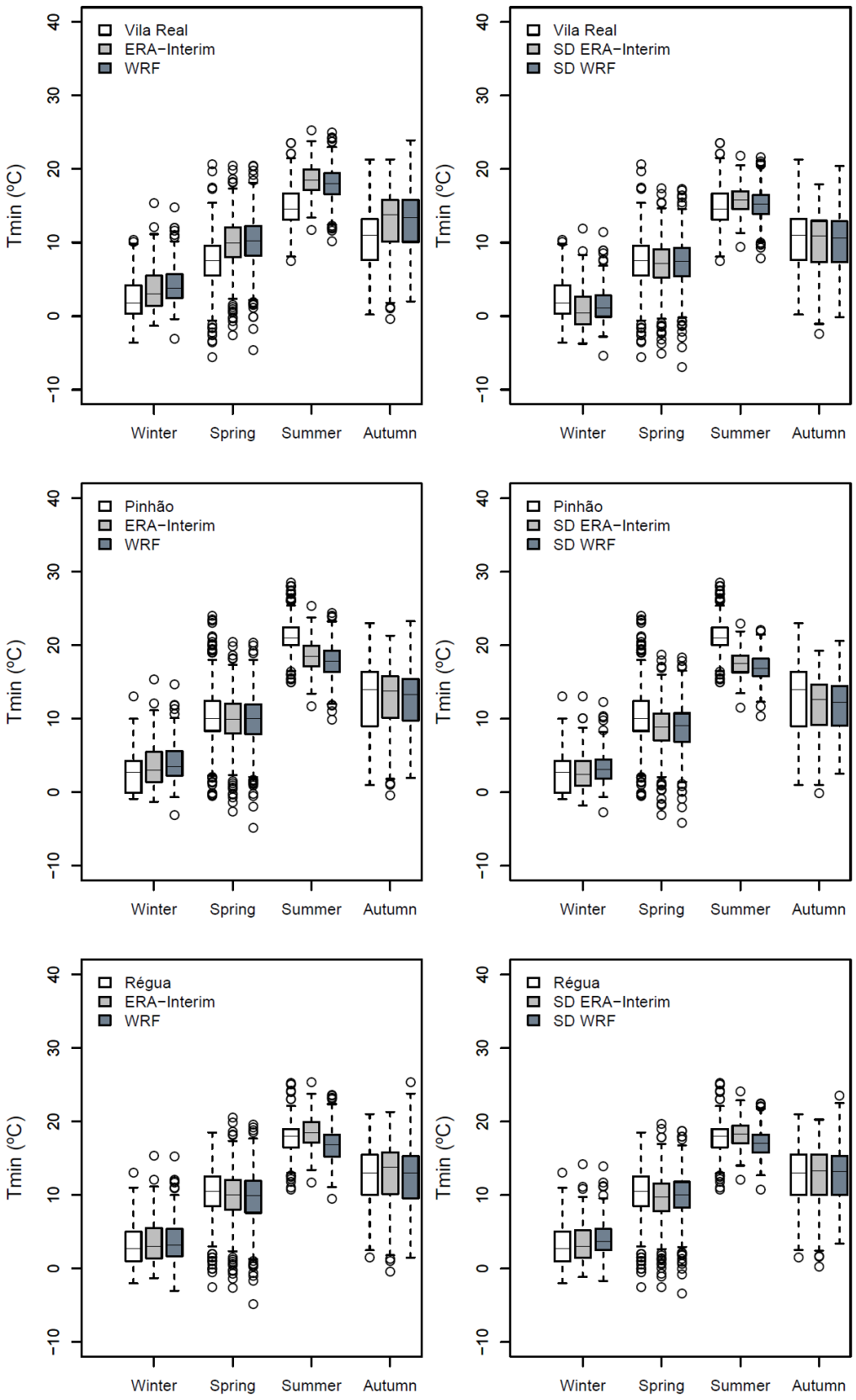

Figure 38 – Boxplot of seasonal daily Tmin from ERA-Interim/WRF and statistically-downscaled time (SD) series based on ordinary least squares for the validation period (2004-2006).

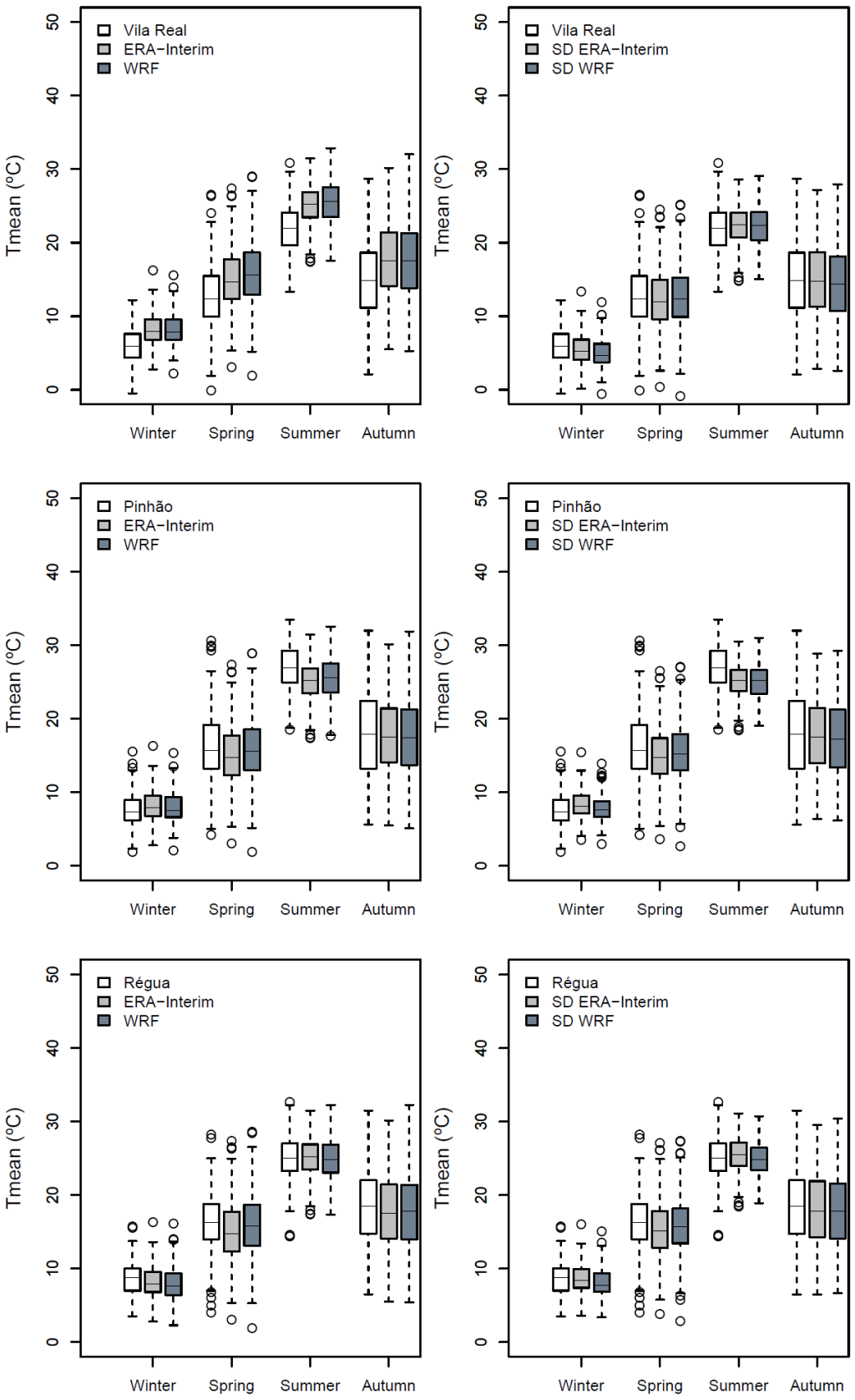

Figure 39 – Boxplot of seasonal daily Tmean from ERA-Interim/WRF and statistically-downscaled time (SD) series based on ordinary least squares for the validation period (2004-2006).

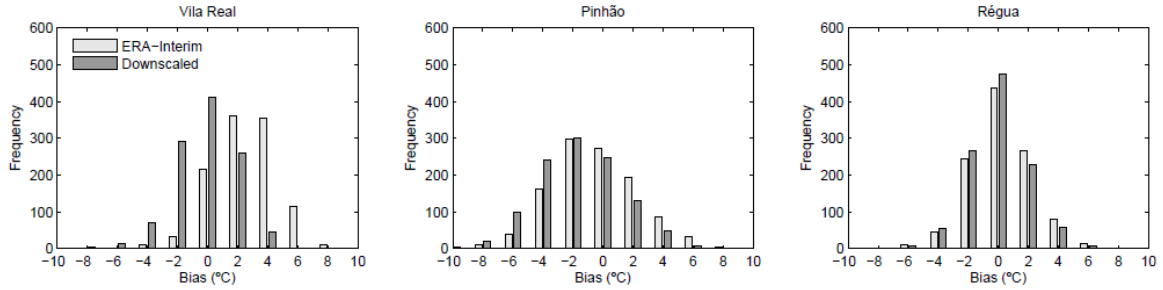

Figure 40 – Bias histograms of the Tmin downscaled time series based on ordinary least squares (gray) and of the ERA-Interim (white).

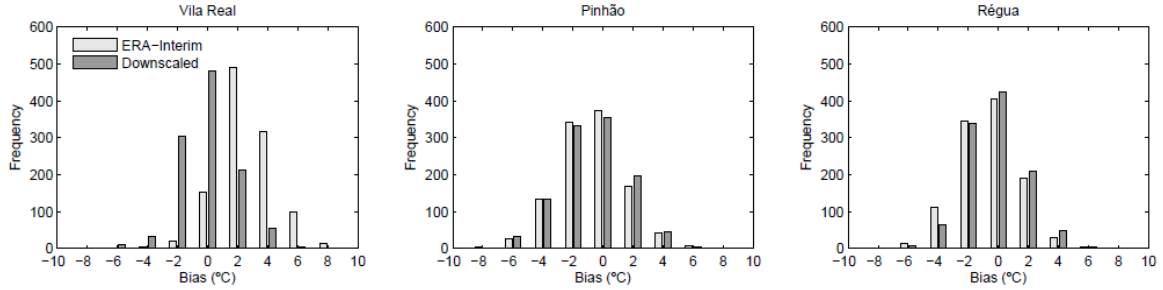

Figure 41 – Bias histograms of the Tmean downscaled time series based on ordinary least squares (gray) and of the ERA-Interim (white).

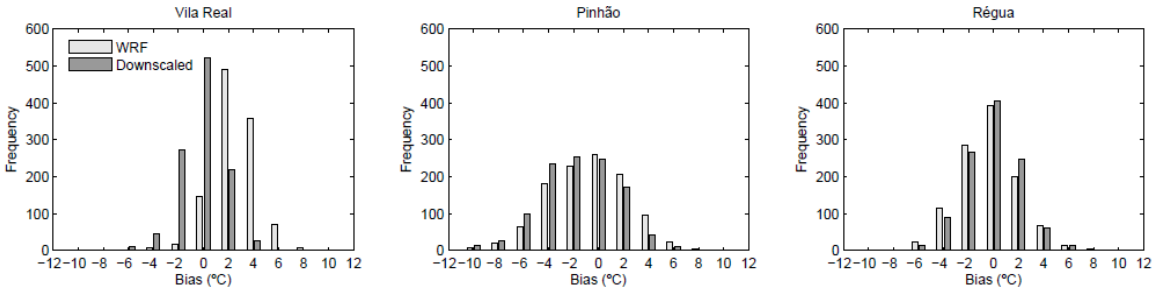

Figure 42 – Bias histograms of the Tmin statistical downscaled time series (gray) and of the WRF model (white).

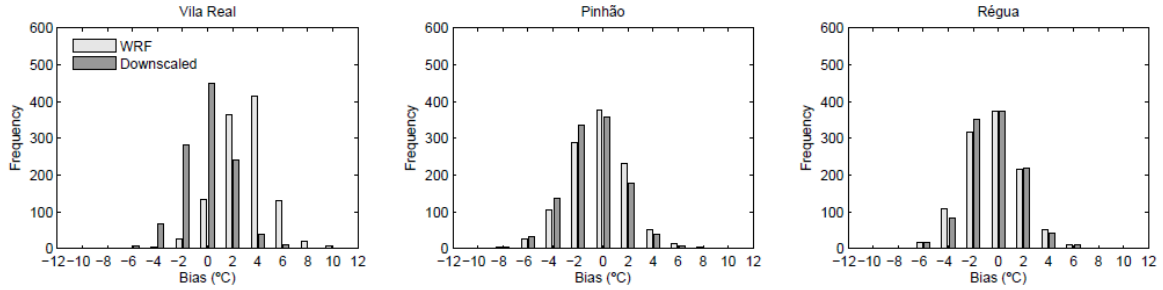

Figure 43 – Bias histograms of the Tmean statistical downscaled time series (gray) and of the WRF model (white).

MATLAB and R scripts example

Main steps of the statistical downscaling of WRF model data at Vila Real (Tmax)

```
                              %%%%%%%%%%%%%%%%%%%%%%%%%
                              %%%%% MATLAB-script %%%%%
                              %%%%%%%%%%%%%%%%%%%%%%%%%

%Read netcdf Tmax and Tmin
Tmaxwrf = ncread( 'Tmax_Tmin.nc', 'Tmax');%Tmax(time,y,x) [7305 135 162]
%Read netcdf LAT and LON
latwrf = ncread('Tmax_Tmin.nc', 'XLAT');%XLAT(y,x) [135 162]
lonwrf = ncread('Tmax_Tmin.nc', 'XLONG');%XLONG(y,x) [135 162]
%Read netcdf time file
timewrf = ncread('Tmax_Tmin.nc','time');%time [7305] "hours since 1989-01-
01 00:00:00"
%Read netcdf height
HGT = ncread('HGT.nc', 'HGT');

%%%%%%%%%%%%%%%%%%%%%%%%%%%%%%%%%%%%%%%%%%%%%%%
%Select WRF domine for the Douro Region
%%%%%%%%%%%%%%%%%%%%%%%%%%%%%%%%%%%%%%%%%%%%%%%

[lin col]=find(lonwrf>=-8.1045 & lonwrf<=-6.40 & latwrf>=40.505 &
latwrf<=42.05);%D4

Tmax_wrf = NaN(7305,1);
lat_wrf = NaN(1);
lon_wrf = NaN(1);
z_wrf = NaN(1);

for i=1:length(lin)

        LAT = unique(latwrf(lin(i),col(i)));
        LON = unique(lonwrf(lin(i),col(i)));

        TMAX = shiftdim(Tmaxwrf(lin(i),col(i),:));

        z = shiftdim(HGT(lin(i),col(i)));

        %%%%%%%%%%%%%%%%%%%%%%%%%%%%%
        %Aplly orographic correction
        %%%%%%%%%%%%%%%%%%%%%%%%%%%%%

        Tmax = TMAX+(z*6/1000);
        Tmin = TMIN+(z*6/1000);

        Tmax_wrf = cat(2, Tmax_wrf, Tmax);

        lat_wrf = cat(1,lat_wrf,LAT');
        lon_wrf = cat(1,lon_wrf,LON');

        z_wrf = cat(1,z_wrf, z');

    end

Tmax_wrf(:,1)=[];
Tmin_wrf(:,1)=[];
lat_wrf(1,:)=[];
```

```
lon_wrf(1,:)=[];
z_wrf(1,:)=[];

%%%%%%%%%%%%%%%%%%%%%%%%%%%%%%%%%%%%%%%%%%%%%%%%%%%%%%%%%%%%%%%%%%%%%%%
%Find WRF closest grid-points to Douro weather stations
%%%%%%%%%%%%%%%%%%%%%%%%%%%%%%%%%%%%%%%%%%%%%%%%%%%%%%%%%%%%%%%%%%%%%%%

%location douro stations
lat_vreal=41.3166667; lon_vreal=-7.7333333;

distvreal=zeros(size(lat_wrf)).*nan;

%Calculate distance between each grid-point and the stations

for j=1:numel(lat_wrf)
     distvreal(j)=distance(lat_wrf(j),lon_wrf(j),lat_vreal,lon_vreal);
end

%Find the minimum distance

mindistvreal=min(min(distvreal));
[linvreal colvreal]=find(distvreal==mindistvreal);

for k = 1:270

    LATwrfvreal = lat_wrf(linvreal,colvreal);
    LONwrfvreal = lon_wrf(linvreal,colvreal);

    Tmaxwrfvreal= shiftdim(Tmax_wrf(:,linvreal,colvreal));
end

%Save WRF time series closest to Vila Real, Pinhão and Régua txt files

dlmwrite('Tmax_wrf_vreal_orogcorrect.txt',Tmaxwrfvreal,'')


clear all; close all

%%%%%%%%%%%%%%%%%%%%%%%%%%%%%%%%%%%%%%%%%%%
%Calibration years 1989-2003 (15years)
%%%%%%%%%%%%%%%%%%%%%%%%%%%%%%%%%%%%%%%%%%%

clear all; close all;

endcalibration=datenum(2003,12,31,22,00,00);
time_wrf=load('timewrf.txt');
a=datenum(1989,1,1)+time_wrf/24;
k=find(a==endcalibration);

%Vila Real
Tmaxwrf_vreal=load('Tmax_wrf_vreal_orogcorrect.txt');
Tmaxwrf_vreal=Tmaxwrf_vreal(1:k,:);


dlmwrite('Tmaxwrf_vreal_orogcorrect_calibrationperiod.txt', Tmaxwrf_vreal,
' ')
%%%%%%%%%%%%%%%%%%%%%%%%%%%%%%%%%%%%%%%%%%%
%Validation years 2003-2006 (3years)
%%%%%%%%%%%%%%%%%%%%%%%%%%%%%%%%%%%%%%%%%%%
clear all; close all;
```

```
startvalidation=datenum(2003,12,31,22,00,00);

endvalidation=datenum(2006,12,30,22,00,00);
time_wrf=load('timewrf.txt');
a=datenum(1989,1,1)+time_wrf/24;

y=find(a==startvalidation);
k=find(a==endvalidation);

%Vila Real
Tmaxwrf_vreal=load('Tmax_wrf_vreal_orogcorrect.txt');

dlmwrite('Tmaxwrf_vreal_orogcorrect_validationperiod.txt', Tmaxwrf_vreal, '
')
```

```
                        ###################
                        ##### R-script ####
                        ###################


######################
# STL decomposition #
######################

library(chron)

library(zoo)

#Calibration period (1989-2003)

Tmax_wrf_vreal = ts(read.table
("Tmaxwrf_vreal_orogcorrect_calibrationperiod.txt"), start=c(1989,1,1),
frequency=365)

#Obtain seasonal cycle (1989-2003)

write.table(file="Tmaxwrf_vreal_stl_saz_calibrationperiod.txt",stl(Tmax_wrf
_vreal[,1],
s.window=365)$time.series[,1],quote=FALSE,col.names=FALSE,row.names=FALSE)

#Seasonal adjustment (1989-2003)

write.table(file="Tmaxwrf_vreal_stl_adj_calibrationperiod.txt",Tmax_wrf_vre
al[,1]-stl(Tmax_wrf_vreal[,1],
s.window=365)$time.series[,1],quote=FALSE,col.names=FALSE,row.names=FALSE)

#Validation period (2004-2006)

Tmax_wrf_vreal = ts(read.table
("Tmaxwrf_vreal_orogcorrect_validationperiod.txt"), start=c(2003,12,31),
frequency=365)

#Obtain seasonal cycle (2004-2006)

write.table(file="Tmaxwrf_vreal_stl_saz_validationperiod.txt",stl(Tmax_wrf_
vreal[,1],
s.window=365)$time.series[,1],quote=FALSE,col.names=FALSE,row.names=FALSE)

#Seasonal adjustment (2004-2006)

write.table(file="Tmaxwrf_vreal_stl_adj_validationperiod.txt",Tmax_wrf_vrea
l[,1]-stl(Tmax_wrf_vreal[,1],
s.window=365)$time.series[,1],quote=FALSE,col.names=FALSE,row.names=FALSE)
```

```
################################################
### Ordinary Least Squares and Robust Regression ##
################################################


library(nlme)
library(MASS)

#Observations Calibration period (1989-2003) seasonally-adjusted time
series
Tmax_vreal=data.matrix(read.table('Tmaxvreal_stl_adj_nan.txt'));

#WRF Calibration period (1989-2003) seasonally-adjusted time series
Tmax_wrf_vreal =
data.matrix(read.table('Tmaxwrf_vreal_stl_adj_calibrationperiod.txt')-
273.15);

#WRF validation period (2004-2006) seasonally-adjusted time series
Tmax_wrf_vreal_0306 =
data.matrix(read.table('Tmaxwrf_vreal_stl_adj_validationperiod.txt')-
273.15);

#Statistical downscaling
#OLS Regression

#Estimate OLS model
lm.TmaxWRFvreal = lm(Tmax_vreal~Tmax_wrf_vreal)

#Extract model coefficients
a_lm.TmaxWRFvreal = data.matrix(coef(lm.TmaxWRFvreal))[1,]
b_lm.TmaxWRFvreal = data.matrix(coef(lm.TmaxWRFvreal))[2,]

#Apply coefficients to seasonally-adjusted WRF time series
TmaxWRFvreal_lm_0306 = a_lm.TmaxWRFvreal +
b_lm.TmaxWRFvreal*Tmax_wrf_vreal_0306

write.table(file="TmaxWRFvreal_lm_0306.txt",TmaxWRFvreal_lm_0306,quote=FALS
E,col.names=FALSE,row.names=FALSE)

#Robust Regression

#Estimate Robust regression model
rlm.TmaxWRFvreal = rlm(Tmax_vreal~Tmax_wrf_vreal)

#Extract model coefficients
a_rlm.TmaxWRFvreal = data.matrix(coef(rlm.TmaxWRFvreal))[1,]
b_rlm.TmaxWRFvreal = data.matrix(coef(rlm.TmaxWRFvreal))[2,]

TmaxWRFvreal_rlm_0306 = a_rlm.TmaxWRFvreal +
b_rlm.TmaxWRFvreal*Tmax_wrf_vreal_0306

#Apply coefficients to seasonally-adjusted WRF time series
write.table(file="TmaxWRFvreal_rlm_0306.txt",TmaxWRFvreal_rlm_0306,quote=FA
LSE,col.names=FALSE,row.names=FALSE)


#################################################################
#ADD WRF SEASONAL CYCLE (2004-2006) TO DOWSCALED ADJ TIME SERIES OLS
#################################################################

#Downscaled based on WRF by OLS seasonally-adjusted time series
Tmax_vreal_lm_wrf=data.matrix(read.table("TmaxWRFvreal_lm_0306.txt"))
```

```
#WRF seasonal cycle (2004-2006)
Tmax_wrf_vreal_saz=data.matrix(read.table("Tmaxwrf_vreal_stl_saz_validation
period.txt"))

#Add seasonal cycle to downscaled time series (adj)
Tmax_wrf_vreal_downscaled = Tmax_vreal_lm_wrf + Tmax_wrf_vreal_saz
write.table(file="Tmax_vreal_downscaled_lm_wrf_seas0306.txt",Tmax_wrf_vreal
_downscaled, quote=FALSE,col.names=FALSE,row.names=FALSE)


########################
#BIO-CLIMATIC INDICES##
########################


#Downscaled based on WRF by OLS
Tmean_vreal_downscaled_lm_wrf=zoo(read.table("Tmean_vreal_downscaled_lm_wrf
_seas0306.txt"), order.by=tm_0306)

Tmean_vreal_downscaled_lm_wrf_grow_04=window(Tmean_vreal_downscaled_lm_wrf,
start = as.Date("2004-04-01"), end = as.Date("2004-10-31"))
Tmean_vreal_downscaled_lm_wrf_grow_05=window(Tmean_vreal_downscaled_lm_wrf,
start = as.Date("2005-04-01"), end = as.Date("2005-10-31"))
Tmean_vreal_downscaled_lm_wrf_grow_06=window(Tmean_vreal_downscaled_lm_wrf,
start = as.Date("2006-04-01"), end = as.Date("2006-10-31"))

#GST Downscaled wrf

GST_vreal_lm_wrf_04 =
sum(Tmean_vreal_downscaled_lm_wrf_grow_04)/length(Tmean_vreal_downscaled_lm
_wrf_grow_04)
GST_vreal_lm_wrf_05 =
sum(Tmean_vreal_downscaled_lm_wrf_grow_05)/length(Tmean_vreal_downscaled_lm
_wrf_grow_06)
GST_vreal_lm_wrf_06 =
sum(Tmean_vreal_downscaled_lm_wrf_grow_06)/length(Tmean_vreal_downscaled_lm
_wrf_grow_06)

# set GDD base temperature (usually 10 °C)
Tbase = 10

# Any temperature below Tbase is set to Tbase
adjust_for_Tbase <- function(x) ifelse(test = x < Tbase, yes = Tbase, no =
x)

#GDD DOWNSCALED

Tmean_vreal_lm_wrf_grow_04_adj =
adjust_for_Tbase(Tmean_vreal_downscaled_lm_wrf_grow_04)
Tmean_vreal_lm_wrf_grow_05_adj =
adjust_for_Tbase(Tmean_vreal_downscaled_lm_wrf_grow_05)
Tmean_vreal_lm_wrf_grow_06_adj =
adjust_for_Tbase(Tmean_vreal_downscaled_lm_wrf_grow_06)

GDD_vreal_lm_wrf_04 = sum(Tmean_vreal_lm_wrf_grow_04_adj-Tbase)
GDD_vreal_lm_wrf_05 = sum(Tmean_vreal_lm_wrf_grow_05_adj-Tbase)
GDD_vreal_lm_wrf_06 = sum(Tmean_vreal_lm_wrf_grow_06_adj-Tbase)

cumGDD_vreal_lm_wrf_04 = cumsum(Tmean_vreal_lm_wrf_grow_04_adj-Tbase)
cumGDD_vreal_lm_wrf_05 = cumsum(Tmean_vreal_lm_wrf_grow_05_adj-Tbase)
cumGDD_vreal_lm_wrf_06 = cumsum(Tmean_vreal_lm_wrf_grow_06_adj-Tbase)

#Huglin Index
```

```
# set HI base temperature (usually 10 °C)
Tbase = 10

#set daylength adjustment due to latitude varying (Tonietto et al 2004)
d = 1.02

Tmax_vreal_downscaled_lm_wrf=zoo(read.table("Tmax_vreal_downscaled_lm_wrf_s
eas0306.txt"), order.by=tm_0306)
Tmax_vreal_downscaled_lm_wrf_grow_04=window(Tmax_vreal_downscaled_lm_wrf,
start = as.Date("2004-04-01"), end = as.Date("2004-10-31"))
Tmax_vreal_downscaled_lm_wrf_grow_05=window(Tmax_vreal_downscaled_lm_wrf,
start = as.Date("2005-04-01"), end = as.Date("2005-10-31"))
Tmax_vreal_downscaled_lm_wrf_grow_06=window(Tmax_vreal_downscaled_lm_wrf,
start = as.Date("2006-04-01"), end = as.Date("2006-10-31"))

Tmin_vreal_downscaled_lm_wrf=zoo(read.table("Tmin_vreal_downscaled_lm_wrf_s
eas0306.txt"), order.by=tm_0306)
Tmin_vreal_downscaled_lm_wrf_grow_04=window(Tmin_vreal_downscaled_lm_wrf,
start = as.Date("2004-04-01"), end = as.Date("2004-10-31"))
Tmin_vreal_downscaled_lm_wrf_grow_05=window(Tmin_vreal_downscaled_lm_wrf,
start = as.Date("2005-04-01"), end = as.Date("2005-10-31"))
Tmin_vreal_downscaled_lm_wrf_grow_06=window(Tmin_vreal_downscaled_lm_wrf,
start = as.Date("2006-04-01"), end = as.Date("2006-10-31"))


HI_vreal_lm_wrf_04 = sum((((Tmean_vreal_downscaled_lm_wrf_grow_04-
Tbase)+(Tmax_vreal_downscaled_lm_wrf_grow_04-Tbase))/2)*d)
HI_vreal_lm_wrf_05 = sum((((Tmean_vreal_downscaled_lm_wrf_grow_05-
Tbase)+(Tmax_vreal_downscaled_lm_wrf_grow_05-Tbase))/2)*d)
HI_vreal_lm_wrf_06 = sum((((Tmean_vreal_downscaled_lm_wrf_grow_06-
Tbase)+(Tmax_vreal_downscaled_lm_wrf_grow_06-Tbase))/2)*d)

#LGS

LGS_vreal_lm_wrf_04=length(which(Tmean_vreal_downscaled_lm_wrf_grow_04>10))
LGS_vreal_lm_wrf_05=length(which(Tmean_vreal_downscaled_lm_wrf_grow_05>10))
LGS_vreal_lm_wrf_06=length(which(Tmean_vreal_downscaled_lm_wrf_grow_06>10))

#Cool night index

Tmin_vreal_downscaled_lm_wrf=zoo(read.table("Tmin_vreal_downscaled_lm_wrf_s
eas0306.txt"), order.by=tm_0306)
Tmin_vreal_downscaled_lm_wrf_grow_04=window(Tmin_vreal_downscaled_lm_wrf,
start = as.Date("2004-09-01"), end = as.Date("2004-09-30"))
Tmin_vreal_downscaled_lm_wrf_grow_05=window(Tmin_vreal_downscaled_lm_wrf,
start = as.Date("2005-09-01"), end = as.Date("2005-09-30"))
Tmin_vreal_downscaled_lm_wrf_grow_06=window(Tmin_vreal_downscaled_lm_wrf,
start = as.Date("2006-09-01"), end = as.Date("2006-09-30"))


CI_vreal_04 = mean(Tmin_vreal_grow_04)
CI_vreal_05 = mean(Tmin_vreal_grow_05)
CI_vreal_06 = mean(Tmin_vreal_grow_06)
```